UNIVERSITÀ
DI PAVIA

PhD in Biomedical Sciences

Department of Brain and Behavioral Sciences

Unit of Neurophysiology

Novel outcome measures and genetic variability in hereditary transthyretin amyloidosis

PhD Tutor: Andrea Cortese, MD, PhD

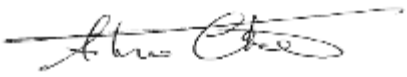

PhD dissertation of: Elisa Vegezzi

Academic Year 2022-2023

Table of contents

1. Introduction

Hereditary transthyretin amyloidosis (ATTRv, "v" for "variant) also known as familial amyloid polyneuropathy (FAP) is a rare, dominantly inherited, systemic disease caused by point mutations in the transthyretin (*TTR*) gene. Mutant TTR protein tends to misfold and accumulates as amyloid extracellular fibrils across different tissues and organs, especially peripheral nerves, and heart, resulting in a toxic gain of function.

ATTRv amyloidosis was first described as FAP in 1952 by Corino Andrade in northern Portugal[1]. After its identification, other endemic foci have been discovered, mostly in northern Sweden[2] and Japan[3]. However, an increasing number of late-onset, often sporadic cases have been recognized worldwide, and more than 150 amyloidogenic mutations have been reported so far[4], with a broad phenotypic variability in terms of age of onset (AOO), severity, and response to disease modifying therapies. The most frequent mutation is V30M (alternatively named, according to the novel nomenclature[5], p.Val50Met), which was the first one identified. ATTRv is a progressive, disabling, and life-threatening condition with a mean survival of 7-10 years if left untreated[6–8].

Different therapies have been approved for ATTRv amyloidosis so far, including the TTR stabilizer tafamidis and, more recently, the RNAi agents patisiran and vutrisiran, and the antisense oligonucleotide inotersen[9,10,11]. Moreover, other treatment options are underway[12].

1.1 Epidemiology

Until 1990 ATTRv amyloidosis was considered as a rare disease with endemic foci in northern Portugal[13], northern Sweden[2] and two areas in Japan[3], with an estimated prevalence in these regions of 1-10 in 10,000. Thereafter, other endemic foci have been reported in Cyprus[14], Majorca[15], and Brazil[16].

However, an increasing number of late-onset, often sporadic, cases have also been diagnosed through biopsy findings and *TTR* gene sequencing[17]. Indeed, ATTRv amyloidosis has been reported so far in 29 Countries, including many Countries in Europe[18], the USA[19], China[20], and India[21].

According to a survey published in 2018, based on the known prevalence in Portugal, Sweden, Japan in addition to that in seven core countries (France, Italy, Turkey, Cyprus, Bulgaria, Germany and the Netherlands), the global population of people with ATTRv amyloidosis was estimated at 10,186, with a range of 5,526-38,46821[22].

According to the national registry, in Italy the prevalence of ATTRv amyloidosis was 4.3/million, although with regional differences[23]. This estimated prevalence was similar to that found in France (3-4/million)[24], The Netherlands (2.6/million), and in Bulgaria (6.2/million)[22].

Similarly to the worldwide distribution, also in Italy the V30M (p.Val50Met) is the most common mutation, mostly in the Northern and Central regions, followed by F64L (p.Phe84Leu), I68L (p.Ile88Leu), and V122I (p.Val142Ile)[23]. These genetic variants are not restricted to a unique area, and the V30M (p.Val50Met) mutation seems to have a different and ancestral origin comparing the Italian haplotype by microsatellite analysis with those of patients with Portuguese and Swedish ancestry[25].

In Southern Italy, E89Q (p.Glu109Gln), F64L (p.Phe84Leu), and T49A (p.Thr69Ala) are the most frequent pathogenic variants, with a clear common ancestry for the E89Q (p.Glu109Gln, Siracusa, Sicily) and the T49A (p.Thr69Ala, Agrigento, Sicily) mutations. Also the Y78F (p.Tyr98Phe) harbors a common ancestry from Bergamo (Lombardy)[23].

1.2 Pathophysiology

1.2.1 Structure and function of *TTR* gene and protein

The *TTR* gene (ENSG00000118271) is located on chromosome 18q11.2-12.1[26] (GRCh38/hg38, chr18:31,591,877-31,598,821, 6,945 bp) and encompasses four exons, three introns, a TATA box-like sequence at nucleotides 24-30, and a CAAT box-like sequence at nucleotides 95–101[27,28].

The first exon contains 95 base pairs (bp) and 26 bp of 5' untranslated region. It encodes for a signal peptide of 20 amino acids along with the first 3 amino acid residues of the mature protein. The other three exons encode for amino acid residues 4-47 (exon 2, 131 bp), 48-92 (exon 3, 136 bp), and 93-127 (exon 4,253 bp)[28,29], respectively.

The immature protein consists of 147 amino acid residues, whose N-terminal region corresponds to a hydrophobic signal peptide of 20 amino acids, which is cleaved to produce the native TTR monomer[30]. This cleavage is necessary to free the first 9 amino acids of the mature TTR monomer, which are fundamental for monomer-monomer assembly into dimers, which represents the first step of the formation of the tetramer[31,32].

TTR is as a transport protein of 55 KDa, mainly synthetized by the liver[33], and the choroid plexus, but also retinal pigment epithelium, pancreas, placenta, and yolk sac[34], and then secreted into the plasma or serum and cerebrospinal fluid. TTR was previously known as prealbumin since it migrates in front of albumin in serum protein electrophoresis[35]. Following the discovery of its role as a transporter of thyroxine (T4), the name was converted into "thyroxine-binding prealbumin"[36]. It was only in 1981 that The International Union of Biochemistry changed the name into "transthyretin" (*trans*ports *thy*roxine and *retin*ol), when it was discovered that this protein was also able to bind retinol complexed with retinol-binding protein 4 (holo-RBP)[37].

Indeed, human TTR has a globular homotetrameric structure with four identical subunits composed of eight beta-strands each, with a molecular weight of approximately 14 KDa, designed with letters from "A" to "H", and one short alpha-helix of 9 amino acid residues between strands "E" and "F"[38,39]. These eight β-strands are connected by loops and are arranged in two groups of twisted β-sheets[40]. Two TTR monomers are arranged into dimers by hydrogen bonding and two dimers then form a tetramer mainly through hydrophobic bonds between loops[40]. The tetramer has two and four bindings sites which are meant for T4 and holoRBP, respectively.

TTR knockout (*TTR*-KO) mice presented with sensory-motor dysfunction and impaired functional recovery in response to crush injuries, with reduced neurite outgrowth and extension, resulting from decreased number of both myelinated and unmyelinated fibres. Moreover, the expression of human *TTR* in *TTR*-KO mice rescued the phenotype, thus highlighting the fundamental role of *TTR* in nerve regeneration and repair[41]. Alongside with its well-established function in the peripheral nervous system (PNS) physiology, *TTR* seems also to play a role in the central nervous system (CNS), being involved in the maintenance of normal cognitive processes during aging by acting on the retinoid signalling pathway[42].

1.2.2 Genetics

To date over 150 mutations have been identified in the *TTR* gene. The vast majority of them is pathogenic and only few mutations are non-amyloidogenic[4]. Indeed, the polymorphism G6S (p.Gly26Ser) has no significant value in a patient with sporadic idiopathic peripheral neuropathy[43], being its allele frequency in Caucasians around 5%[44]. T119M (p.Thr139Met) variant is taught to be protective and when in compound heterozygous

state with the common V30M (p.Val50Met) mutation, it seems to slow down the tetramer dissociation, which represents the first misfolding event, thus resulting in a later age-of-onset (AOO)[45]. Most variants are point missense mutations, while only a single deletion in exon 4 encompassing 3 nucleotides has been reported so far[46]. Patients who are compound heterozygous, meaning that they carry one pathogenic and one non-pathogenic variant, as well as patients who are homozygous for pathogenic mutations, have also been described.

The V30M (p.Val50Met) variant accounts for ATTRv amyloidosis in the regions where the disease is endemic (Portugal, Sweden, Japan, Cyprus, Majorca, and Brazil)[2,3,13–16]. This mutation is also the most common one among smaller disease clusters and scattered families worldwide[19]. The carrier frequency in the Swedish population is high (~1.5%)[47] while it is lower in non-endemic regions[34]. Carrier frequency also deeply varies according to racial backgrounds, as for the V122I (p.Val142Ile) variant which typically occurs in the Afro-American, West African, and Hispanic populations[48,49], although cases across Caucasians, especially in Italy (Tuscany), have been reported so far[50,51]. In Tuscany, a founder effect rather than an admixture from African population has been demonstrated[52].

Distinct founder mutations have also been reported including T60A (p.Thr80Ala) in northwest Ireland (Donegal) and populations of Irish ancestry[53], E89Q (p.Glu109Gln) in southwest Bulgaria, S50A (p.Ser70Arg) in Mexico[54], F64L (p.Phe84Leu) in Sicily[23], S77T (p.Ser97Tyr)[55] and S77F[6] (p.Ser97Phe) in France, and A97S (p.Ala117Ser) in Taiwan and China[56]. However, the E89Q (p.Glu109Gln) variant has also been reported in Italy (Sicily)[57] and Turkey[58].

The penetrance of *TTR* mutation is highly variable. A penetrance which approaches 100% has been reported in families with multiple affected members from endemic regions[59]. In non-endemic regions penetrance seems to increase with age[60]. Different studies including patients from Portugal, Sweden, France, and Brazil showed that penetrance varies with age and increases up to the 9th decade, when it approaches 100%, even in case of mutations which are associated to a late-onset phenotype[59–61].

Anticipation, which means the occurrence of a disease at a significantly earlier AOO in the offspring/younger generations, has been observed in ATTRv amyloidosis. Indeed, a parent-of-origin effect with mother-son pairs showing the largest differences in AOO, up to >=10 years, has been observed across Portuguese, Swedish, and Japanese families[47,62,63,64]. However, although anticipation is more pronounced in mother-son pairs, it has also been reported in mother-daughter and father-son transmission, suggesting that different factors, other than gender, could play a role[64]. Differences in penetrance according to gender of the

transmitting parent has also been reported, with a higher penetrance in case of maternal transmission[61,65].

Various *TTR* haplotypes associated with V30M (p.Val50Met) mutations in ATTRv patients have been reported so far across different Countries. The first approach to genetic variation in ATTRv amyloidosis involved the characterization of intragenic haplotypes and was mainly focused on the origin of the V30M (p.Val50Met) mutation across different ethnicities. Five different haplotypes have been initially described using six to seven most informative intronic single nucleotide polymorphisms (SNPs) located at positions 1218 (intron 1), 2422 and 2537 (intron 2), 5198, 5610, and 5708 (intron 3), respectively: haplotype I (GCACGT), II (TGGCGT), III (TGGACG), IV (GCAAGT), and V (GGGAGT)[66,67]. One major disease haplotype, type I (GCACGT), have been invariably reported among Portuguese ATTRv patients carrying V30M (p.Val50Met) mutation, typically presenting with early-onset and severe phenotype[67]. Although haplotype I was also found in Swedish ATTRv V30M (p.Val50Met) carriers, with typical late-onset and milder phenotype[67], an independent founder effect was further demonstrated using polymorphic microsatellites flanking *TTR* gene[68,69]. Haplotype I has also been reported in French ATTRv V30M (p.Val50Met) families of Portuguese descent[70], while haplotype II and III have been detected in French ATTRv patients not of Portuguese origin carrying the same commonest mutation[6,70]. Haplotype III was also demonstrated to segregate in Italian, British, Turkish, and Japanese ATTRv kindreds with V30M (p.Val50Met) variant[66,67] and even to be associated to the V30M (p.Val50Met) mutation in Portuguese ATTRv patients, although in a single study[71]. Moreover, ATTRv patients from Majorca, Brazil, and Japan (prefectures of Nagano and Kumamoto) carrying V30M (p.Val50Met) mutation seem to share the same haplotype I of Portuguese ATTRv patients, although some recombination events have probably occurred locally[68,69].

More recently, it has been shown that Italian ATTRv patients carrying V30M (p.Val50Met) mutation seem to harbor a different haplotype, defined by 11 microsatellites surrounding *TTR* gene, from both Portuguese and Swedish patients, which has probably independently arose between 850 and 900 years ago[25].

Five novel different haplotypes (named from “A” to “E”) have been further reported according to eight intragenic SNPs, four of which overlapping with those from previous studies[72]. Interestingly, for the rs72922947 SNP (minor allele A in haplotype C [TTGAGCTT]), which is located in the intron 2 of *TTR* gene, a *trans*-acting effect (i.e., when transmitted by the non-carrier parent) influencing an earlier onset (i.e., very early [<=30 years], and early [<=40 years]) in Portuguese ATTRv V30M (p.Val50Met) patients has been

hypothesized[72]. Also, the rs62093482 SNP, although not apparently affecting AOO[72,73], seems to be unique to the Swedish ATTRv V30M (p.Val50Met) patients[73].

To better understand the heterogeneity which underlies ATTRv amyloidosis, previous studies have also looked at genetic modifiers of AOO, and a possible role of *cis* and *trans*-acting elements from *TTR* gene, including coding and non-coding variants in *TTR* itself, and other genes as Retinol Binding Protein 4 (*RBP4*)[74,75], Androgen Receptor (*AR*)[74], Complement C1q A Chain (*C1QA*), Complement C1q C Chain (*C1QC*)[76–78], Amyloid P Component, Serum (*APCS*)[74–76], Biglycan (*BGN*), Heat Shock Protein 27 (*HSP27*), Mitogen Activated Protein Kinase 1 (*MEK1*), Mitogen Activated Protein Kinase 2 (*MEK2*), Neutrophil Gelatinase-Associated Lipocalin (*NGAL*), Tyrosine 3-Monooxygenase/Tryptophan 5-Monooxygenase Activation Protein Zeta (*YWHAZ*)[79] has been hypothesized.

1.2.3 TTR amyloid fibrils: morphology, formation, and tissue toxicity

ATTRv is a protein misfolding disease. Indeed, the dissociation of mutant TTR subunits results in misfolding and aggregation of TTR amyloid fibrils in extracellular spaces, leading to systemic organ dysfunction[80,81].

The morphology of TTR fibrils varies according to AOO, and specific causal mutation[82–84]. Indeed, amyloid fibrils of ATTRv V30M (p.Val50Met) patients from Sweden have two different compositions[85]. In some patients there is large amount of truncated, mostly C-terminal, TTR protein, starting at position around amino acid 50, in addition to the full-length protein (fibril type A). In other patients, only the full-length protein seems to be present in the amyloid deposits (fibril type B)[85]. These deposits have been first recognized in the cardiac tissue[85] and, later on, in the abdominal adipose tissue along with other tissues[78,84]. These amyloid fibrils have different morphology in the microscope. Type A fibrils are short, and haphazardly arranged. Also, they have a faint color and birefringence as well as a smooth appearance when stained with Congo red. Contrarily, type B fibrils are longer and parallel arranged into bundles. They are strongly stained by Congo red, and have a granular appearance, rendering a “glittering” effect in polarized light[85].

The fibril type seems to be related to the phenotypic differences seen in ATTRv V30M (p.Val50Met) patients. Indeed, type A fibrils, which more easily incorporates wild-type TTR fibres[84], are mainly found in patients with a later AOO (over 50 years) and with an

increased left ventricular wall thickness, while patients with fibrils type B are usually characterized by an earlier AOO and normal cardiac wall thickness[82]. Portuguese and Brazilian (said to be of Portuguese origin) ATTRv V30M (p.Val50Met) patients from endemic areas exhibited long thick amyloid fibrils, similar to those detected in Japanese patients from endemic foci[83,87]. Contrarily, the amyloid deposits in ATTRv patients harboring other mutations seem to be similar to those of patients with late-onset ATTRv V30M (p.Val50Met) amyloidosis from non-endemic foci in Japan[83,88]. Interestingly, patients with senile systemic amyloidosis (SSA) who have been investigated so far have type A fibrils, suggesting that the presence of fragmented TTR is fairly common while full-length TTR seems to be clustered in certain subsets of patients from endemic foci[85]. In patients, especially elderly men, who undergo liver transplantation, cardiac amyloidosis can exacerbate, due to the deposition of wild-type TTR[89,90]. This also occurs in the peripheral nerves, although the ratio of wild-type relative to mutant TTR is lower than in the heart[91,92].

It is still unknown why there are two different compositions of amyloid fibrils. The fibril type seems to remain unchanged over time, and patients who have been longitudinally followed up to 10-15 years still not display fragments in their deposits[86]. A difference in protease activity or the presence of two different structures of amyloid fibrils, with a cleavage site which could be more or less exposed, may be at play[88].

The native tetrameric assemblies of all *TTR* variants are less stable *in vitro* than those of wild-type *TTR*, and dissociated protomers tend to self-aggregate[93] although the mechanism underlying the fibrillogenesis *in vivo* is still unknown.

One proposed pathogenic pathway for ATTRv amyloidosis involves proteolytic cleavage of TTR[94,95]. Evidence suggests that carboxy-terminal fragments of TTR produced by this cleavage promote amyloid fibril formation[96]. In particular, the residue 49-127 C-terminal is a major component of *ex vivo* TTR amyloid fibrils, especially in the heart[97], regardless of the presence, nature, and position of any *TTR* amyloidogenic mutation[85]. It has been shown that the proteolytic cleavage of the highly aggressive S52P (p.Ser72Pro) ATTRv variant at 48-49 peptide bond makes the tetramer deeply unstable with the release of 49-127 peptide under physiological fluid agitation, which tends to self-aggregate together with the full-length protein[98]. A mechano-enzymatic process common to different amyloidogenic variants (V30M, p.Val50Met; L55P, p.Leu75Pro; V122I, p.Val142Ile) and wild-type *TTR*, namely a susceptibility to trypsin cleavage at position 48 under shear stress, as in the heart, has been further proposed. This results in the formation of specific truncated fragments which tend to aggregate into fibrils. Interestingly, the T119M (p.Thr139Met) variant, which is

taught to be protective as mentioned above, is neither cleaved nor forms fibrils under the same biochemical forces[99].

The deposition of amyloid fibrils causes tissue damage. The blood-nerve barrier, meaning the barrier made of tight junctions between endothelial cells of the endoneurial microvessels which divides the vascular lumen and the interstitium in the peripheral nervous system, is disrupted in ATTRv amyloidosis, regardless of the presence of amyloid deposits around it. This enables the entry of mutant TTR into the endoneurial space[92].

The amyloid fibrils exhibit also toxic effects on Schwann cell membranes. Non-demyelinating Schwann cells, which wrap around small-diameter nerve fibres, become distorted and atrophic when adjacent to long and thick amyloid fibrils of early-onset ATTRv V30M (p.Val50Met) amyloidosis. Indeed, small-fibre axonal loss occurs predominantly in early-onset ATTRv V30M (p.Val50Met) amyloidosis. Contrarily, large, myelinated fibres seem to be resistant to the damage caused by the deposition of amyloid fibrils because the contact of these fibres with the aggregates is usually partial[83,100]. *In vitro* models showed that TTR oligomers rather than mature fibrils are toxic[101] and this could explain the loss of large fibres in late-onset ATTRv V30M (p.Val50Met) patients, in which fewer deposits of mature amyloid fibrils are present[102] (**Fig**. **1**).

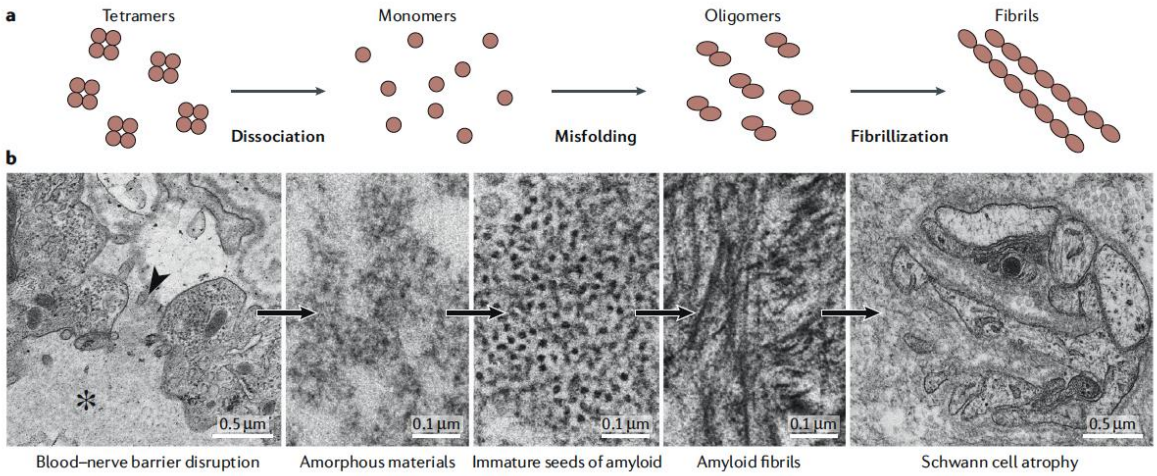

Fig. **1**. Mechanistic models of amyloid fibril formation (**a**) and toxicity of amyloid fibrils (**b**)[103].

1.3 Clinical spectrum

1.3.1 Natural history

ATTRv is a progressive, disabling, and life-threatening condition with a mean survival of 7-10 years if left untreated[6,7,8].

Relaying on broad observational studies on the Portuguese early-onset ATTRv V30M (p.Val50Met) patients, Coutinho and colleagues defined three different stages based on walking capability. Stage I corresponds to a progressive sensory neuropathy determining walking difficulties but without any assistance needed. Stage II is a sensory-motor polyneuropathy with preserved walking capability, although with required assistance. In stage III the patient is wheelchair-bound or bedridden[104].

Contrarily, the natural history of late-onset ATTRv V30M (p.Val50Met) amyloidosis and ATTRv amyloidosis related to other mutations is characterized by a more rapid disease progression, with gait disability occurring earlier, which is paralleled by a faster progression of Neuropathy Impairment Scale (NIS) (*see further*)[7,105].

1.3.2 Clinical presentation

ATTRv amyloidosis is mainly a neuropathic condition. However, given its multisystemic features, which can include also cardiac, eye, and kidney abnormalities, ATTRv amyloidosis should be managed in a multidisciplinary setting, with the neurologist playing a pivotal role.

1.3.2.1 Hereditary transthyretin amyloidosis-polyneuropathy

ATTRv polyneuropathy (ATTRv-PN) is the most common form of ATTRv amyloidosis and most frequently associated to V30M (p.Val50Met) mutation. Clinical presentation and disease course differ considerably between patients with early- and late-onset PN phenotype.

Early-onset ATTRv PN phenotype is typically found in Portugal and endemic regions in Japan. The AOO is usually <50 years, and the disease is nearly always associated with a positive family history with high penetrance. Patients present with an axonal lengh-dependent sensory-motor polyneuropathy, causing mostly sensory disturbances (e.g., paraesthesia, lightning pain), which start distally and further extends to the proximal segments. A small-

fibre neuropathy, which typically determines loss of nociception and thermal sensation, is also at play. Autonomic dysfunction, meaning orthostatic hypothension (light headedness, fainting upon moving from lying to standing), gastrointestinal (gastroparesis, early satiety and crisis of vomiting, diarrhoea, or alternating diarrhoea-constipation, and faecal incontinence), and genitourinary (urinary retention or incontinence, incomplete emptying, erectile dysfunction) symptoms, is present in up to 75% of patients. Also, cardiac conduction defects are frequent, often requiring pacemaker implantation. Involuntary weight loss and fatigue can be unspecific presenting symptoms of the disease. Disese course is usually slower, with a longer median survival, if compared to late-onset phenotype[104,106].

Late-onset ATTRv PN phenotype is found in both endemic and non-endemic regions. The AOO is tipically >50 years, there is no family history, and variable penetrance. It is characterized by an axonal lengh-dependent sensory-motor polyneuropathy affecting all sensory modalities. Autonomic dysfunction is usually milder while cardiomyopathy is typically observed, althugh the extent of peripheral nerves and cardiac involvement relies on the *TTR* pathogenic variant[7,106,107]. A positive history of carpal tunnel synndrome is common (23-63% of patients) in late-onset ATTRv V30M (p.Val50Met) amyloidosis and other variants, while is less frequent in early-onset ATTRv V30M (p.Val50Met) cases[108].

In non-endemic regions ATTRv PN may be misdiagnosed as chronic inflammatory demyelinating polyradiculoneuropathy, with slowing of motor conduction velocities (up to 30 m/s in the lower limbs), sensory loss of all-modalities, diffuse areflexia, and elevated proteins in the cerebrospinal fluid[109,110]. Also, multifocal neuropathy with upper-limb onset (17.6%)[7,111], ataxic neuropathy / gait disorders (e.g., S77T, p.Ser97Tyr variant in northern France, 11-23%)[24], and pure motor neuropathy (<1%)[112,113], have been described.

1.3.2.2 Hereditary transthyretin amyloidosis-cardiomyopathy

ATTRv cardiomyopathy (ATTRv-CM) is overall present as an infiltrative cardiomyopathy with myocardial thickness >13mm in nearly 56% to 63% of ATTRv patients, being more common in late-onset cases[9,11]. It usually presents as a hyperthrophic restrictive cardiomyopathy causing heart failure, otherwise known as heart failure with preserved ejection fraction, which is fairly undistinguishable from ATTRwt-cardiomyopathy (*see further*). Conduction blocks, ventricular arrhytmias, or sudden cardiac death may occur. However, ATTRv-CM remains latent for long time thus being underdiagnosed[114].

V122I (p.Val142Ile), which is commonly seen in 3-4% of Afro-Americans, and Ile111Met (p.Ile131Met) typically present with a cardiac phenotype, while other mutations with a cardiac involvement are more frequent in Caucasian, Hispanic, and Asian populations[115,116].

Low-voltage ECG in right praecordial leads, and asymmetrical septal / ventricular wall thickening ("pseudohypertrophy" with sparkling apperance do to amyloid deposition in the extracellular matrix rather than muscle hypertrophy) with impaired diastolic relaxation and reduced global longitudinal strain, are consistent with ATTRv-CM[117]. Also, myocardial thichening along with late gadolinium enhancement are typically seen at cardiac magnetic resonance imaging[118].

Additionally, nuclear whole-body imaging with radiolabeled phosphonates such as diphosphono-1,2-propanodicarboxylic acid (DPD), hydroxymethylene diphosphonate (HMDP), or pyrophosphate (PYP) has been shown to be very sensitive in detecting cardicac involvement in ATTRv amyloidosis[119–122].

1.3.2.3 Leptomeningeal amyloidosis and other organ involvement

Leptomeningeal amyloidosis is a rare manifestation of ATTRv amyloidosis. It is most frequently associated to non-V30M (p.Val50Met) variants, including L12P (p.Leu32Pro), A25T (p.Ala45Thr), G53G (p.Gly73Glu), T114C (p.Tyr134Cys), A18G (p.Asp38Gly), and T69H (p.Tyr89His)[123]. However, also patients harboring V30M (p.Val50Met) variant may exhibit leptomeningeal involvement ~11 years after liver transplantation, due to ongoing production of variant TTR by the choroid plexus[124].

Amyloid tends to deposit in the media and adventitia of medium-size and small-size cortical arterioles and veins, along with veins in the subarachnoid space and leptomeninges. Ischemic stroke and intracerebral / subarachnoid hemorrhage causing headache, transient focal neurological deficits (i.e., amyloid spells), seizures, and cognitive impairment, are common manifestations[125].

Other organs can be involved in ATTRv amyloidosis. Renal disease, which leads to nephrotic syndrome and renal failure is encountered in approximately one third of Portuguese patients with V30M (p.Val50Met) variant, especially in late-onset cases[126,127]. Also, ocular involvement, manifesting as dry eyes and keratoconjunctivitis, vitreous opacity, cataract, secondary open-angle glaucoma, and retinal amyloid angiopathy may be present in up to 25% of patients harboring V30M (p.Val50Met) variant[128].

1.3.3 Genotype-phenotype correlation

The extent of PNS and cardiac involvement in ATTRv amyloidosis has led to the classification of phenotypes as neurological, cardiac, or mixed according to the clinical presentation. However, when the disease progresses, a combination of neuropathy and cardiomyopathy is usually seen.

These different phenotypes depend on both underlying causative variant and AOO. For example, as mentioned above the V122I (p.Val142Ile) and L111M (p.Leu131Met) variant typically present with a cardiac phenotype[129], while S50A (p.Ser70Arg) and A97S (p.Ala 117Ser) are typically neuropathic[130,131]. However, in two randomized clinical trials enrolling patients with different genotypes, an infiltrative cardiomyopathy (meaning a myocardial thickness >13mm) was present in up to 56-63% of cases[9,11].

Also, AOO affects the presenting phenotype regardless of the underlying mutation as occurs for ATTRv V30M (p.Val50Met) patients (early-onset *vs* late-onset phenotype, as mentioned above)[102].

The phenotypic spectrum of *TTR* variants is shown in **Fig**. **2**.

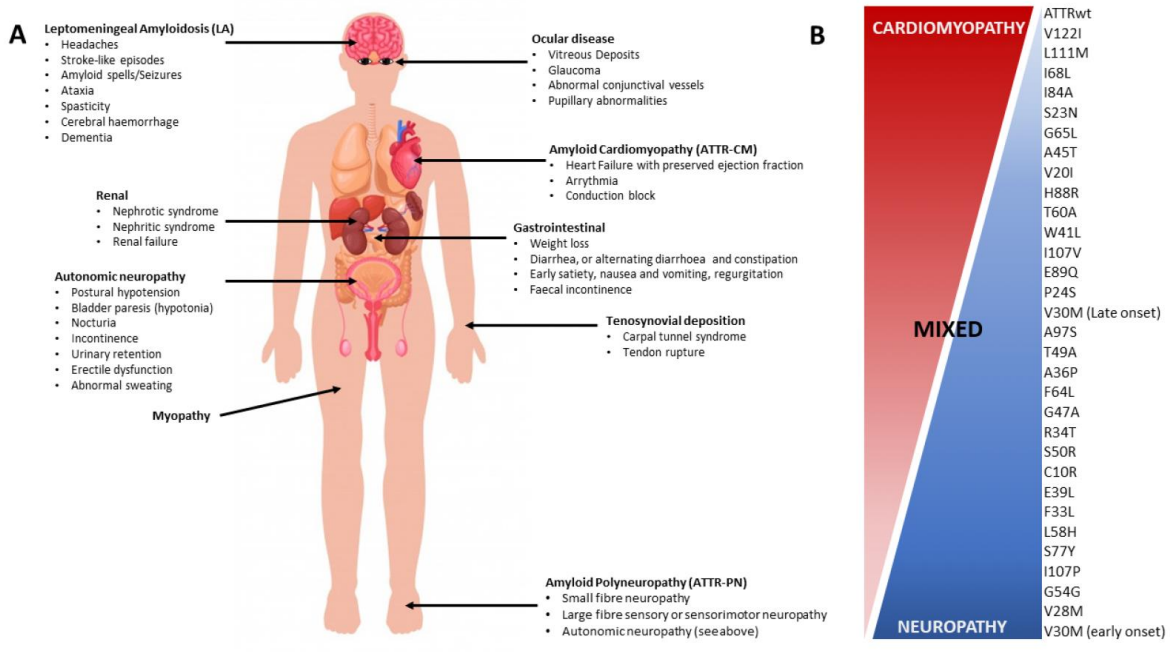

Fig. **2**. Clinical features (**A**) and genotype-phenotype correlations (**B**)[132].

1.4 Wild-type ATTR amyloidosis

ATTRwt, also known as senile systemic amyloidosis, is a common disease of ageing, which typically presents in the sixth-eighth decades with heart failure with preserved ejection fraction, as for ATTRv-CM, atrial fibrillation, and ventricular arrhythmias, occasionally requiring implantable devices[133].

At pathological level, between 10-25% of individuals aged over 80 years has wild-type amyloid deposition in the heart (myocardium), although this is not necessarily paralleled by clinical manifestations[134].

Carpal tunnel syndrome and spinal stenosis are common features, while neuropathy is typically absent[7,114].

1.5 Diagnosis and assessment

1.5.1 Suspicion index and red flags

The suspicion index of ATTRv amyloidosis is raised upon different clinical presentations and symptoms according to the area of origin. Indeed, in endemic foci, for patients with a known family history of ATTRv amyloidosis, any onset of length-dependent sensory axonal polyneuropathy, with a predominant impairment of temperature and pain sensation, or autonomic dysfunction, *plus* >=1 among unexplained weight loss, cardiac arrhythmia, vitreous opacity, or renal abnormalities should point to ATTRv amyloidosis (**Fig**. **3**)[135]. The diagnosis of ATTRv amyloidosis is usually made within 1 year of onset of symptoms since families in which ATTRv amyloidosis has been identified are regularly monitored in referral Centres.

Contrarily, in non-endemic areas, for patients without a family history of ATTRv amyloidosis, the disease should be considered if they present with progressive idiopathic, sensory-motor axonal polyneuropathy or atypical CIDP *plus* >=1 among bilateral carpal tunnel syndrome, autonomic dysfunction, gait disorders, or as for patients from endemic areas, unexplained weight loss, cardiac abnormalities (hypertrophy or rhythm disorders), vitreous opacity, or renal impairment (**Fig**. **3**)[135]. In these cases, the diagnosis can be delayed up to 4 years, due to different factors, among others the lack of family history[24,109,136], the

variable clinical presentation which can mimic other conditions, especially CIDP[109,110], a delay in diagnostic tests, and a negative result of biopsy testing[108,136,].

The diagnostic workup is showed in **Fig**. **4**.

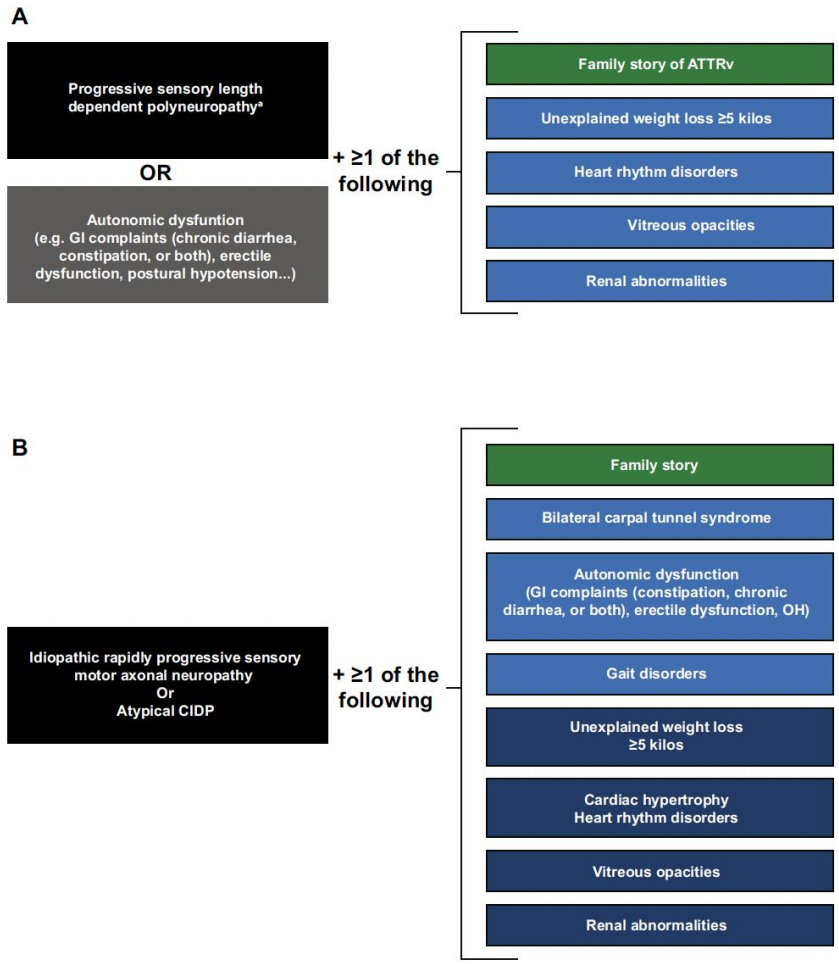

Fig. **3**. Suspicion index and red flags of ATTRv amyloidosis in endemic (**A**) and non-endemic (**B**) areas[135].

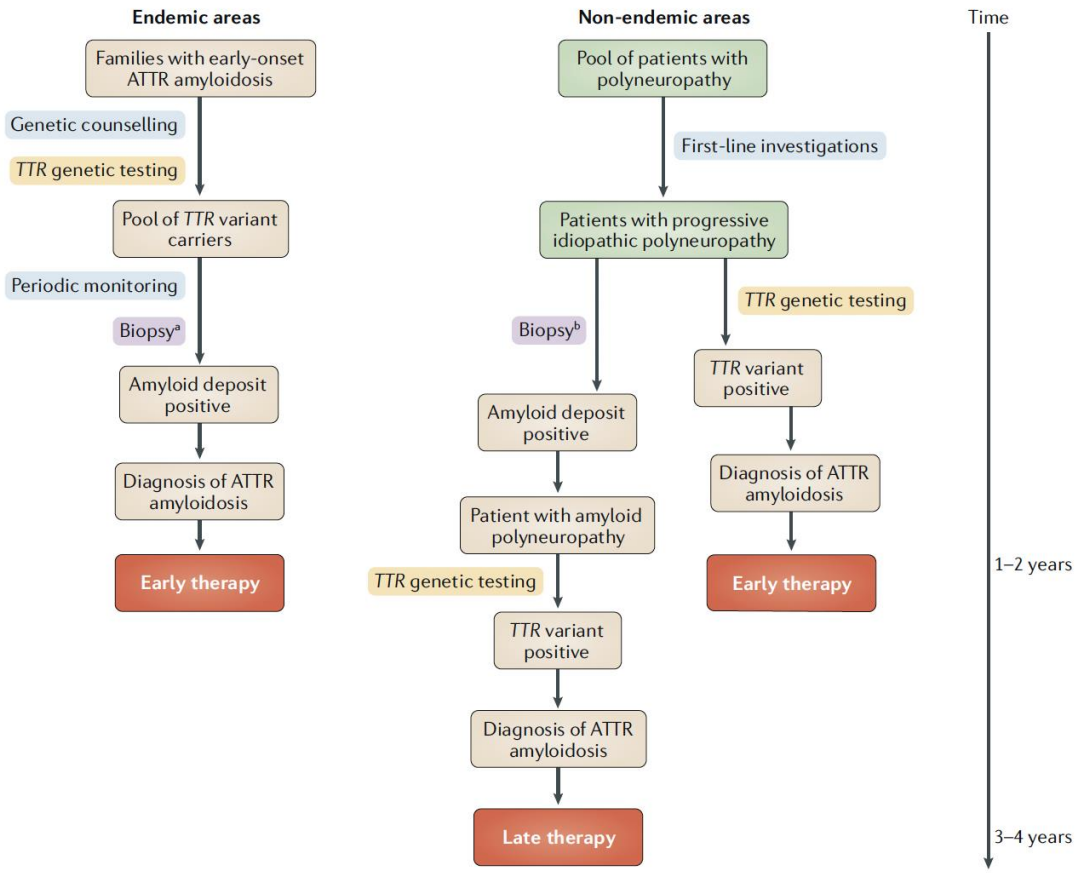

Fig. **4**. Diagnosis of ATTRv amyloidosis in endemic and non-endemic areas. [a]Biopsy of the labial salivary gland is proposed at symptom onset. [b]Biopsy of the labial salivary gland, nerve, or aspirated fat tissue. TTR: transthyretin[103].

1.5.2 Misdiagnosis

Misdiagnosis of ATTRv amyloidosis is fairly common as a consequence of both variable clinical presentation and electrodiagnostic findings.

Indeed, a proportion of patients between 32% and 74% has been misdiagnosed[24,109], while ~18% of patients have received multiple misdiagnoses[24,111]. As mentioned above, the most common misdiagnosis is CIDP, which can present with sensory-motor impairment with diffuse areflexia. Also, in ATTRv-PN CSF proteins can be raised up to 1g/ml, and electrodiagnostic findings can fulfill the European Federation of Neurological Sciences-Peripheral Nerve society criteria for CIDP in a significant proportion of cases (12.5-15%)[109,110]. Other possible misdiagnoses are lumbar spinal stenosis[24,109] and, although infrequently, motor neuron disease[112,113]. Most common misdiagnoses are detailed in **Fig**. **5**.

Phenotype	Genotypes	Misdiagnoses
Length-dependent small-fibre polyneuropathy and/or autonomic neuropathy	*TTR* Val30Met mutation (early-onset disease)	• Diabetic polyneuropathy • Fibromyalgia • Immunoglobulin light-chain amyloidosis • Chronic digestive disease
All-fibre polyneuropathy	*TTR* Val30Met mutation (late-onset disease) and other *TTR* variants	• CIDP • Idiopathic axonal polyneuropathy • Lumbar canal stenosis • Vasculitic peripheral neuropathy • Toxic peripheral neuropathy • Alcoholic neuropathy • Paraproteinaemic peripheral neuropathy
Upper-limb-onset polyneuropathy	*TTR* Val30Met mutation (43%) and other *TTR* variants (Phe64Leu, Ser77Tyr, Tyr78Phe and Ile107Val)	• Carpal tunnel syndrome • Idiopathic polyneuropathy • CIDP • Paraneoplastic neuropathy • Cervical radiculopathy
Motor neuropathy	*TTR* Val30Met, Phe64Leu, Ile68Leu, Tyr78Phe, Val93Met and Ile107Val	• ALS • Motor CIDP • Motor neuropathy • Motor neuron disease

Fig. **5**. Main misdiagnoses of ATTRv-PN[103].

1.5.3 Diagnostic and assessment tools

Diagnostic tools for ATTRv amyloidosis include: *TTR* gene sequencing looking for *TTR* amyloidogenic variants, and tools aimed at detecting amyloid deposits, i.e., biopsy and bone scintigraphy with DPD, HMDP, or PYP.

TTR gene, located on chromosome 18q11.2-12.1[26], is rather small, encompassing only four exons. To date over 150 mutations have been identified, the vast majority of which is pathogenic[4]. Sanger sequencing remains the gold standard for *TTR* gene sequencing, since it allows for the identification of rare and also unknown variants.

A *TTR* variant alone cannot confirm the diagnosis of ATTRv amyloidosis since the penetrance in carriers is incomplete. *TTR* gene sequencing can be used to support or exclude a diagnosis of ATTRv amyloidosis in patients with idiopathic neuropathy, and for predictive genetic counseling in at-risk individuals with a known family history of ATTRv amyloidosis.

To confirm the diagnosis of ATTRv amyloidosis, the presence of amyloid deposits in significant tissues should be determined. A biopsy of salivary glands, skin, or abdominal fat is usually performed, according to the Centre expertise, while other more invasive biopsies (i.e., nerve and myocardial biopsy) are typically avoided. For example, in Portugal and France a salivary gland biopsy is preferred, with a sensitivity which reaches 91% in V30M (p.Val50Met) carriers. Contrarily, in USA, UK, The Netherlands, Germany, and Sweden an

abdominal fat pad, which however harbors quite a variable sensitivity (14-83%) is usually performed[135]. Indeed, a negative biopsy result should not rule-out the diagnosis of ATTRv amyloidosis, if the suspicion index is high, since the sensitivity varies according to the tissue sample, the pathogenic mutation, the patient's age, and also relies on the expertise of the pathologist[137]. Apple-green or yellow birefringence of Congo red-stained biopsies under polarized light points to the presence of amyloid fibrils[103,135]. Proteomic analysis based on mass-spectrometry can be used to identify certain type of amyloid fibrils[138].

Bone scintigraphy with DPD, HMDP, or PYP could be useful in patients with neuropathy, hypertrophic cardiopathy, harboring a pathogenic *TTR* variant but with a negative tissue biopsy[119]. Also, a diagnosis of ATTRv amyloidosis can be made even without a tissue biopsy if bone scintigraphy abnormalities are graded 2 or 3 at Perugini score (i.e., uptake equal to/greater than bone uptake), and if echocardiographic/cardiac MRI criteria are met.

1.5.4 Assessment of neuropathy

The assessment of the somatic neuropathy includes nerve conduction studies[139] while for objective testing of autonomic neuropathy the measurement of heart rate variability during normal breathing, deep breathing, and during tilt from supine position to standing can be used[140]. Also, a reliable assessment of early autonomic dysfunction can be achieved through a sudomotor test called Sudoscan based on the measurement of electrochemical skin conductance in both hands and feet[141].

Useful clinical scales include polyneuropathy disability (PND) score[142] to assess the locomotion, the NIS[143], and the Compound Autonomic Dysfunction Test (CADT)[144].

Each PND score corresponds to a different stage of ATTRv polyneuropathy. Score I refers to the presence of only sensory disturbances with preserved walking capability; score II refers to a patient with impaired walking capability, although still able to walk without assistance; score IIIa indicates the need of one walking aid (stick or crutch); IIIb stands for the need of two walking aids (stick or crutch); score IV refers to a wheelchair-bound or bedridden patient[142].

NIS along with its subset, NIS-lower limb (NIS-LL), is a clinical scale which was first designed to grade the neurological impairment in diabetic neuropathy. It encompasses a composite evaluation of sensory disturbances, motor impairment, and four limb-deep tendon

reflexes, with a greater emphasis on weakness. The total score is graded on a scale which ranges from 0 (no neurological impairment) to 244 (greatest neurological impairment). NIS-LL is a subset of NIS items specific to neuropathy in the lower-limbs. Its score ranges from 0 to 88, with higher scores indicating greater impairment[143].

The use of these scales will be further deepened in the section entitled "*Assessment in clinical trials*".

1.5.5 Assessment of cardiomyopathy

Cardiac assessment is aimed at revealing the presence of both heart conduction defects and infiltrative cardiomyopathy.

Electrocardiogram, 24-hour electrocardiogram Holter monitoring, intracardiac electrophysiological studies, or implantation of prophylactic pacemaker can be used to detect conduction and/or bundle branch block, or other cardiac arrhythmias.

Echocardiography with strain imaging[117], cardiac MRI[118], and bone scintigraphy with DPD, HMDP, or PYP[119–122] can be used to detect the cardiac involvement. The detection of cardiac uptake of DPD or PYP is highly sensitive and specific for the diagnosis of cardiac amyloidosis, with a positive predictive value (>99%) when there is no concurrent monoclonal gammopathy, and therefore can be used as an equivalent of a positive biopsy[119].

The use of the New York Heart Association (NYHA) classification in ATTRv amyloidosis is questionable since it harbors a high inter-operator variability and it is also not reliable because of the concurrent physical limitations due to the underlying neuropathy[145].

Plasma biomarkers as the amino-terminal prohormone of brain natriuretic peptide (NT-proBNP) and troponin have a prognostic value in ATTRv-CM[146]. A new staging system based on cut points of NT-proBNP and estimated glomerular filtration rate (eGFR) has also been proposed[147].

1.5.6 Other assessments

Ocular investigations should include Shirmer test, assessment of visual acuity and intraocular pressure, slit lamp, and fundus examination. Also, kidney function has to be assessed by measuring proteinuria, microalbuminuria, and eGFR[148]. The nutritional status can be evaluated by a modified body mass index (mBMI, kg/m^2 x albumin - g/l)[142].

1.5.7 Assessment in clinical trials

To date, most outcome measures used in ATTRv-PN are based on clinical examination and functional impairment. In particular, NIS, along with its subset NIS-LL, which was first designed to grade neurological impairment in diabetic neuropathy as previously mentioned, has become the most used outcome measure in different clinical trials and observational studies in ATTRv amyloidosis[149,150,151].

To better capture the multisystem involvement in ATTRv amyloidosis, two other scales have been adopted. The NIS + 7 scale combined the NIS with seven additional assessments to better characterize and quantify the neuropathic impairment. Five out of these seven items are nerve conduction study parameters focused on three nerves in the lower limbs (i.e., peroneal, tibial, and sural nerves), while the other two encompasses a vibration detection threshold, a sensory measure taken at the great toe, and heart rate response to deep breathing, which are meant to capture the extent of autonomic dysfunction. This scale ranges from 0 (no neurological deficits) to 270 (no detectable peripheral nerve function)[149,152].

More recently, NIS + 7 has been further modified (i.e., mNIS + 7) to better quantify both the sensation over the whole body (rather than the distal sites) and the autonomic function. Two different versions have been developed, one by Ionis (mNIS + 7 $_{Ionis}$, 0-346.3)[152,153] and the other one by Alnylam (mNIS + 7 $_{Alnylam}$, 0-340)[154]. Both tools introduce the smart somatotopic quantitative sensation testing, but whereas mNIS + $7_{Alnylam}$ uses only this assessment to quantify the sensory loss, mNIS + 7_{Ionis} still retains the vibration detection threshold.

Finally, the mNIS + $7_{Alnylam}$ uses an alternative measure of autonomic dysfunction (postural hypotension), whilst mNIS + 7_{Ionis} maintains the heart rate response to deep breathing.

The differing components of the NIS + 7, mNIS + $7_{Alnylam}$, and mNIS + 7_{Ionis} are shown and described in more detail in **Fig**. **6**.

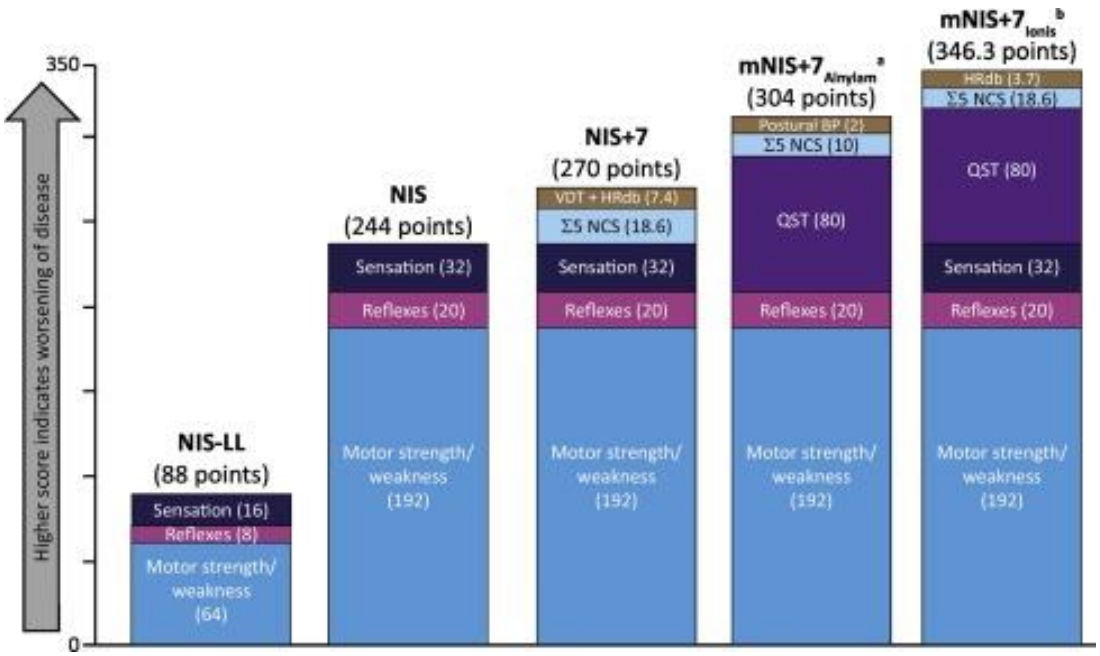

Fig. **6**. Composition and scores of NIS and other NIS-based scales. *BP* blood pressure, *HRdb* heart rate with deep breathing, *mNIS + 7* modified Neuropathy Impairment Score + 7, *NCS* nerve conduction studies, *NIS* Neuropathy Impairment Score, *NIS + 7* Neuropathy Impairment Score + 7, *QST* quantitative sensation testing, *VDT* vibration detection threshold[155].

Other clinical scales include the Composite Autonomic Symptom Score 31 (COMPASS-31) questionnaire for assessment of autonomic symptoms, the Rasch-built Overall Disability Scale (R-ODS) survey for assessment of activities of daily living[156], the Norfolk Quality of Life- Diabetic Neuropathy (QoL- DN) questionnaire to measure quality of life[157], and the timed 10-minute walk test and handgrip strength test (dynamometer) to assess motor function[152].

Six-minute walking test, echocardiogram parameters, troponin I, and NT-proBNP are used to assess cardiac function while proteinuria and eGFR can quantify kidney impairment.

1.6 Novel diagnostic and prognostic biomarkers

1.6.1 Plasma neurofilaments, neurophysiology, and nerve MRI

Plasma neurofilament light chain (NfL), which can reflect axonal damage/degeneration, has proved as an effective biomarker in ATTRv amyloidosis since their levels are significantly raised in ATTRv-PN compared to controls, and correlate with disease severity[158–160]. Also, NfL can distinguish presymptomatic V30M and non-V30M (p.Val50Met) carriers from symptomatic patients[159,161], and the reduction of their levels after therapy (gene silencing, *see further*) parallels the improvement of NIS[158].

Also, some neurophysiological parameters have been investigated in ATTRv amyloidosis as promising prognostic tools. Indeed, the dorsal sural nerve amplitude seems to be an early marker of nerve damage in ATTRv presymptomatic carriers[162]. Moreover, the cutaneous silent period, a nociceptive reflex mostly mediated by the A-delta afferent fibres, could be used to easily assess the small fibres, which seem to be involved also in ATTRv late-onset cases, since its latency was found to be slightly but significantly prolonged in ATTRv presymptomatic patients[163].

Also, nerve MRI has been studied in ATTRv amyloidosis as a possible diagnostic and prognostic biomarker. Indeed, the early and objective recognition and localization of nerve injury had proven challenging so far.

MRI neurography of sciatic and sural nerve, which provides high spatial resolution and large anatomical coverage, was shown to be able to detect *in vivo* nerve lesions in ATTRv amyloidosis, which occurred in a non-diffuse pattern, with a clear focus at the tight level, where nerve injury was greater, although symptoms in ATTRv amyloidosis typically start and prevail distally. Indeed, both ATTRv symptomatic patients and asymptomatic carriers (carrying V30M, p.Val50Met; or L58H, p.Leu78His; or T69H, p.Tyr89His mutations) showed a strong increase in proton spin density (p), while a significant increase in apparent T_2 relaxation time (T_{2app}) was found only in ATTRv symptomatic patients.

Therefore, MRI neurography can accurately distinguish patients with ATTRv amyloidosis from healthy controls. Also, more importantly, it can detect early and even subclinical nerve lesions in asymptomatic carriers, as shown by p increase, which points toward a change in the macromolecular organization of the extracellular compartment, possibly due to the endoneurial deposit of mutant TTR[164,165].

However, the underlying macromolecular alterations leading to the observed increase of p (as well as of T_{2app}) remain mostly unclear. Magnetization transfer contrast imaging is an MRI technique that is sensitive to protons bound to macromolecular structures, such as myelin lipids or collagen. Magnetization transfer ratio (MTR) of the sciatic nerve, which reflects myelin integrity, was highest in healthy controls, decreased in asymptomatic carriers, and decreased even more in patients with manifest ATTRv polyneuropathy, independent of the underlying *TTR* gene mutation. Then, MTR showed promising results as it differentiated both symptomatic ATTRv patients and asymptomatic carriers from healthy controls and correlated with disease severity (NIS-LL) and electrophysiological parameters[166].

In conclusion, the *in vivo* detection, localization, and quantification of nerve injury in ATTRv amyloidosis might improve early diagnosis and initiation of disease modifying therapies. Also, it might help unravelling novel biomarkers for early monitoring of microstructural nerve injury, which would allow for the development of future therapeutic strategies.

1.7 Disease modifying therapies

The management of ATTRv amyloidosis requires a multidisciplinary approach. Care includes symptomatic treatment and strategies aimed at: 1) lowering TTR production, 2) stabilizing of TTR tetramers, and 3) reducing TTR deposits.

1.7.1 Liver transplantation

Orthotopic liver transplantation (LT) is known to be an effective treatment for ATTRv amyloidosis since it causes prompt replacement of variant TTR by the donor wild-type TTR in the plasma[167]. Also, histopathological examination of abdominal fat tissues demonstrated a significant decrease or disappearance of amyloid deposits with a raised contribution of wild-type TTR to the composition ratio in amyloid fibrils after liver transplantation[168].

LT is associated with an improvement or stabilization of the peripheral neuropathy with greater effects on V30M (p.Val50Met) ATTRv-PN. The overall survival rate varies between 85% and 73% at 5 and 10 years of follow-up, respectively[167,169,170].

Although widely accepted, this therapeutic approach has some limitations including shortage of donors, procedure-related morbidity, and mortality (~10%), and long-term immunosuppression. To overcome organ shortage, domino-liver transplantation in which a liver of a patient affected by ATTRv amyloidosis is transplanted into another patient, was previously adopted. However, unfortunately recipients developed polyneuropathy about 10 years after the procedure[171]. Also, some patients developed oculoleptomeningeal disease due to ongoing mutant TTR production by the choroid plexus and retinal pigment cells, which was not prevented by LT[172].

LT is then considered a 2nd line treatment option for those patients who are refractory or intolerant to other pharmacological treatments, of for which no other treatment option is currently available.

1.7.2 TTR tetramer stabilizers

Diflunisal (Dolobid, Merck&Co) is an oral non-steroidal anti-inflammatory drug which acts as TTR stabilizer, preventing it from dissociation, by binding to the T4 binding site of TTR protein[173]. A randomized, placebo-controlled, double-blind, multicentre, international study showed efficacy of diflunisal (250 mg two times/day) in ATTRv-PN (late-onset V30M, p.Val50Met and other mutations) with slowing of disease progression (NIS and NIS+7) at 2-year-follow-up by 60% and improvement of quality of life (36-Item Short-Form Health Survey [SF-36])[149].

However, 52% of patients discontinued the treatment because of disease progression and liver transplantation. Also, significant side effects, including gastrointestinal symptoms and renal impairment were reported[174]. Indeed, rapid disease progression of late-onset ATTRv amyloidosis could not be halted by the TTR stabilizer over 2 years of follow-up[149].

Tafamidis (Vyndaqel, Pfizer) is an oral TTR stabilizer which binds to the T4 binding site of both wild-type and variant TTR, preventing its dissociation[175]. In a first multicentre, placebo-controlled, phase III clinical trial including early-onset V30M (p.Val50Met) ATTRv patients, mostly of Portuguese origin, no neuropathy progression (NIS and NIS-LL) was seen in 60% of patients who received tafamidis (20 mg/day) *vs* 38% of patients who received placebo. Also, a greater increase in quality of life (Norfolk QoL–DN) was detected in the tafamidis group[176].

The short- and long-term efficacy of tafamidis has been further evaluated in late-onset V30M (p.Val50Met) ATTRv patients and ATTRv patients harboring different pathogenic variants. Tafamidis did not prevent progression of disability by 43-55% after 1-year-follow-up[151,177,178].

The European Medicine Agency (EMA) approved tafamidis in 2011 for stage 1 ATTRv-PN, although 30%-40% of the patients were considered non-responders[179]. More recently, in 2019, tafamidis (Vyndamax, 61 mg/day in free acid, equivalent to the 80 mg dosage administered in the study) has also been approved by Food & Drug Administration (FDA) (and later on by both EMA and Italian Medicines Agency [AIFA]) for the treatment of ATTRv- and ATTRwt-related cardiomyopathy[180].

Acoramidis (AG10/ALXN2060, Eldos Therapeutics, 800 mg/twice a day), which binds to TTR tetramer more selectively than diflunisal and tafamidis[181], is under investigation in phase III Eldos AG10 study (ATTRIBUTE-CM-NCT03860935) for patients with ATTRv- and ATTRwt-related cardiomyopathy[182].

1.7.3 TTR fibril removal

Doxycycline (100 mg twice/day), which prevents the formation of amyloid fibrils *plus tauroursodeoxycholic acid* (Doxy-TUDCA, 250 mg three times/day), a biliary acid which reduces the aggregation of non-fibrillary TTR, has been reported to stabilize both neurological and cardiac function (NIS-LL and Kumamoto score) over 12 month-follow-up in a phase II, open-label study, with an acceptable toxicity profile[183].

The monoclonal antibody *dezamizumab* targeting the amyloid serum component (SAP), which is known to contribute to the stability of amyloid aggregates, has not shown reduction of the amount of cardiac amyloid, and is currently no longer under study, even due to an unfavourable risk/benefit ratio[184].

However, there are currently two other monoclonal antibodies under investigation for the removal of amyloid fibrils from tissues: *NI006* (Neuroimmune; CPHPC) and *NN6019-0001* (formerly known as *PRX004*)[184].

1.7.4 Gene therapy

Gene silencing therapies using antisense oligonucleotides (ASOs) or small-interfering RNAs (siRNAs) have emerged as safe and effective strategies for treating ATTRv and ATTRwt amyloidosis.

Inotersen (Tegsedi, Alkcea Therapeutics) is a short ASO complementary to the target mRNA, able to prevent RNA translation and protein expression. A phase III study (NEURO-TTR) has established efficacy of inotersen (300 mg/week, administered subcutaneously), measured by reduced decline in mNIS+7 and Norfolk QOL-DN, in adult-onset ATTRv patients with stage I and II ATTRv-PN. Effectiveness was found to be independent of type of pathogenic variant, disease stage, and presence of cardiomyopathy. Thrombocytopenia and glomerulonephritis were evident in 3% of patients[11]. Inotersen is currently approved for the treatment of stage I and II ATTRv-PN.

To improve its safety profile, inotersen has been ligand-conjugated to allow for receptor-mediated uptake by hepatocytes. A phase I study (NCT03728634) has showed improved potency and safety of *eplontersen* (AKCEA-TTR- LRx), with no reported serious adverse events[185]. In phase III NEURO-TTRansform (NCT04136184, Ionis Pharmaceutical, AstraZeneca) eplontersen showed significantly lowered serum transthyretin concentration, less neuropathy impairment measured by mNIS+7, and better quality of life (Norfolk QOL-DN) compared with a historical placebo[186]. Also phase III study to evaluate safety and efficacy of eplontersen is underway in ATTR-CM (CARDIO-TTRansform, NCT04136171, Ionis Pharmaceutical, AstraZeneca)[187].

SiRNA drugs are a class of small non-coding 21-23 nucleotide long double-stranded RNA molecules that target and cleave complementary mRNA, leading to “knockdown” of target gene expression.

Patisiran (Onpattro, Alnylam Pharmaceuticals) is a TTR-specific siRNA which targets the 3’ untranslated region of TTR mRNA. A phase III study (APOLLO) has shown efficacy of patisiran (0.3 mg/kg administered intravenously, three times/week) measured by improvement in mNIS+7, in ATTRv-PN. Patisiran was generally safe with only mild to moderate infusion-related reactions reported[9], although premedication with cortisone and antihistamines to limit infusion-related allergic reactions is required. Patisiran is currently approved for the treatment of stage I and II ATTRv-PN.

Patisiran has also been reported as effective in improving functional capacity, as measured by the 6 minute walking test and quality of life, in patients affected by either ATTRv- and ATTRwt-related cardiomyopathy staged NYHA Class I-III (APOLLO-B, NCT03997383)[188] (results presented at XVIII International Symposium on Amyloidosis (Heidelberg, Germany, September 2022).

Vutrisiran (Amvuttra, Alnylam Pharmaceuticals) is a second-generation siRNA that, compared to patisiran, has a higher affinity for hepatocytes due to conjugation with *N*-acetyl galactosamine, and does not require any premedication since lipid nanoparticles are absent. It targets a highly conserved mRNA sequence across all known TTR variants, including wild-type TTR. In the phase III, global, open-label study HELIOS-A vutrisiran (25 mg every three months) has shown a significant improve in mNIS+7 in ATTRv-PN[10]. Vutrisiran is currently approved for the treatment of stage I and II ATTRv-PN.

The efficacy of vutrisiran is currently under investigation in patients affected by either ATTRv- and ATTRwt-related cardiomyopathy staged NYHA Class I-III (HELIOS-B, NCT04153149)[189].

The use of clustered, regularly interspaced short palindromic repeats and associated Cas9 endonuclease (CRISPR-Cas9) is an alternative strategy to achieve *in vivo* gene editing, thus aimed at modifying or repairing a specific point of a target DNA using a guide RNA. Since ATTRv amyloidosis is a monogenic disorder and the knockdown of *TTR* has limited physiological effects, this disease seems to be a perfect candidate for CRISPR-Cas9 gene editing.

NTLA-2001 consists of a single-guide RNA targeting human *TTR* with a human codon-optimized mRNA sequence of Streptococcus pyogenes (Spy)-Cas9 protein. In a small cohort of patients affected by ATTRv-PN, administration of NTLA-2001 led to a dose-dependent decrease of TTR protein concentration in serum through targeted knockout of *TTR*, with only mild infusion-related adverse events[12].

The whole landscape of available treatments for ATTRv and ATTRwt amyloidosis is summarized in **Fig**. **7**.

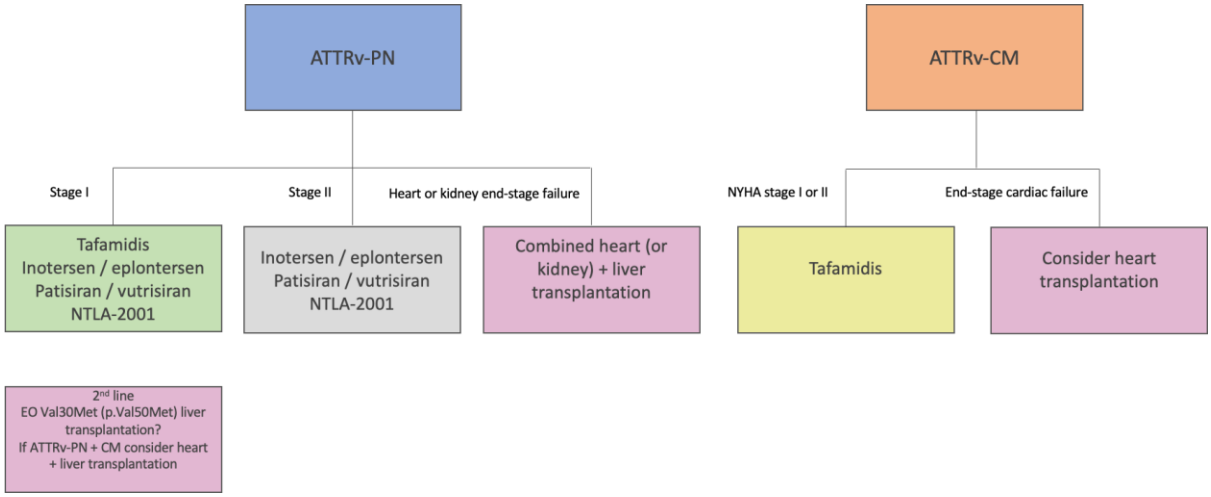

Fig. **7**. Decision tree in ATTRv-PN and CM. ATTRv: hereditary transthyretin amyloidosis; EO: early-onset; CM: cardiomyopathy; NYHA: New York Heart Association; PN: polyneuropathy. Adapted from Adams et al, *Current Opinion in Neurology*, 2020[190].

2. Muscle quantitative magnetic resonance imaging (MRI) as a novel outcome measure in hereditary transthyretin amyloidosis with polyneuropathy

2.1 Study rationale

ATTRv is a progressive, disabling, and life-threatening condition with a mean survival of 7-10 years if left untreated[6–8]. The increasing availability of disease modifying therapies, including the TTR stabilizer tafamidis, and, more recently, the RNAi agent patisiran, the antisense oligonucleotide inotersen[9,11], together with other treatment options underway[12], has deeply changed the natural history of ATTRv amyloidosis from an invariably lethal to a treatable condition. There is compelling evidence that all these therapies are more effective if started early in the disease course.

Unfortunately, the definition of disease onset is often cumbersome and we still lack effective biomarkers to define and predict it, to track disease progression, and to monitor treatment efficacy.

Similarly to other neuromuscular disorders, the identification of sensitive and responsive outcome measures has always proven challenging in ATTRv amyloidosis. To date, clinically-based scales as NIS and NIS-LL[149–151], NIS+7[149,152], and mNIS+7[152–154] have been used in clinical trials to assess progression and treatment response, however all of them have limitations including inter-rater variability[9,191,192] and their dependence on patient's motivation.

Muscle quantitative MRI (qMRI) has been extensively used as an outcome measure in muscle diseases[193–196]. In particular, in Duchenne muscular dystrophy, both fat substitution (fat fraction, FF) and water T2 content provided sensitive noninvasive measures of disease progression across different muscles over time and response to corticosteroid treatment[193].

Also, in motoneuron diseases (amyotrophic lateral sclerosis, ALS and spinal bulbar muscular atrophy, SBMA) qMRI revealed significant fat substitution compared to controls, which correlated with clinical measures, and identified distinct patterns of muscle involvement[197]. Moreover, STIR and relative T2-weighted signal turned out as objective surrogate markers of muscle denervation, and significantly increased over 12 months[198].

More recently, the quantification of intramuscular fat (FF), which indirectly reflects axonal degeneration, showed high responsiveness to change over 12 months in patients with

genetic neuropathies including Charcot-Marie Tooth 1A (CMT1A)[199], and hereditary sensory neuropathy type 1 due to SPTLC1 and SPTLC2 mutations[200]. Also, in both CMT1A and hereditary neuropathy with liability to pressure palsies (HNPP), FF showed a proximal-to-distal gradient consistent with a length-dependent axonal loss[201,202], with a prominent involvement of the antero-lateral compartment of the calf and a higher responsiveness in case of calf FF>10% in CMT1A[201].

The role of muscle qMRI as possible outcome measure has not been investigated in ATTRv amyloidosis so far.

2.2 Aim

To assess in a cross-sectional study the role of qMRI of skeletal muscle as an outcome measure in ATTRv-PN and compare it with previously validated and functionally relevant clinical outcomes (PND score, NIS, and NIS-LL).

2.3 Material and methods

2.3.1 Study design and patient recruitment

We performed a prospective cross-sectional study assessing muscle qMRI of the lower limbs in symptomatic patients diagnosed with ATTRv-PN (n=24) who were enrolled among those who attended the Amyloidosis Research and Treatment Centre (IRCCS Fondazione Policlinico S. Matteo) in Pavia (Italy) between September 2017 and August 2018.

ATTRv-PN patients were defined as symptomatic when PND scored[163] >=1. Healthy controls (HCs), group-matched for age and sex, were also enrolled (n=12). Exclusion criteria for all participants were pregnancy and safety-related MRI contraindications.

2.3.2 Data acquisition: clinical and functional testing and electrophysiological revision

All patients underwent detailed assessment including demographic records, past medical history, and full neurological examination. Patients were rated using PND scoring system[163], NIS, and NIS-LL[149–151]. PND score was graded as follows: PND=1 (sensory disturbances with preserved walking capability), PND=2 (sensory-motor symptoms with unassisted gait), PND=3 (sensory-motor symptoms with assisted gait), and PND=4 (wheelchair-bound or bedridden). In a subset of n=17 patients who underwent nerve conduction studies (NCSs) at the same time from MRI, compound muscle action potential (CMAP) of peroneal and tibial nerve, and sensory nerve action potential (SNAP) of sural nerve, measured form peak to peak, were reviewed in detail and considered for further analysis. For each patient the most affected side was considered unless the asymmetry was due to other conditions (e.g., radiculopathy).

2.3.3 Magnetic resonance imaging

Muscle MRI was performed at Mondino Foundation IRCCS. Participants were examined on a 3T scanner (MAGNETOM Skyra, Siemens, Erlangen, Germany) lying supine and feet-first. The acquisition protocol included calf- and thigh-level centered T1-weigthed, short tau inversion recovery (STIR), a 2D multi-echo T2-weighted spin-echo (SE) (ME-SE) (number

of echoes 17, number of slices 7, repetition time (TR) 4,100 ms, first echo time (TE) and echo spacing 10.9 ms, bandwidth 250 Hz/px, matrix size 192 × 384, resolution 1.2 × 1.2 mm2, slice thickness 10 mm, gap between slices 30 mm), and a 3D gradient-echo (ME-GRE) (number of echoes 6, TR 35 ms, first TE/echo spacing 1.7/1.5 ms, flip angle 7°, bandwidth 1,050 Hz/px, matrix size 396 × 432 × 52, resolution 1.0 × 1.0 × 5.0 mm3). The sequence had a monopolar readout with interleaved echo spacing (even and odd echoes acquired in subsequent repetitions). Imaging of thigh and calf took approximately 35 and 25 minutes, respectively.

2.3.4 MRI data analysis: quantitative muscle MRI

A single observer with a 5-year training expertise and blinded to study groups outlined for each participant regions of interest (ROIs) on the 1st echo of the ME-SE sequence at mid-thigh (12 muscles) and mid-calf level (6 muscles) using ITK-SNAP software[203]. ROIs were then transferred to the 1st echo of the ME-GRE acquisition and manually adjusted to ensure proper alignment. All ROIs were verified by two expert neuroradiologists with more than 5-year expertise in neuromuscular imaging.

The ME-SE sequence was processed using a bi-component extended phase graph algorithm, implemented in Python, for quantification of water T2 (wT2)[204,205], using an open-source toolbox[206]. The Fatty Riot algorithm was used offline for the calculation of fat/water images from the ME-GRE acquisition[207,208], and then FF maps were obtained (FF= F/F+W*100%) from each ROI. Average values of FF and wT2 were calculated for the global ROI and for each muscle at thigh and calf level.

Fig. **8** shows the muscles of the lower limbs which have been assessed. The tibialis posterior (TP) was not evaluated according to the poor quality of visualization at calf MRI.

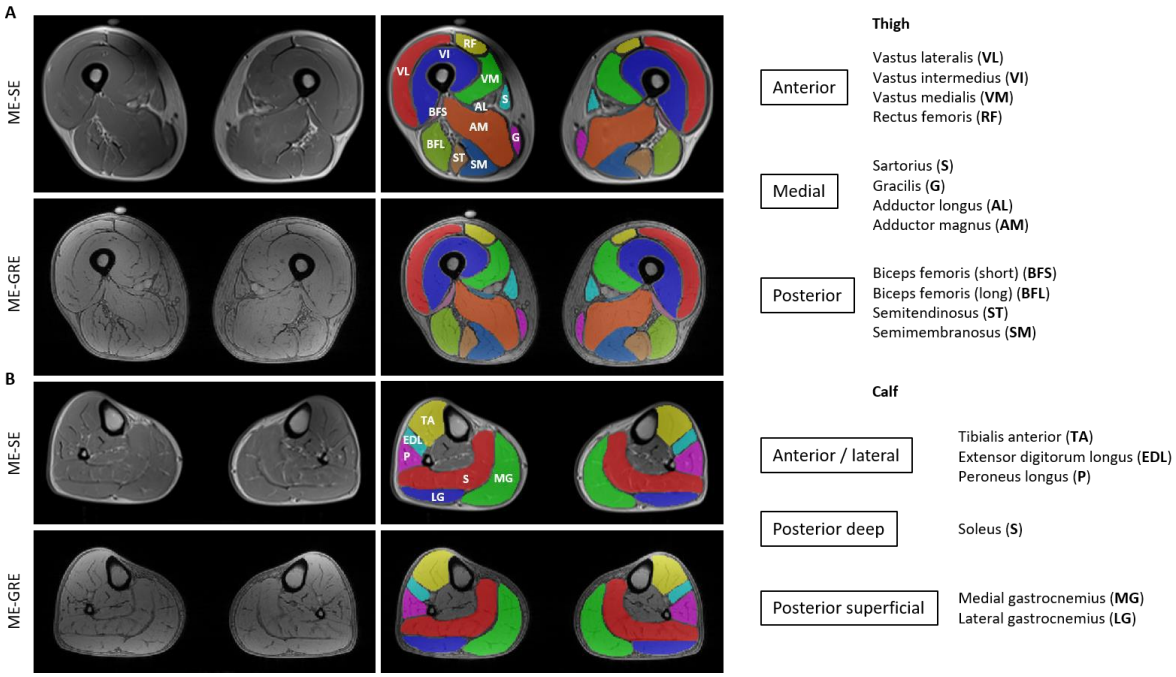

Fig. **8**. Thigh and calf single muscle ROIs and compartments**.** Thigh (A) and calf (B) single muscle ROI of a healthy control superimposed on ME-SE sequence (1st echo) to extract water T2 values and on ME-GRE sequence (1st echo) to obtain fat fraction (FF) maps. Thigh and calf compartments are reported on the right.

2.3.5 Statistical analysis

Statistical analyses were performed with SPSS version 22 (SPSS, Armonk, NY) with a significance α level of 0.05. Quantitative measures are reported as mean ± standard deviation (SD) or median and interquartile range (IQR) as appropriate according to their distribution. For intergroup comparisons 2-sample t-test and Mann-Whitney U test were applied as appropriate. Correlations of MRI parameters with clinical and electrophysiological measures were investigated with Spearman (ρ) or Pearson coefficients as appropriate according to data distribution. Graphics were obtained using Prism-GraphPad version 9.2.0 (332).

2.4 Results

2.4.1 Participant clinical and demographic records

We enrolled patients with ATTRv-PN (n=24) and healthy controls, group-matched for age and sex (n=12). Seventeen/24 (71%) patients were males, median age at enrollment was 63.5 years (range 42-77), and median disease duration was 5 years (range 4-11).

TTR mutations were: V30M (n=6, 25%), F64L (n=5, 21%), E89Q (n=3, 13%), Y78F (n=3, 13%), T49A (n=2, 8%), A109S (n=2, 8%), I68L (n=1, 4%), S77T (n=1, 4%), A49M (n=1, 4%).

The distribution of PND score was the following: PND=1 (n=11, 46%), PND=2 (n=9, 37.5%), PND=3 (n=3, 12.5%) and PND=4 (n=1, 4%). Median NIS total and NIS-LL were 25.5 (range 0-170.5) and 14.5 (range 0-88), respectively. Twenty-one/24 (87.5%) were on treatment including tafamidis (n=15, 71%), diflunisal (n=3, 14%), patisiran (n=2, 10%), and inotersen (n=1, 5%). Seventeen/24 (71%) agreed also to undergo NCS evaluation.

Nine/12 (75%) HCs were males and median age at enrollment was 59 years (range 46-68). Demographic and clinical data of the participants are summarized in **Table 1** and **2**.

Demographics and clinical measures	**ATTRv patients (n=24)**	**Control group (n=12)**	***p* Value**
Sex, M/F	17/7	9/3	0.80
Age, y	63.5 (42-77)	59 (46-68)	0.14
Median disease duration (range), y	5 (4-11)	NA	
Treatment, N/tot	21/24	NA	
Tafamidis	15/24		
Diflunisal	3/24		
Inotersen	2/24		
Patisiran	1/24		
Mutation		NA	
V30M	6/24		
F64L	5/24		
E89Q	3/24		
Y78F	3/24		
T49A	2/24		
A109S	2/24		
I68L	1/24		
S77T	1/24		
A49M	1/24		
PND score		NA	
0	NA		
1-2	20/24		
3-4	4/24		
Median NIS (range)	25.5 (0-170.5)	NA	
Median NIS-LL (range)	14.5 (0-80)	NA	

Table 1. Demographic and clinical data of ATTRv patients and healthy controls.

ATTRv patient	Age, y/sex	Mutation	Disease duration, y	Treatment	PND score	NIS	NIS-LL
01	77/M	F64L	5	Diflunisal	4	170.5	80
02	58/F	E89Q	7	Tafamidis	2	5	5
03	57/M	V30M	10	-	1	14	6
04	68/M	A109S	11	Inotersen	3	170	72
05	71/M	Y78F	3	Tafamidis	1	14	7
06	71/M	I68L	3	Tafamidis	1	6	6
07	57/M	F64L	3	Tafamidis	2	58	29
08	73/F	S77T	5	Tafamidis	2	30	20
09	55/M	E89Q	6	Inotersen	2	37	20
10	46/M	A49M	4	Tafamidis	2	24	14
11	62/F	Y78F	8	Tafamidis	1	6	4
12	68/M	Y78F	8	Tafamidis	1	27	15
13	63/M	V30M	4	Tafamidis	2	36	20
14	64/M	V30M	4	Tafamidis	1	4	2
15	64/F	F64L	7	Tafamidis	1	10	8
16	61/M	V30M	4	Tafamidis	1	13	8
17	42/F	V30M	9	-	1	0	0
18	65/M	F64L	2	Tafamidis	2	42.75	20.75
19	75/M	A109S	8	Patisiran	2	60	37
20	45/M	T49A	11	Diflunisal	3	103.75	62.25
21	49/F	T49A	5	Tafamidis	2	34	24
22	72/M	F64L	4	-	1	16	10
23	60/F	E89Q	3	Tafamidis	1	4	2
24	69/M	V30M	4	Diflunisal	3	98.5	55.5

Table 2. Clinical data of ATTRv patients.

2.4.2 Muscle fat fraction and water T2 distinguish patients with hereditary transthyretin amyloidosis from healthy controls

We found that FF was significantly higher in ATTRv patients compared to healthy controls at thigh (ATTRv *vs* controls: median 9.8%, IQR 7.3% *vs* median 6.5%, IQR 2.5%; p=0.002) and calf level (ATTRv *vs* controls: median 9.9%, IQR 6% *vs* median 7.1%, IQR 3.1%; p=0.017).

Similarly, wT2 was significantly higher in ATTRv patients compared to healthy controls, both in the thighs (ATTRv *vs* controls: median 44.8 ms, IQR 5.6 ms *vs* median 40.8 ms, IQR 1.8 ms; p=0.000) and in the calves (ATTRv *vs* controls: median 47.2 ms, IQR 12.2 ms *vs* median 42 ms, IQR 2.7 ms; p=0.000) (**Table 3**) (**Fig**. **9**).

No significant difference was seen between patients carrying V30M (p.Val50Met) and other mutations (*data not shown*).

Quantitative imaging measures	**ATTRv patients (n=24)**	**Healthy controls (n=12)**	***p* Value**
MRI, thigh level			
FF, %	9.8 (4.1-31.3)	6.5 (4.2-9.0)	0.002
wT2, ms	44.8 (39.7-64.6)	40.8 (39.0-42.8)	<0.001
MRI, calf level			
FF, %	9.9 (4.0-42.8)	7.1 (4.1-11.5)	0.017
wT2, ms	47.2 (39.7-75.2)	42.0 (39.6-44.8)	<0.001

Data presented as median (range) as appropriate to distribution; p values calculated with Mann-Whitney U test

Table 3. Fat fraction and water T2 of ATTRv patients and healthy controls.

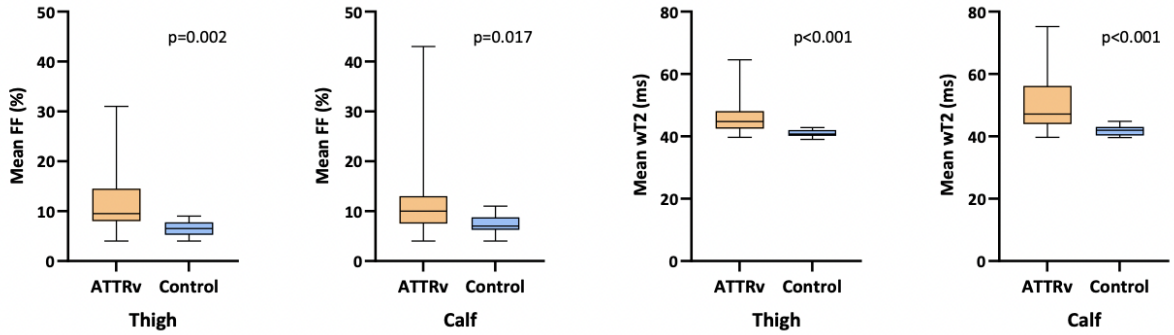

Fig. 9. Quantitative muscle MRI imaging: thigh and calf compartments in ATTRv patients and healthy controls**.** Overall thigh and calf fat fraction (FF) and water T2 (wT2) are significantly higher in ATTRv compared to healthy controls. Boxes represent median and IQR and whiskers show range.

2.4.3 Quantitative MRI parameters correlate with clinical outcomes

We next assessed the role of qMRI as a biomarker of disease severity by looking at the correlation between qMRI measures and previously validated scales of disability (PND score) and neurological impairment (NIS and NIS-LL).

Thigh and calf FF correlated well with PND score (thigh: r=0.626, p=0.001; calf: r=0.623, p=0.002), NIS (thigh: r=0.553, p=0.005; calf: r=0.621, p=0.002), and NIS-LL (thigh: r=0.553, p=0.005; calf: r=0.624, p=0.002) (**Fig**. **10**). These positive associations were independent from sex, age, treatment, and mutation in a multivariable linear regression model (**Table 4**).

Similarly, water T2 significantly correlated with PND score (thigh: r=0.630, p=0.001; calf: r=0.690, p<0.001), NIS (thigh: r=0.725, p<0.001; calf: r=0.802, p<0.001), and NIS-LL (thigh: r=0.714, p<0.001; calf: r=0.785, p<0.001).

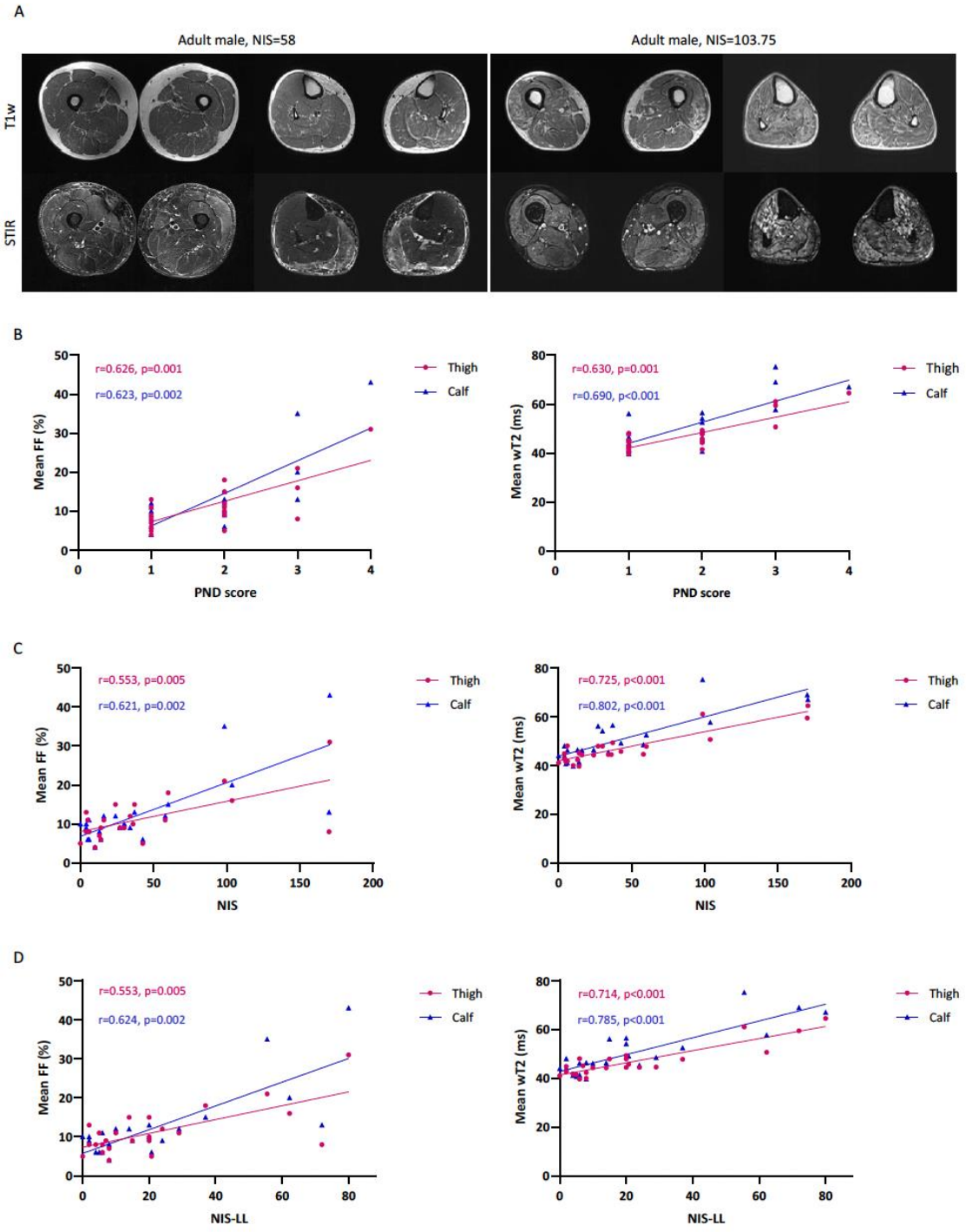

Fig. **10**. Correlation of muscle quantitative MRI measures with functional rating scales in ATTRv amyloidosis**.** Representative examples of T1-weighted (T1w) and short tau inversion recovery (STIR) sequences of the thighs and calves of two patients affected by ATTRv amyloidosis with moderate (left) and severe (right) disease. The patient with greater disability (right) has more prominent fat infiltration and a higher water T2 content (A). Moderate to strong positive correlation was observed between mean fat fraction (FF) and water T2 (wT2) at thigh (purple) and calf (blue) level and PND score (B), Neuropathy Impairment Score (NIS) (C) and NIS-lower limb (NIS-LL) (D).

	*NIS	NIS-LL	PND score
†Age	β=0.047, *p*=0.802	0.004, 0.984	-0.119, 0.468
Sex	-0.238, 0.227	-0.218, 0.240	-0.089, 0.594
Treatment	0.069, 0.722	0.099, 0.591	0.180, 0.291
Mutation	0.076, 0.698	0.069, 0.711	0.022, 0.896
Thigh FF	0.525, **0.012**	0.596, **0.004**	0.697, **0.000**
†Age	-0.025,0.880	-0.071, 0.234	-0.201, 0.165
Sex	-0.202, 0.234	-0.186, 0.227	-0.068, 0.629
Treatment	0.078, 0.647	0.111, 0.473	0.184, 0.214
Mutation	0.213, 0.223	0.222, 0.166	0.243, 0.110
Calf FF	0.683, **0.001**	0.732, **0.000**	0.802, **0.000**
†Age	-0.169, 0.148	-0.208, 0.078	-0.319, 0.023
Sex	-0.091, 0.427	-0.087, 0.444	0.009, 0.947
Treatment	-0.037, 0.742	0.003, 0.980	0.106, 0.417
Mutation	0.086, 0.445	0.087, 0.438	0.057, 0.660
Thigh wT2	0.925, **0.000**	0.926, **0.000**	0.915, **0.000**
†Age	-0.071, 0.610	-0.110, 0.409	-0.218, 0.170
Sex	-0.095, 0.609	-0.089, 0.519	-0.001, 0.994
Treatment	-0.056, 0.702	-0.020, 0.887	0.070, 0.668
Mutation	0.206, 0.161	0.211, 0.135	0.222, 0.174
Calf wT2	0.840, **0.000**	0.856, **0.000**	0.828, **0.000**

*Dependent variable
†Independent variable; standardized regression coefficients (β) and p values (*p*) are shown
Level of significance (α) of 0.05

Table 4. Multivariate linear regression model.

2.4.4 Quantitative MRI parameters correlate with nerve conduction study measures

Quantitative MRI parameters also showed significant correlation with several neurophysiological parameters. In particular, FF and wT2 negatively correlated with peroneal nerve CMAP (thigh: FF: r=-0.504, p=0.039; wT2: r=-0.645, p=0.005; calf: FF: r=-0.748, p=0.001; wT2: r=-0.623, p=0.013), tibial nerve CMAP (thigh: wT2: r=-0.699, p=0.003; calf:

FF: r=-0.757, p=0.002; wT2: r=-0.726, p=0.003), and sural SNAP (thigh: wT2: r=-0.669, p=0.003; calf: FF: r=-0.770, p=0.001; wT2: r=-0.645, p=0.009) (**Fig**. **11**) amplitudes.

Interestingly, in 7/17 (42%) ATTRv patients with unexcitable or severely reduced motor and sensory action potentials in the lower limbs (peroneal and tibial CMAP <= 1mV, sural SAP <= 1 microV) qMRI showed changes ranging from +8% to +16% of FF at thighs and +9% to +20% at calves, compared to an average in controls of 6.5% and 7.1%, respectively, correlating with clinical severity.

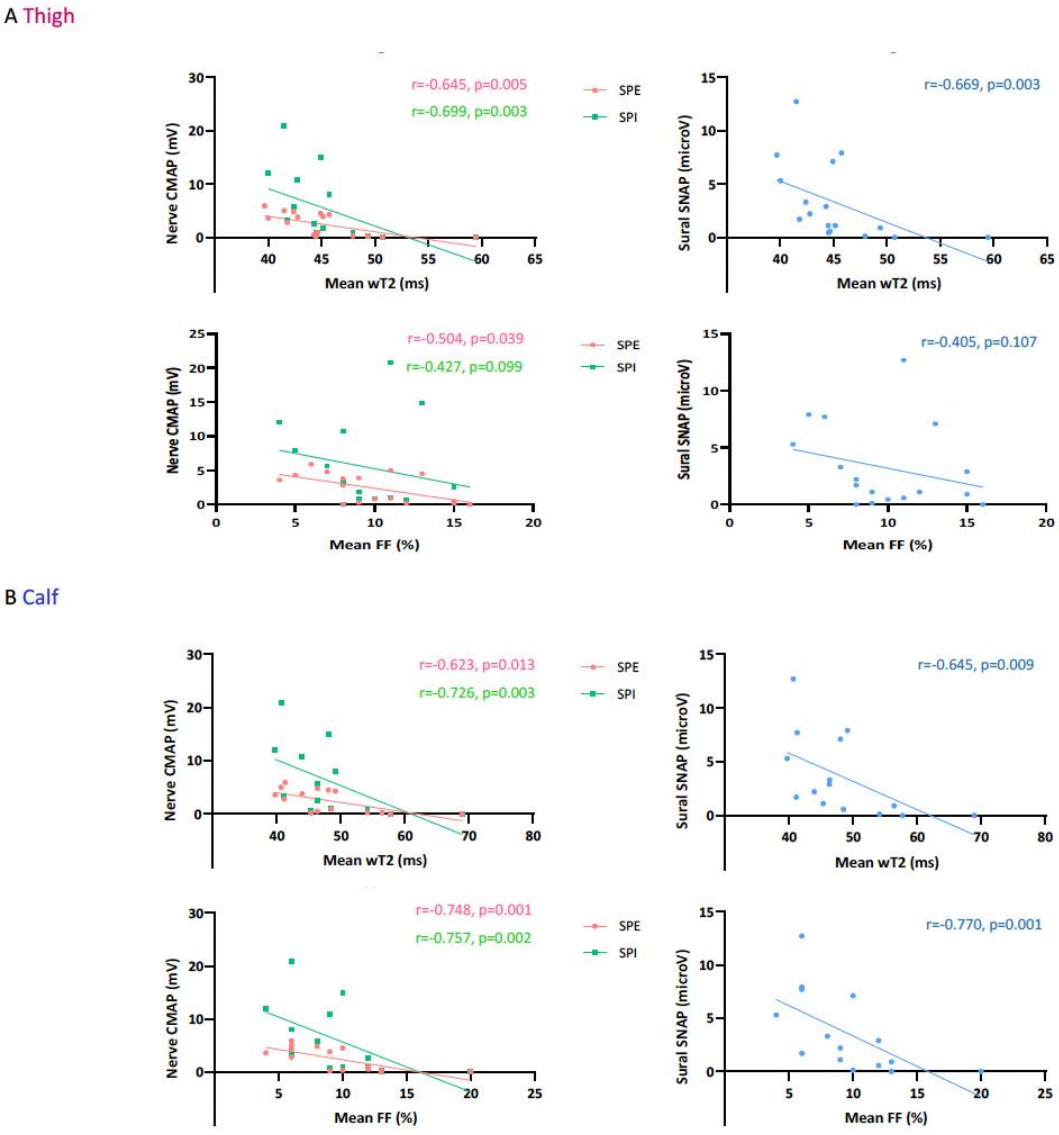

Fig. **11**. Correlation of muscle quantitative MRI measures with NCS parameters in ATTRv amyloidosis**.** Negative correlation between NCS parameters namely peroneal compound muscle action potential (CMAP) (pink), tibial CMAP (green) and sural sensory nerve action potential (SNAP) (light blue) and water T2 and fat fraction (FF) at thigh (A) and calf (B) level.

2.4.5 Muscle fat fraction and water T2 do not exhibit length-dependent changes

ATTRv amyloidosis typically presents with a length-dependent pattern of weakness, namely lower limbs are more affected than upper limbs and distal limb segments are more affected than proximal ones[209].

In our cohort, calf muscles were significantly weaker compared to thigh muscles as measured by NIS-LL (NIS-LL score at calf *vs* thigh: median 7, IQR 28.5 *vs* median 0, IQR 6; p=0.023).

Despite these clinical findings, thighs showed a similar degree of fat replacement compared to calves (thighs median FF 9.8%, IQR 7.3% *vs* calves median FF 9.9%, IQR 6.0%; p=0.8). Similarly, no significant difference was appreciated between wT2 at thigh and calf level (thighs median wT2 44.8, IQR 5.6 *vs* calves median wT2 47.2, IQR 12.2; p=0.147) (**Fig**. **12**).

2.4.6 Pattern of fat infiltration: posterior thigh involvement

Quantitative MRI identified a prominent involvement of the medio-posterior compartment of the thighs with a relative sparing of the quadriceps (median 12.8%, IQR 8.6% *vs* median 7.7%, IQR 5.5%; p=0.010), despite the similar involvement at clinical examination (NIS-LL score anterior *vs* posterior region at thigh: median 0, IQR 2 *vs* median 0, IQR 3; p=0.963).

At calf level, no significant difference in FF between different compartments was appreciated (deep posterior *vs* superficial posterior: p=0.925; deep posterior *vs* antero-lateral: p=0.336; superficial posterior *vs* antero-lateral: p=0.250; posterior *vs* antero-lateral: p=0.229) (**Fig**. **12**).

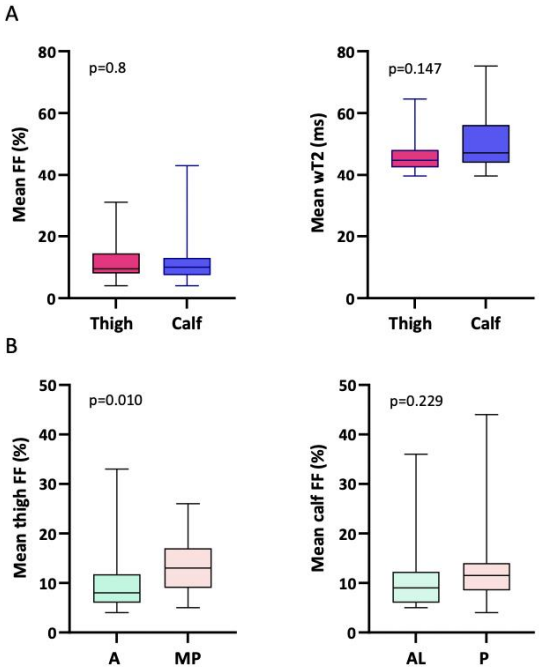

Fig. **12**. Muscle quantitative MRI imaging: thigh and calf compartments in ATTRv amyloidosis**.** Fat fraction (FF) and water T2 (wT2) were not significantly different between thigh and calf level (A). Fat substitution prevailed in the medio-posterior thigh compartment compared to the anterior region while no difference was seen at calf between the antero-lateral and posterior region (B).

2.5 Discussion

In this study we assessed the role of muscle qMRI as a novel outcome measure in a cohort of ATTRv patients with polyneuropathy. We showed that qMRI reveals significant difference between ATTRv patients and healthy controls and strongly correlates with previously validated clinical measures.

ATTRv amyloidosis is a progressive and highly debilitating hereditary disease, which is fatal within a decade without treatment[6–8]. Early diagnosis is key to promptly start an appropriate anti-amyloidogenic treatment. Therefore, there is a need for reliable and objective measures to establish the disease onset, track its progression and monitor the response to treatments.

To date, most outcome measures used in ATTRv-PN are based on clinical examination and functional impairment. In particular, NIS, along with its subset NIS-LL, which was first designed to grade neurological impairment in diabetic neuropathy[143], has become the most used outcome measure in different clinical trials and observational studies in ATTRv amyloidosis[149–151]. However, it does not encompass the autonomic and cardiac involvement of the disease. Also, even if performed by expert and preliminarily trained clinicians, NIS and NIS-LL are limited by intra- and inter-rater variability[9,191,192] along with patient's motivation. To better capture the multisystem involvement in ATTRv amyloidosis and reduce its variability[105], novel compound scales, NIS+7 and mNIS+7, have been developed. Although NIS+7 and mNIS+7[149–154], provide a thorough evaluation of ATTRv amyloidosis, they are time-consuming and require a bespoke setting and specific training of the examiners[155].

Quantitative MRI may represent an attractive option to overcome shortcomings in clinical examination as it is relatively rapid, with high intra- and inter-operator reproducibility of manual muscle segmentation[203] and analysis can also be automated in all ATTRv patients. In particular, previous studies have shown that muscle quantitative MRI has a very good reproducibility with an interclass correlation coefficient > 0.9 both for intra- and inter-rater agreement[210]. The future implementation of robust machine learning algorithms for automatic segmentation of muscles may be the key to overcome the limitations related to manual segmentation[211,212].

Recently, MRI neurography of sciatic and sural nerve was shown to be able to accurately distinguish patients with ATTRv amyloidosis from controls and, importantly, to detect subclinical and early nerve lesions in asymptomatic carriers[164,165]. Similarly, magnetization transfer ratio of the sciatic nerve showed promising results as it differentiated both

symptomatic ATTRv patients and asymptomatic carriers from healthy controls and correlated with electrophysiology[166].

Muscle qMRI has been extensively applied as disease biomarker for the study of muscle dystrophies and other myopathies, including Duchenne muscular dystrophy, where both fat fraction and water T2 content provided sensitive noninvasive measures of disease progression over time[193]. More recently, quantification of intramuscular fat showed high responsiveness to change over 12-month time in genetic neuropathies, and currently represents the most sensitive outcome measure for the assessment of the slow progression of CMT1A[199].

Prompted by these encouraging results, we decided to assess the role of muscle qMRI in ATTRv amyloidosis with polyneuropathy. We evaluated both acute (tissue water content as expressed by T2 signal) and chronic (fat replacement as expressed by FF) changes in the lower limb muscles. We found that water T2 and FF were significantly higher in ATTRv patients compared to healthy controls and were able to differentiate the two groups. Their increase might be explained by axonal damage due to the underlying neuropathy resulting in acute (as defined by water T2) and chronic (as defined by FF) denervation. More important, we observed a moderate to strong positive correlation between muscle qMRI parameters (mean FF and wT2) at both thigh and calf level and patients' functionally relevant clinical measures (PND score, NIS, and NIS-LL scales). Therefore, muscle qMRI represents a reliable surrogate measure of disease severity in ATTRv amyloidosis, which is independent of participant's effort and with a high intra-rater agreement[203]. In addition, qMRI may help clinicians to monitor disease progression in ATTRv patients in more advanced stages of the disease, when widespread reduction or unexcitability of motor and sensory action potentials limits the role of electrophysiology in assessing progression and response to treatment.

Interestingly, in ATTRv qMRI showed a similar degree of fat replacement and water content of thigh and calf muscles, which was unexpected considering the length-dependent involvement of lower limb muscles at neurological examination. This finding differed from previous studies on slowly progressive neuropathies, CMT1A and hereditary neuropathy with liability to pressure palsies, where qMRI showed a higher degree of fat substitution at calves[201,202]. However, it is worth noting that previous pathological studies have shown in ATTRv amyloidosis conspicuous amyloid deposition in dorsal roots and sympathetic ganglia[213]. Also, previous MR neurography studies have detected in ATTRv carriers the presence of early and prominent changes of the proximal nerve tracts compared to distal ones[164], which is in agreement with our finding of significant fat replacement in the proximal muscles of the lower limbs.

Finally, skeletal muscle MRI showed a distinctive pattern in ATTRv patients with preferential involvement of posterior muscles and a relative sparing of quadriceps in the thighs, while in the calves all muscles appeared to be equally affected. This pattern has not been previously described in other acquired and genetic neuropathies. Indeed, patients affected by chronic inflammatory demyelinating polyneuropathy had fat infiltration both at biceps femoris and quadriceps[214], while in CMT1A a predominant degeneration of antero-lateral compartments of calves was reported[201]. Therefore, although this observation warrants further confirmation in larger cohorts, it may be a clue to suspect ATTRv amyloidosis in patients with unexplained axonal neuropathy and, maybe in the future, to help differentiating ATTRv amyloidosis from other genetic and acquired neuropathies.

Our study has some limitations. First, we recruited mostly ATTRv patients with mild and moderate neuropathy, while the more advanced stages of the disease were underrepresented. Second, a muscle biopsy was not performed in any case. Therefore, we cannot rule out the presence of a coexisting myopathy. However, needle EMG was available for n=17 patients and did not show myopathic changes in any of them. Also, amyloid myopathy is infrequent in previous case series[215]. Third, although the time required for muscle MRI was limited to one hour and was mostly well tolerated by all subjects, patients with more advanced neuropathy showed lower tolerance of a prolonged supine position, which partly explains their lower recruitment. However, in general, good collaboration from the patient was fundamental to obtain images suitable to quantitative analysis. Hopefully, in the near future compressed sensing and parallel imaging will allow to shorten the acquisition time making this evaluation easier to perform.

Longitudinal studies are warranted in order to assess the role of qMRI as noninvasive, objective, and sensitive biomarker for the diagnosis and monitoring over time of ATTRv-PN patients, especially in presymptomatic and early symptomatic stages of the disease.

3. Genetic modifiers in hereditary and acquired transthyretin amyloidosis

3.1 Study rationale

As mentioned above, ATTRv amyloidosis is clinically heterogenous, and there is considerable variability in terms of AOO, penetrance, clinical phenotype, progression, and response to disease-modifying treatments across different populations, as well as inside single families, which cannot be entirely explained by the specific point mutation in the *TTR* gene. Also, factors favoring wild-type TTR deposition in senile systemic amyloidosis, are still largely unknown. Therefore, a role of genetic modifiers has been hypothesized.

Previous studies have looked at genetic modifiers of AOO in ATTRv amyloidosis, and possible role of *cis* and *trans* elements from *TTR* gene, including coding and non-coding variants in *TTR* itself, and other genes as *RBP4*[74,75], *AR*[74], *C1QA*, *C1QC*[76–78], *APCS*[74–76], *BGN*, *HSP27*, *MEK1*, *MEK2*, *NGAL*, *YWHAZ*[79] has been suggested. However, these studies were mostly limited to single populations endemic for V30M (p.Val50Met) mutation (i.e., Swedish, and Portuguese patients), and genes tested were chosen because of their possible functional relevance to the disease ("biased approach"). Also, variants identified as possible modifiers often failed independent replication across different populations. Hence, this genetic variability has never been looked at in an "unbiased way".

Stemming from these premises, our study aims to identify loci harboring genetic variations in ATTR amyloidosis by performing a genome-wide association study (GWAS). Long-read sequencing (LRS) techniques will be further adopted to better characterize meaningful GWAS loci and the *TTR*-containing region itself.

Indeed, even though there have been previous attempts to sequence the *TTR* locus, also including neighboring regions, up to ~ 6,000 bp up- and downstream, to identify variant-disease associations, these were based on canonical sequencing methods (i.e., Sanger sequencing by dye terminator chemistry approach) which nevertheless cannot generate reads longer than ~ 1000 bp from a single DNA molecule[71,216].

The definition of the linkage phase of individual haplotypes, a process known as haplotype phasing or haplotyping, traditionally involved either population-based or pedigree-based inferential methods, which statistically infer haplotypes from the unphased genotypes of multiple related or unrelated individuals, and direct methods, including cloning, which

apply experimental techniques to high-molecular weight genomic DNA derived from a single individual[217].

While population-based haplotype inference is challenged by low-frequency variants (i.e., with minor allele frequency, MAF < 1%), private variants (i.e., variants that are found in a single individual or pedigree, and then which are absent from reference panels), and *de novo* variants, pedigree-based haplotype inference relies on the availability family DNA, and is unable to phase *de novo* variation which has arisen in the last generation[217].

By contrast, second-generation next-generation sequencing (NGS) technologies, such as Illumina sequencing by synthesis, typically produce fairly short reads (up to 300 bp), that usually span no more than a single variant. For instance, also in this case, the haplotype can be phased solely by statistical inference from population genotyping data[217]. To overcome these issues, different *ad hoc* library preparations that preserve haplotype information in short-read sequencing data have been proposed, however they require additional sample preparation time and costs[218–220].

Third-generation sequencing technologies, such as PacBio single-molecule real time (SMRT) and Oxford Nanopore (ONT), can facilitate rapid and direct haplotyping due to long sequencing reads (>10 kb) by analysis of single DNA molecules in real-time[217,221]. Albeit long-read sequencing helps reconstructing haplotypes by mitigating the intrinsic limitation that the distance between subsequent heterozygous markers can be larger than the read itself, to phase over longer stretches of homozygosity, repeat-rich regions, including segmental duplications, and centromeres, still proves challenging[221].

To date, this technique has never been applied to resolve haplotype structure to identify variant-disease associations in ATTR amyloidosis.

The identification of loci harboring genetic variations across different populations and ethnicities, either at *TTR* gene (in cis- or trans) or at genome-wide level, both by genotype arrays and novel sequencing methods, which can directly resolve haplotype phasing, is of utmost importance since it will help to predict AOO in ATTRv patients, prompting earlier diagnosis, closer monitoring, and treatment initiation, and it will also possibly enable clinicians to stratify these patients based on a genetic risk score.

3.2 Aim

1) To perform a GWA analysis to identify loci harboring genetic variations that modify:
    a. AOO and penetrance
    b. phenotype, clinical severity, and progression
    c. response to anti-amyloidogenic treatments

   of ATTRv and ATTRwt amyloidosis.
2) To characterize by LRS the *TTR*-containing region across different populations
    a. To detect and confirm the *TTR* pathogenic mutation from each ATTRv patient
    b. To accurately assign (that is "phasing") nearby variants (*cis* or *trans*) associated with the *TTR* mutation which define different intragenic haplotypes.

3.3 Materials and methods

3.3.1 Study design and patient recruitment

3.3.1.1 Experimental plan design

The GWAS will be performed on:

1) a discovery cohort of n=1500 patients affected by V30M (p.Val50Met) ATTRv amyloidosis and showing a continuous range of AOO of the disease, from early to very late
2) an independent cohort of n=1000 V30M (p.Val50Met) ATTRv amyloidosis patients (replication cohort)
3) a cohort of n=1500 ATTRv amyloidosis patients carrying non-V30M (p.Val50Met) mutations
4) a cohort of n=1500 patients affected by ATTRwt amyloidosis *plus* a cohort of n=1500 age-, gender-, and ancestry-matched healthy controls (complementary case-control GWAS).

Long-read sequencing of *TTR* locus and GWAS significant loci in most informative early onset, severe, and treatment resistant cases will be performed to identify coding and non-coding variants, short indels, larger structural variants, short-tandem repeats, retrogenes, acting as possible genetic modifiers (*see following sections for detailed description*).

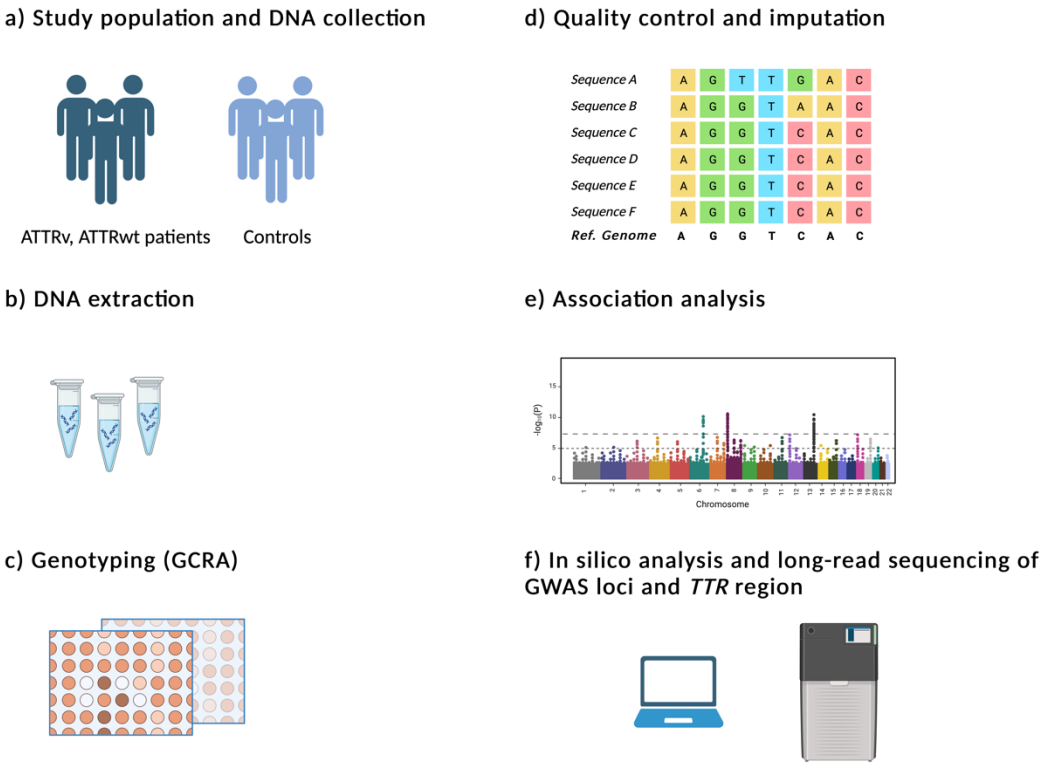

Fig. 13. Graphical summary of experimental plan.

3.3.1.2 Patient enrollment, DNA samples, and clinical data collection

The study population (all aged >=18 years of age) will entail:

1) patients affected by ATTRv amyloidosis, carrying either V30M (p.Val50Met) or non-V30M (p.Val50Met) mutations in *TTR* gene, or carriers at risk of developing the disease. The presymptomatic carriers will be defined as asymptomatic subjects five years (or more) before the mean AOO in the family or within five years (or later) the AOO in the family
2) patients affected by ATTRwt amyloidosis
3) age-, gender-, and ancestry-matched healthy controls (HCs) (partners and carers of patients will be enrolled). Additional genotyping data are already available from healthy controls belonging to different ethnic backgrounds at UCL Institute of Neurology.

The majority of the DNA samples from living or deceased patients have been already collected and are stored in -80°C freezers and are thus available for the present study together

with thorough clinical information. Few Centres will be prospectively collecting fresh blood from patients whose DNA was not previously stored, or if the already collected material is exhausted.

For most stored DNA samples, generic consent for genetic testing (including when performed in external Centres) has already been collected. This is of particular relevance for DNA samples from deceased individuals. A bespoke consent to the present study will be obtained from all patients undergoing fresh blood collection, and from all prospectively followed up patients.

The following demographic and clinical information were collected for all enrolled cases:

1) Centre (with local ID and family ID, whenever available)
2) disease group (i.e., ATTRv symptomatic or presymptomatic, ATTRwt, HC)
3) self-reported ethnicity (white Caucasian, Black or African American, Asian, mixed)
4) sex (male/female)
5) year of birth
6) year of most recent follow-up
7) in case of ATTRv amyloidosis, mutation in the *TTR* gene, according to Amyloid nomenclature, 2020 (ISA)[5] (of note: all the already reported *TTR* mutations are also covered on our custom Global Clinical Research arrays [GCRA], in order to confirm the reported genotype)
8) zygosity of the *TTR* mutation
9) family history of ATTRv amyloidosis, relatedness to other enrolled cases, and parent-of-origin (father or mother)
10) if diagnosis of ATTRv amyloidosis was made during the presymptomatic screening (in case of presence of family history of ATTRv amyloidosis)
11) year of diagnosis
12) presence of bilateral carpal tunnel syndrome and AOO
13) presence of polyneuropathy (i.e., sensory-motor symptoms and/or neurophysiology) and AOO of different PND stages (1 to 4)
14) presence of pain and AOO
15) presence of cardiomyopathy (i.e., symptoms or echocardiographic [diastolic interventricular septum thickness > 12 mm], or cardiac magnetic resonance abnormalities consistent with amyloidosis, or bone tracer scintigraphy with Perugini score 2 or 3) and AOO

16) presence of cardiac rhythm defects requiring pacemaker implantation and AOO
17) presence of diarrhea and/or orthostatic hypotension and AOO
18) presence of lumbar spinal stenosis and AOO
19) presence of renal involvement (proteinuria) and AOO
20) presence of eye involvement (vitreous opacity) and AOO
21) maximum wall thickness, New York Heart Association (NHYA) stage, N-terminal pro B-type natriuretic peptide (NT-proBNP), and estimated glomerular filtration rate (eGFR) at most recent follow-up
22) occurrence of heart failure requiring hospitalization and AOO
23) type of treatment (liver transplant, anti-amyloidogenic therapy) and year
24) if deceased, year, and cause of death (if related or unrelated to ATTRv/ATTRwt amyloidosis)

In order to capture the multisystem involvement of ATTRv amyloidosis, we will also generate a progression score on the basis of principal component analysis (PCA) of prospectively acquired longitudinal changes into six broad domains, defined *a priori*: motor, sensory, autonomic, cardiological, renal, and eye. This approach was successfully implemented to model disease progression in Huntington disease, a polyglutamine repeat expansion disorder, which, similarly to ATTRv amyloidosis, has variable and multisystemic clinical expressivity and a complex genetic architecture which can modify the effect of the size of CAG repeat expansion in *HTT* gene, influencing disease onset, and progression[222].

3.3.2 Genome-wide association study

We will perform our GWAS using the Illumina GCRA at the University College London Genomics. This new array is designed to give a denser mapping along the genome and will better capture the ethnic diversity across the ATTRv/ATTRwt different populations.

To detect meaningful rare variants not included in the standard GCRA, we have increased the backbone of Illumina GCRA with a custom content entailing different significant single nucleotide polymorphisms (SNPs) (*see below*).

Interestingly, anticipation and parent-of-origin effect, which have both been reported in ATTRv amyloidosis, are well characterised biological mechanisms in repeat-expansion disorders, thus highlighting the importance of considering variations in short tandem repeats as possible genetic modifiers in ATTRv amyloidosis.

Standard quality control (QC) procedures will be performed using PLINK v1.9, including controlling for coverage and call rates (5% of missing data allowed per SNP and individual), and Hardy-Weinberg equilibrium (SNPs with $p < 10^{-6}$ in an exact test will be removed). Relatedness and non-European ancestry will be assessed by identity-by-descent analysis and ADMIXTURE analysis, respectively.

In ATTRv amyloidosis discovery and replication cohorts, association analyses will be performed with the mixed linear model (MLM) functions included in GCTA v1.26, specifically the leave-one-chromosome-out (LOCO) procedure. This analysis will account for relatedness and ancestry.

While our primary association analysis in ATTRv amyloidosis will use AOO, we will perform secondary association analyses using measures of disease progression, including validated outcome scales of disability (e.g., PND score), and an *ad hoc* PCA-based compound score, as well as the report of response to disease modifying therapies. In cases carrying non-V30M (p.Val50Met) mutations we will use standardised residual AOO and residual disease progression measures, after correcting for the effects of the specific *TTR* mutation.

A case-control GWAS design will be applied to test for the presence of loci conferring increased susceptibility in ATTRwt amyloidosis *vs* age-, gender- and ancestry-matched healthy controls.

3.3.3 Long-read sequencing of *TTR* locus

3.3.3.1 DNA extraction and long-range PCR

Genomic DNA (gDNA) was extracted from peripheral blood leukocytes using Flexigene (Qiagen) or QIAamp DNA mini kit (Qiagen), or from saliva using QIAamp DNA mini kit (Qiagen).

The *TTR*-containing region (GRCh38/hg38: chr18:31,591,877-31,598,821; transcript size: 6,945 bp, including untranslated regions) (**Fig**. **14**) was amplified as a single amplicon of 9,227 bp, entailing all four exons, and three introns, by long-range PCR. Sequences for PCR primers were designed with Primer3Plus software, and the presence of hairpins and secondary structures was ascertained with AutoDimer v1.0 (primer sequences: Fw GGTTCTCACAGTCATCTCTACTTTCT; Rv: CCGAGATTTGGGGTTATTTGTGATAG).

To amplify the *TTR*-containing region, the PCR reaction was performed in a final volume of 10 µl with 50 ng of gDNA, and 0.4 µM of primers, using 0.4 µl of LongAmp® *Taq* DNA polymerase, according to manufacturer's protocol (New England *BioLabs*). Thermocycling conditions were the following: 3 min 94°C, 30 cycles (30 sec 94°C, 30 sec 60°C, 8 min 65°C), and 10 min 65°C.

The PCR products were then run on an agarose gel (1%) for 45 minutes at 90V and visualised on GelDocTM XR+ with Image LabTM Software (Bio-Rad).

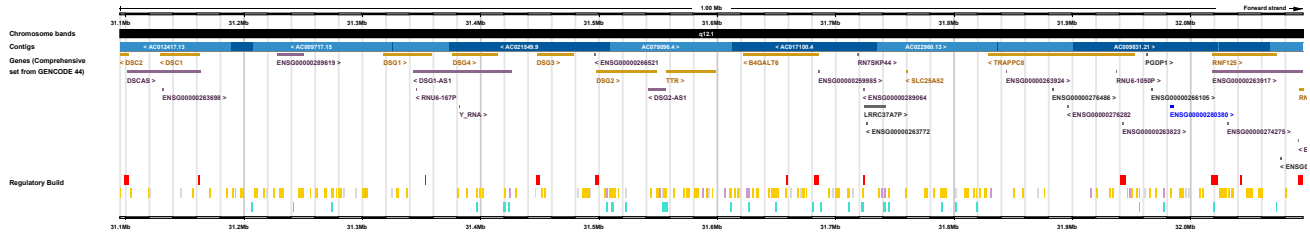

Fig. **14**. *TTR*-containing region (GRCh38/hg38) visualized on *e*!Ensembl.

3.3.3.2 Barcoding, library preparation, and long-read sequencing

After the optimization of the long-range PCR reaction, barcoded primers were customized according to PacBio requirements as follows:

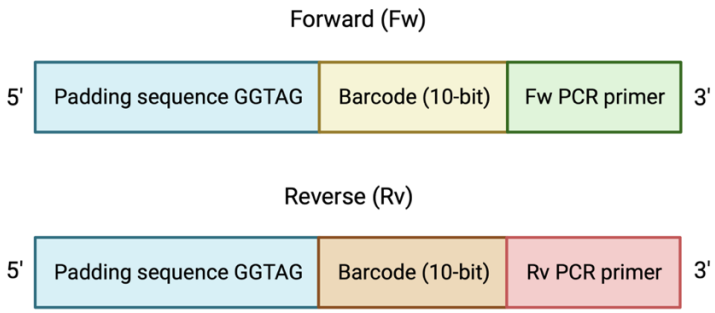

An asymmetric barcoding strategy was adopted, which means completely different barcode sequences used for the forward and reverse PCR primers for each patient DNA sample. This was done to minimize the total number of PCR primers required. An example amplicon containing the mentioned asymmetric barcoded primers, with the 5-base padding sequence, is reported below (**Fig**. **15**).

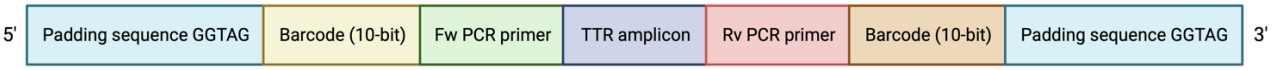

Fig. **15**. PCR primers (Fw and Rv) with asymmetric barcodes and 5-base padding sequence.

Using 50 ng of gDNA from each patient, a total of n=323 DNA samples from symptomatic ATTRv patients were amplified using asymmetric barcoded primers in an optimized long-range PCR reaction (*as described above*). As it was not possible or practical to confirm successful PCR amplification on agarose gel electrophoresis for all the samples, products of PCR reactions were quantified using a microplate-based fluorometric approach (Invitrogen Quant-iT™ PicoGreen™ dsDNA Assay Kit). A successful amplification was defined as an increase of > 50% in the total mass of dsDNA in the reaction (i.e., > 75 ng of dsDNA post-PCR compared to 50 ng pre-PCR).

After equimolar pooling (60 ng from each PCR reaction, for a total mass of 19.440 µg and a volume of 1016.8 ul), libraries were prepared using the SMRTbell Prep Kit 3.0 (PN 102-141-700, Pacific Biosciences, Menlo Park, CA, USA). Briefly, 1.5 µg of gDNA was

used for the library preparation. High-quality gDNA was sheared using Megaruptor 3 System (Diagenode, Denville, New York, USA). After quality control, the total pooled input DNA amount was diluted to 500 ng, and damage repair & A-tailing, non-barcoded hairpin adapter ligation, and final exonuclease treatment were performed. SMRTbell beads (Pacific Biosciences, Menlo Park, CA, USA) were used for all the purification steps (1.3 x clean-up). Library size and quality were assessed using FEMTO Pulse System (Agilent Technologies M5330AA), and Qubit fluorometer with Qubit 1X dsDNA HS Assay Kit (Thermo Fisher Scientific Q33230). Sequencing primer 3.2 and Sequel II DNA Polymerase 2.2 were annealed and bound, respectively, to the final SMRTbell library. Libraries were loaded at a concentration of 70 pM and sequencing was performed using a single 8M SMRT cell on the Sequel IIe System (Pacific Biosciences, Menlo Park, CA, USA). Secondary analysis (circular consensus sequencing [CCS] mode to generate highly accurate [>=Q20] single molecule long reads [HiFi reads]) was performed using Pacific Biosciences SMRT Link v11.1. The sequencing data were then processed and analyzed.

PacBio CCS reads were demultiplexed with command "lima-->split-named-->peek-guess-->preset HIFI-ASYMMETRIC". Reads from each demultiplexed sample were aligned to the hg38 reference with "Minimap2-ax map-hifi". Coverage and sequencing depth in the region of interest were obtained with standard samtools commands. Only samples with 100% coverage of the region and a minimum read depth > 15 were kept for further analysis. Variant calling was performed with DeepVariant v1.5, with standard options. For the purpose of haplotype identification, only biallelic SNPs variants were kept (filtering with "bcftools view-v snps-M2"), followed by phasing with WhatsHap. For subsequent downstream processing and data visualisation, we used the Python library Pandas.
The workflow is reported below (**Fig**. **16**).

We looked for coding and non-coding single nucleotide variants of possible functional relevance to the disease-causing mechanisms. Also, we will look at short indels, larger structural variants (i.e., deletions, duplication, and inversions), and short tandem repeats. Importantly to this last aspect, SMRT long-read sequencing has proved able to accurately sequence structural variants and repeated regions, which are known to be a challenge for both traditional and short-read NGS technologies.

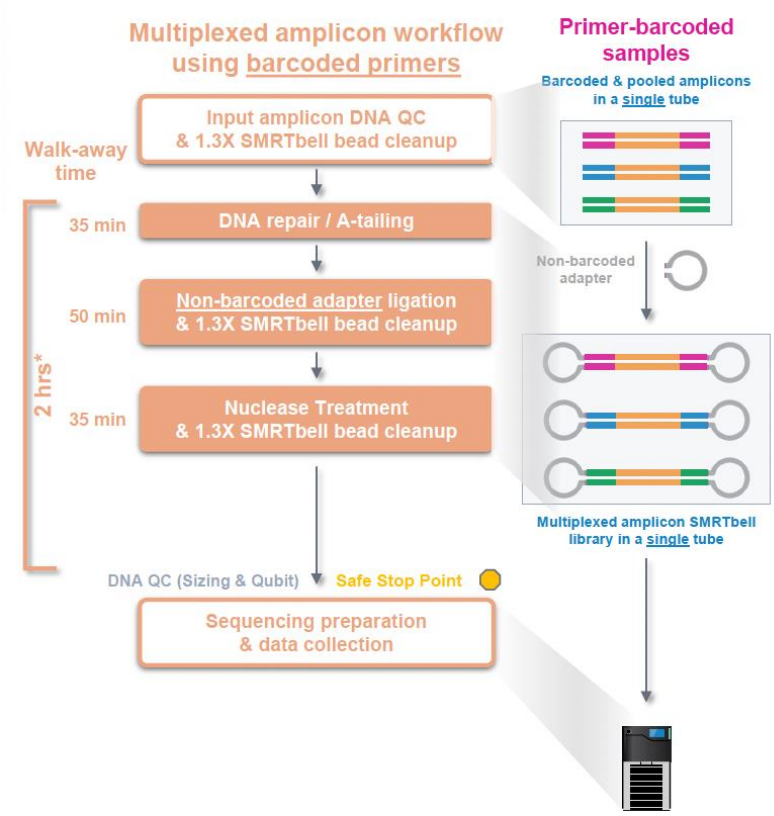

Fig. **16**. Amplicon SMRTbell library construction workflow overview using barcoded primers.

3.4 Results

3.4.1 Enrolled Centres and DNA sample collection

From June 2021 to September 2023 n=52 Centres have been enrolled across the globe, encompassing n=19 different Countries (**Fig**. **17**).

Fig. **17**. World map showing all collaborating Centres.

During the same timeframe, n=3596 DNA samples have been received (n=1910 from ATTRv patients; n=665 from ATTRwt patients, and n=1031 from controls).
The global enrollment status is better detailed in **Table 5**.

	ATTRv		ATTRwt	Controls	Total
	V30M	nV30M			
DNA samples received	1910		655	1031	3596
	1248	662			
DNA samples being prepared for shipping by collaborating Centres	2177		327	255	2759
Total expected DNA samples for the GWA study	4087		982	1286	6355

Table 5. Global enrollment of the *TTR* GWA study.

The detailed breakdown of the DNAs which have been already received or being prepared for shipping is reported below (**Table 6** and **7**).

	Country	Centre / contact person	ATTRv		ATTRwt	Controls
			V30M	nV30M		
1	Italy	Pavia / L. Obici – A. Cortese	230	170	500	500
		Padua / C. Briani	1	6	0	0
		Rome / M. Luigetti	26	24	0	0
		Rome / G. Antonini	8	4	14	0
		Verona / G. Fabrizi	19	63	16	0
2	France	Creteil / V. Planté-Bordeneuve	68	0	0	0
3	UK	London / M.M. Reilly	56	0	0	0
4	Spain	Zaragozza / S. Menao	2	4	29	50
		Barcelona / R. Rojas Garcia	40	0	0	0
		Palma / E. Cisneros-Barroso	56	0	0	20
5	Portugal	Lisbon / I. Conceicao	139	0	0	0
6	Germany	Munich / T. Trenkwalder – K. Knoll	0	0	96	459
7	Bulgaria	Sofia / A. Todorova – I. Tournev	45	323	0	0
8	Brasil	São Paulo / W. Marques – P. Tomaselli	109	34	0	2
		Rio de Janeiro / M. Waddington-Cruz	33	0	0	0
9	Sweden	Umea / I. Anan	400	0	0	0
10	US	Boston / T. Prokaeva	17	33	0	
			1910		655	1031

Table 6. DNA samples received and ready for genotyping.

	Country	Centre / contact person	ATTRv		ATTRwt	Controls
			V30M	nV30M		
1	Italy	Genoa / P. Mandich	17	29	32	55
		Florence / F. Cappelli	30		100	200
		Bologna / P. Guaraldi	50		0	0
		Messina / M. Russo	50		0	0
		Palermo / V. Di Stefano	20		0	0
		Bari / G. Milella	20		0	0
2	France	Creteil / V. Planté-Bordeneuve	0	50	0	0
		Paris / D. Adams - A. Echaniz-Laguna	200		0	0
3	UK	London / G. Gillmore	150	250	0	0
4	Spain	Huelva / A. Gragera	50	0	0	0
		San Sebastian / P. Iruzubieta Agudo	16	1	0	0
		Madrid / F. De Frutos	50		0	0
		Barcelona / D. Sánchez-Tejerina	20		0	0
		Barcelona / C. Casasnovas Pons	60		15	0
		Valencia / T. Sevilla	50		0	0
5	Portugal	Porto / T. Coelho – C. Lemos	300	0	0	0
6	Germany	Heidelberg / U. Hegenbart – S. Shoenland	40		150	0
		Berlin / K. Hahn	15		0	0
		Aachen / M. Dohrn	10		0	
7	Switzerland	Lausanne / M. Theaudin	40		0	0
		Zurich / R. Schwotzer	10		0	0
8	Cyprus	Nicosia / K. Kleopa	100	0	0	0

9	US	New York / T. Brannagan – M. Maurer	10	30	0
10	Mexico	Mexico City / K. Soto	30	0	0
11	Argentina	Buenos Aires / M.L. Posadas Martinez – M. Saez	20	0	0
		Buenos Aires / R. Reisin	50	0	0
		Chaco / M. Tomei	15	0	0
12	Brasil	São Paulo / W. Marques – P. Tomaselli	100	0	0
13	Bolivia	Santa Cruz de la Sierra / C. Petit	20	0	0
14	Japan	Kumamoto / M. Tasaki	20	0	0
		Matsumoto / Y. Sekijima	50	0	0
15	Taiwan	Taipei / Y-C. Lee	100	0	0
		Taipei / H. Ching Hsu	8	0	0
16	Malesia	Kuala Lumpur / T. Chen Yin	20	0	0
17	Singapore	Singapore / Z. Chen	6	0	0
			2177	327	255

Table 7. DNA samples identified by participating Centres and being prepared for shipping.

N=998 DNA samples from ATTRv symptomatic patients (V30M, p.Val50Met + other mutations) out of n=1910 (n=1031 symptomatic ATTRv patients, and n=879 presymptomatic ATTRv carriers) DNA samples received have been already plated (C=20 ng/ul, according to GCRA requirements) in order to be genotyped by December 2023.

3.4.2 Custom content design

After comprehensive literature and Genomics England review[223] we have designed a custom content entailing different meaningful variants, which can act as potential genetic modifiers. The following variants have been added to the backbone of standard GCRA:

- all already reported pathogenic mutations in the *TTR* gene (for quality control)[4]

- the known T119M (p.Thr139Met) modifier in the *TTR* gene[45], together with previously published or functionally relevant SNPs in non-coding intronic or flanking regions of the *TTR* gene (expression quantitative trait loci [eQTL], promoter, and regulatory regions)[72,73,224–228]
- all already reported mutations/relevant SNPs in other "amyloidogenic" genes, including Fibrinogen alpha chain (*FGA*), Apolipoprotein A-I (*APOA1*), Apolipoprotein A-II (*APOA2*), Gelsolin (*GSN*), Cystatin 3 (*CST3*), Beta-2-microglobulin (*B2M*), Lysozyme (*LYZ*)[4], Amyloid Precursor Protein (*APP*)[229], Complement C3b/C4b receptor 1 (*CR1*)[230], Unc-5 Netrin Receptor C (*UNC5C*)[231]
- additional SNPs in distant genes, which were previously shown to modify AOO of ATTRv amyloidosis in specific populations, including *RBP4, AR, C1QA, C1QC, APCS, BGN, HSP27, MEK1, MEK2, NGAL, YWHAZ*[74–79]
- additional SNPs in pathways/genes relevant to light-chain amyloidosis, multiple myeloma, and monoclonal gammopathy of unknown significance[232–235] (e.g., SNPs related to carpal tunnel syndrome[236–238], developmental hip dysplasia[239], trigger finger[240,241], lumbar spinal stenosis[242], rotator cuff tear[243–248]; also, SNPs in Cyclin D1 [CCND1][234,237], and Serpin Family E Member 1 [*SERPINE1*][237] have been included)
- relevant SNPs in Ataxin-2 (*ATXN2*). Indeed, so far, a possible relevance to AOO of CAG intermediate repeats (>22) in *ATXN2* has been suggested for ATTRv amyloidosis[249] as well as for other neurological diseases (e.g., repeat-expansion disorders)[250–252]
- other relevant SNPs which have been shown to act as genetic modifiers in different acquired neurological disorders characterized by CNS involvement which can mimic CNS involvement due to ATTRv amyloidosis (e.g., subarachnoid haemorrhage[253], dementia[254])
- extra SNPs with MAF<=5% located:
  +/- 100 kb up- and downstream *TTR* (n=360, of which n=40 already included in the standard array)
  +/- 10 kb up- and downstream *ATXN2*

to explore regulatory regions nearby (**Table 8**).

Gene	Genomic coordinates (GRCh38/hg38)	Ref.
AAK1	chr2:69,457,997-69,643,739	[242]
ACE	chr17:63,477,061-63,498,373	[255]
ACE2	chrX:15,561,033-15,600,960	[255,256,257,258]
ACOT9/SAT1	chrX:23,701,055-23,743,276	[248]
ADAMTS10	chr19:8,580,240-8,610,715	[237,238]
ADAMTS14	chr10:70,672,506-70,762,441	[237]
ADAMTS17	chr15:99,971,437-100,341,975	[237,238]
AEBP1	chr7:44,104,345-44,114,560	[238]
AKR1C2	chr10:4,987,775-5,003,857	[237]
AOC1	chr7:150,852,517-150,861,504	[237,238]
APCS	chr1:159,587,826-159,588,865	[75]
APOA1	chr11:116,835,751-116,837,622	[4]
APOA2	chr1:161,222,292-161,223,628	[4]
APP	chr21:25,880,550-26,170,770	[229]
AR	chrX:67,544,021-67,730,619	[74]
ARHGAP26	chr5:142,770,377-143,229,007	[232]
ARMS2	chr10:122,454,653-122,457,352	[237]
ASTN2	chr9:116,423,112-117,415,057	[248]
ATXN2	chr12:111,452,214-111,599,315	[249–252]
B2M	chr15:44,711,517-44,718,145	[4]
BGN	chrX:153,494,980-153,509,546	[79]
BMP2	chr20:6,767,686-6,780,246	[237]
C1QA	chr1:22,636,628-22,639,678	[76,77,78]
C1QC	chr1:22,643,633-22,648,108	[76,77,78]
C5orf63	chr5:127,051,304-127,073,502	[248]
CCDC180	chr9:97,307,659-97,378,751	[259]
CCND1	chr11:69,641,156-69,654,474	[234,237]
COL11A1	chr1:102,876,473-103,108,522	[236,237,238]
COL5A1	chr9:134,641,803-134,844,843	[236,244]
CR1	chr1:207,496,157-207,641,765	[230]
CREB5	chr7:28,412,518-28,825,894	[239]
CST3	chr20:23,633,657-23,637,955	[4]
DIRC3	chr2:217,319,167-217,756,593	[238,240]
EDN1	chr6:12,290,361-12,297,194	[253]
EFEMP1	chr2:55,865,967-55,923,782	[237,238]
ESRRB	chr14:76,376,137-76,501,837	[247]
EVX2	chr2:176,077,472-176,083,962	[238]
FDPS	chr1:155,308,866-155,320,665	[237]
FGA	chr4:154,585,275-154,590,742	[4]
FMNL2	chr2:152,335,174-152,649,826	[259]
FRMPD4	chrX:12,138,473-12,724,523	[248]
FTO	chr16:53,704,156-54,121,941	[237]

GCK	chr7:44,144,275-44,189,439	[238]
GFPT1	chr2:69,319,780-69,387,227	[242]
GLCCI1	chr7:7,968,796-8,089,080	[244]
GSN	chr9:121,268,162-121,332,842	[4]
HLA-DRB1	chr6:32,578,775-32,589,848	[260]
HP	chr16:72,054,505-72,061,055	[253]
HSPB1	chr7:76,302,673-76,304,292	[79]
IFITM3	chr11:319,676-320,860	[261]
IFT43	chr14:75,985,763-76,083,742	[238]
ITGB5	chr3:124,761,948-124,887,365	[238]
KALRN	chr3:124,033,369-124,726,325	[238]
KCNH2	chr7:150,944,961-150,978,321	[238]
KIAA1755	chr20:38,210,503-38,260,735	[238]
KLHL1	chr13:69,700,597-70,108,452	[241]
LCN2	chr9:128,149,453-128,153,453	[79]
LINC00890/ALG13	chrX:111,681,170-111,760,649	[248]
LNPK	chr2:175,923,882-176,002,267	[237]
LOXL1	chr15:73,926,462-73,952,136	[237]
LTBP1	chr2:32,946,953-33,399,509	[237,238]
LYZ	chr12:69,348,381-69,354,234	[4]
MAP2K1	chr15:66,386,912-66,491,544	[79]
MAP2K2	chr19:4,090,321-4,124,122	[79]
MKNK2	chr19:2,037,471-2,051,244	[237]
MKX	chr10:27,672,874-27,745,819	[237]
MS4A1	chr11:60,455,847-60,470,752	[254]
MUC13	chr3:124,905,442-124,934,751	[238]
MYL7	chr7:44,138,864-44,141,332	[238]
MYO1F	chr19:8,520,778-8,577,442	[238]
NCBP1	chr9:97,633,821-97,673,748	[259]
NFU1	chr2:69,396,126-69,437,435	[242]
NOS1	chr12:117,208,142-117,361,626	[253]
OAS1	chr12:112,906,962-112,919,903	[262,263,264]
PLD2	chr17:4,807,152-4,823,430	[238]
POLE2	chr14:49,643,555-49,688,214	[241]
PSMA4	chr15:78,540,444-78,552,417	[265]
RALGPS1	chr9:126,914,782-127,223,166	[237]
RBP4	chr10:93,591,694-93,601,235	[74,75]
RGMB	chr5:98,773,663-98,796,494	[237]
RNF213	chr17:80,260,852-80,398,794	[266]
RYR1	chr19:38,433,691-38,587,564	[253]
SAP30BP	chr17:75,667,338-75,708,059	[246]
SASH1	chr6:148,342,838-148,552,044	[246]
SERPINE1	chr7:101,127,104-101,139,247	[237]
SLC39A8/UBE2D3	chr4:102,261,666-102,345,482	[248]

SMAD6	chr15:66,702,236-66,782,849	[238]
SNAP47	chr1:227,735,435-227,781,226	[237]
SOX17	chr8:54,457,935-54,460,892	[265]
STAG1	chr3:136,336,236-136,752,378	[237]
STK24	chr13:98,445,185-98,577,107	[248]
SYCP1	chr1:114,854,863-114,995,370	[259]
TBC1D2	chr9:98,199,011-98,255,649	[259]
TGFB3	chr14:75,958,097-75,981,995	[238]
TGFBR1	chr9:99,105,113-99,154,192	[244]
THSD7A	chr7:11,370,365-11,832,198	[244]
TIMP2	chr17:78,852,977-78,925,387	[244]
TMEM106B	chr7:12,211,294-12,243,367	[267]
TMEM176B	chr7:150,791,301-150,800,364	[238]
TMEM176A	chr7:150,800,769-150,805,118	[238]
TNC	chr9:115,019,575-115,118,157	[244]
TNFRSF6B	chr20:63,696,652-63,698,684	[235]
TNFRSF19	chr13:23,570,412-23,676,093	[235]
TPTE2	chr13:19,422,877-19,561,532	[232]
TSPO	chr22:43,151,559-43,163,242	[268]
TTLL5	chr14:75,661,246-75,955,079	[237,238]
TTR	chr18:31,591,877-31,598,821	[4]
UMPS	chr3:124,730,452-124,749,273	[238]
UNC5C	chr4:95,162,504-95,548,973	[231]
VCAN	chr5:83,471,744-83,582,302	[237]
WNT4	chr1:22,117,313-22,143,097	[237]
YWHAZ	chr8:100,916,523-100,952,020	[79]
ZBTB38	chr3:141,368,504-141,449,792	[237]
ZNF438	chr10:30,844,632-31,031,865	[237]
ZNF782	chr9:96,816,269-96,854,514	[259]
ZNF804A	chr2:184,598,529-184,939,492	[244]

Table 8. Custom content of Illumina GCRA. The columns report the additional genes containing meaningful SNPs, with genomic coordinates (GRCh38/hg38), and references from literature.

3.4.3 Long-range PCR amplification of TTR-containing region and amplicon-based long-read sequencing

The *TTR*-containing region has been amplified in n=323 DNA samples from symptomatic patients affected by ATTRv amyloidosis, divided as follows:

	Country	**Centre / contact person**	**ATTRv**	
			V30M	**nV30M**
1	Sweden	Umea / I. Anan	92	0
2	Portugal	Lisbon / I. Conceicao	85	2
3	Bulgaria	Sofia / A. Todorova – I. Tournev	4	25
4	Italy	Pavia / L. Obici – A. Cortese	5	25
		Rome / M. Luigetti	10	9
5	France	Creteil / V. Planté-Bordeneuve	26	0
6	Spain	Barcelona / R. Rojas Garcia	5	2
7	US	Boston / T. Prokaeva	1	1
8	Brasil	São Paulo / W. Marques – P. Tomaselli	16	15
			323	

Table 9. Distribution of DNA samples from symptomatic ATTRv patients amplified by long-range PCR (n=323).

The most frequent pathogenic variants in our population were: V30M (p.Val50Met, 244/323, 75%), E89Q (p.Glu109Gln, 24/323, 7%), V122I (p.Val142Ile, 20/323, 6%), and F64L (p.Phe84Leu, 13/323, 4%).

The overall distribution of *TTR* mutations in our sample population is reported below (**Fig**. **18**).

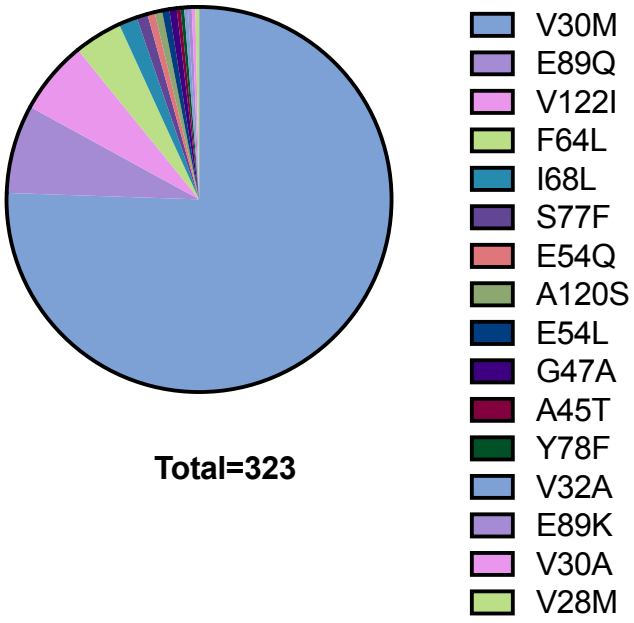

Fig. **18**. Distribution of *TTR* mutations across the DNA samples from ATTRv symptomatic patients amplified by long-range PCR and undergoing amplicon-based sequencing (n=323).

A representative example of the PCR amplicons of *TTR*-containing region (9,227 bp) from DNA obtained from randomly selected samples from n=8 different participating Centres is shown below (**Fig**. **19**).

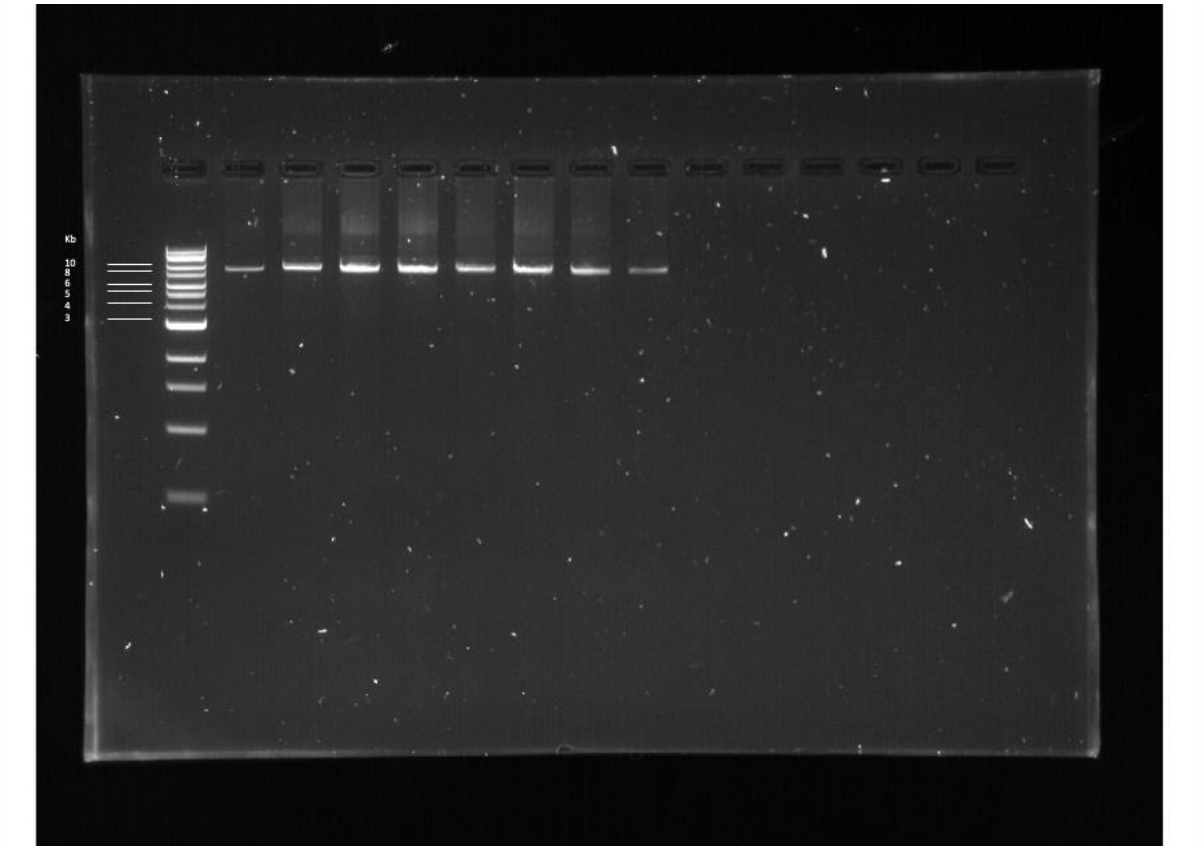

Fig. **19**. PCR amplicons of *TTR*-containing region (9,227 bp) from n=8 DNA samples from different enrolled Centres (Ladder: Quick-Load® 1 kb Extend DNA Ladder).

Overall, n=323 DNA samples from ATTRv symptomatic patients have been sequenced, although n=122 samples failed sequencing because of off-target/non-specific sequencing (insufficient coverage [<100%] or mean depth [<15%]).
The distribution of DNA samples, by Country and mutation, from ATTRv symptomatic patients which underwent effective amplicon-based sequencing is shown in **Table 10** and **Fig**. **20**.

	Country	Centre / contact person	ATTRv	
			V30M	nV30M
1	Sweden	Umea / I. Anan	9	0
2	Portugal	Lisbon / I. Conceicao	70	2
3	Bulgaria	Sofia / A. Todorova – I. Tournev	7	6
4	Italy	Pavia / L. Obici – A. Cortese	4	26
		Rome / M. Luigetti	8	8
5	France	Creteil / V. Planté-Bordeneuve	24	0
6	Spain	Barcelona / R. Rojas Garcia	5	2
8	Brasil	São Paulo / W. Marques – P. Tomaselli	15	15
			201	

Table 10. Distribution of DNA samples from symptomatic ATTRv patients which underwent effective amplicon-based sequencing (n=201).

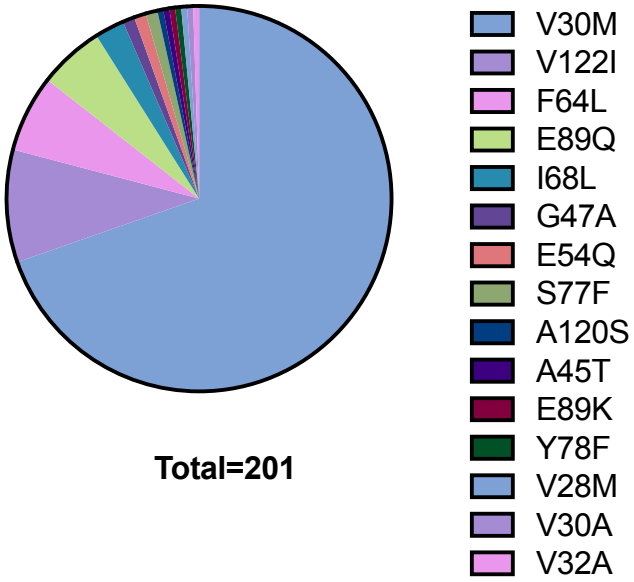

Fig. **20**. Distribution of *TTR* mutations across the DNA samples from ATTRv symptomatic patients amplified by long-range PCR which underwent effective amplicon-based sequencing (n=201).

PacBio sequencing statistics are shown in **Table 11**.

Median counts (=median number of total reads) (min, max)	**Median counts on target (=median number of reads in *TTR*) (min, max)**	**Median coverage (median % of *TTR* region covered) (min, max)**	**Median mean_depth on *TTR* region (min, max)**
14,972 (26, 36741)	14,865 (26, 36733)	100 (100, 100)	14,837,3 (24,0308, 36616,5)

Table 11. PacBio sequencing statistics.

An example of long-read sequencing of the *TTR* region in a Swedish (*above*) and Portuguese (*below*) patients both carrying V30M (p.Val50Met) variant is shown below (**Fig. 21**).

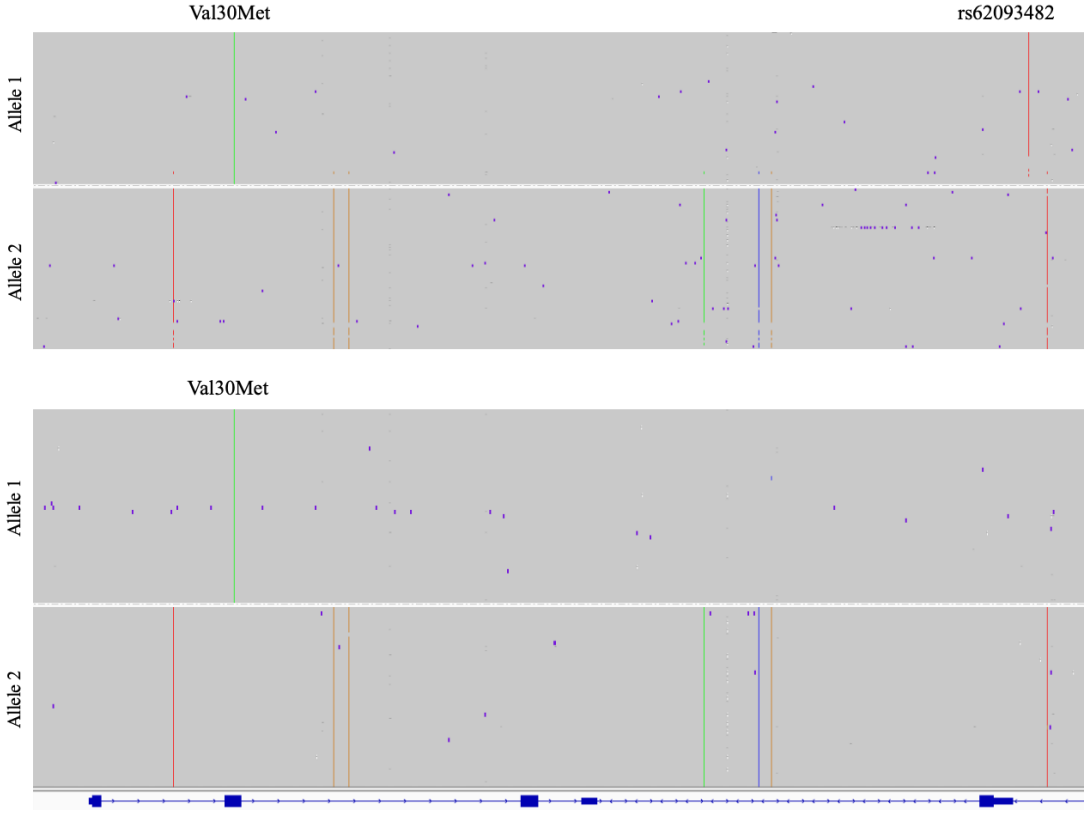

Fig. 21. Integrative Genomics Viewer (IGV) visualization of PacBio mapped reads to the *TTR*-containing region of two patients carrying V30M (p.Val50Met) mutation, from Sweden (*above*) and Portugal (*below*), respectively. In the Swedish patient the common rs62093482 SNP is highlighted (*see below for details*).

3.4.4 Confirmation of *TTR* pathogenic mutations and frequency of G6S (p.Gly26Ser) polymorphism

TTR pathogenic variants were confirmed in all the *TTR* samples sequenced by long-read sequencing (n=201/201, 100%). In n=2 cases, one for Portugal (Lisbon) and one from Bulgaria (Sofia), the V30M (p.Val50Met) variant was in homozygous state.

The G6S (p.Gly26Ser) polymorphism was found in 21/402 alleles (5%).
This polymorphism was *in trans* with a pathogenic *TTR* variant in 16/21 (76%) alleles (n=14 V30M, p.Val50Met; n=1 E89Q, p.Glu109Gln; n=1 V122I, p.Val142Ile), while it was *in cis* in 5/21 alleles (24%) (n=3 V30M, p.Val50Met; n=1 A45T, p.Ala65Thr; n=1 V30A, p.Val50Ala).

3.4.5 TTR intragenic haplotype analysis

Overall, in our sample population n=8 more common haplotypes have been identified, of which n=2 were more frequently observed among ATTRv patients carrying the V30M (p.Val50Met) pathogenic variant. Indeed, V30M-1 haplotype, defined only by the V30M (p.Val50Met) mutation itself, was found in 105/402 alleles (26%), while V30M-2 haplotype, defined by the V30M (p.V30M) mutation plus seven intronic variants, in 15/402 alleles (4%). The other haplotypes identified, ordered by frequency, were: F64L haplotype defined by F64L (p.Phe84Leu) mutation plus six intronic variants (12/402 alleles, 3%); E89Q haplotype defined only by the E89Q (p.Glu109Gln) variant itself (11/402 alleles, 3%); V122I-1 haplotype defined by the V122I (p.Val142Ile) mutation plus five intronic variants (10/402 alleles, 2%); V30M-3 haplotype defined by the V30M (p.V30M) mutation plus one variant, rs62093482, located in the 3' untranslated region (3' UTR) (8/402 alleles, 2%); V122I-2 haplotype defined by the V122I (p.Val142Ile) mutation plus eight intronic variants (6/402 alleles, 1.5%); and I68L haplotype defined by the I68L (p.Ile88Leu) variant and eight intronic variants (5/402 alleles, 1%). (**Fig**. **22** and **23**).

Six SNPs (rs723744, rs1080093, rs1080094, rs3764476, rs7235277, and rs3794884) were common between four different haplotypes (V30M-2, F64L, V122I-2, and I68L).
Table 12 showed all the genetic variants in the region of interest, while all different haplotypes are better detailed in **Table 13**.

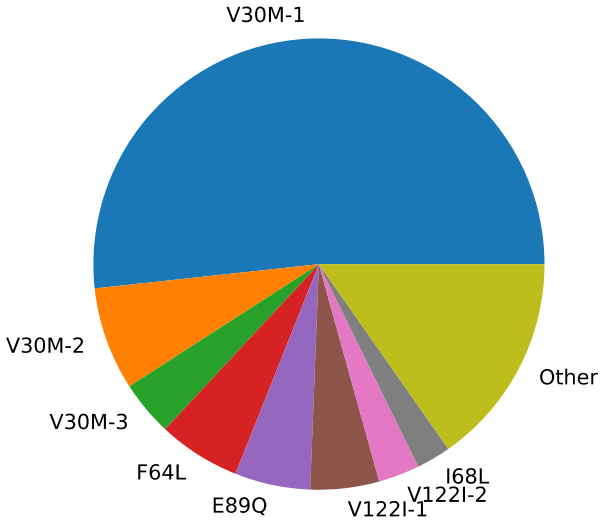

Fig. **22**. Haplotype count across our sample population.

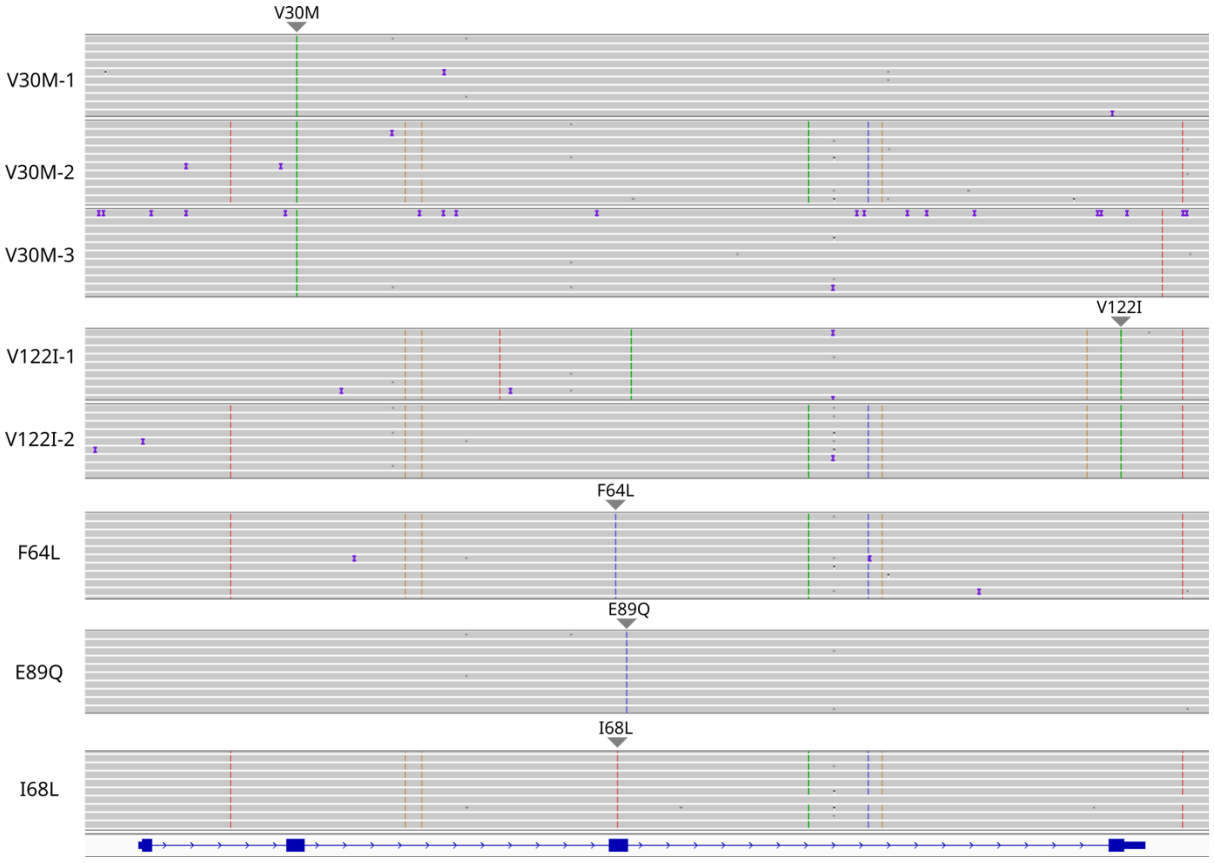

Fig. **23**. IGV graphical representation of n=8 more common haplotypes in our sample population.

dbSNP ID	Pos.	Ref.	Alt.	Protein variant
rs906976449	31590853	T	A	
rs116409170	31591070	C	T	
rs3794885	31591160	A	G,T	
rs79748512	31591221	G	A	
	31591234	C	T	
rs1157253322	31591913	A	T	
rs377052919	31591970	C	T	
rs9304103	31592074	A	G	
rs7231173	31592180	A	G	
rs113997467	31592439	A	G	
rs723744	31592513	G	T	
rs73420308	31592770	T	A	
rs945529882	31592810	C	T	
rs1800458	31592902	G	A	G6S (p.Gly26Ser)
	31592955	T	C	
	31592968	G	A	V28M (p.Val48Met)
rs28933979	31592974	G	A,C	V30M (p.Val50Met)
rs79977247	31592975	T	C,G	V30A (p.Val50Ala)
	31592981	T	C	V32A (p.Val52Ala)
rs121918078	31593019	G	A	A45T (p.Ala65Thr)
rs121918090	31593026	G	C	G47A (p.Gly67Ala)
rs916691210	31593233	G	A	
rs1080093	31593717	C	A,G	
rs112618844	31593727	C	T	
rs72922947	31593821	G	A	
rs1080094	31593832	A	G	
rs17740912	31594051	T	G	
rs13381331	31594224	G	A	
rs141035204	31594368	A	T	
rs1217994235	31594602	G	A	
	31594604	C	G	
rs888005533	31594747	C	A	
rs59882235	31595044	T	A	
rs769870882	31595113	C	T	
	31595139	G	C	E54Q (p.Glu74Gln)
	31595140	A	T	
rs121918091	31595169	T	C	F64L (p.Phe84Leu)
	31595171	T	G	F64L (p.Phe84Leu)
rs121918085	31595181	A	T	I68L (p.Ile88Leu)
rs121918071	31595209	C	A	S77F (p.Ser97Phe)

rs958191819	31595212	A	T	Y78F (p.Tyr98Phe)
rs121918082	31595244	G	C	E89Q (p.Glu109Gln)
	31595244	G	A	E89K (p.Glu109Lys)
rs75517067	31595274	G	A,C	
rs934648359	31595576	C	T	
rs189110087	31595625	G	A	
	31595638	T	C	
rs753737001	31595652	T	C	
rs3764476	31596497	C	A,T	
rs1341626812	31596748	G	A	
rs7235277	31596910	G	C	
	31596951	A	T	
rs3794884	31597008	T	G	
	31597019	T	C	
	31597054	T	C	
rs73420309	31597169	C	T	
rs1667250	31597193	C	T	
rs114136663	31597247	G	A	
rs114664116	31597457	G	C	
rs58678032	31597853	A	T	
rs1791227	31597868	T	A,C	
rs75717327	31598093	T	C,G	
rs1667251	31598416	T	G	
rs79483763	31598477	T	C	
rs36204272	31598550	G	C	
rs2276382	31598648	G	A	
rs876658108	31598649	G	T	A120S (p.Ala140Ser)
rs76992529	31598655	G	A	V122I (p.Val142Ile)
rs12226	31598696	C	A,T	
rs62093482	31598936	C	T	
rs58172837	31599020	G	A	
rs1791228	31599077	C	T	
rs7231903	31599118	T	C	
rs557189384	31599213	C	A	
rs954344068	31599229	C	T	
rs75032823	31599265	G	A	
rs142786948	31599606	T	C	
rs77973165	31599879	A	G	
rs77724619	31599899	A	C	
rs1422296199	31599985	G	A	

Table 12. Genetic variants in the region of interest (*TTR*). The columns show the identification code in dbSNP (dbSNP ID), whenever available, the hg38-based coordinate positions (Pos.), the reference (Ref.) and alternative (Alt.) nucleotides of each variant, and the protein variant for each pathogenic mutation.

Haplotype name	*TTR* pathogenic mutation	*TTR* SNPs											
		rs116409170	**rs723744**	**rs1080093**	**rs1080094**	**rs141035204**	**rs75517067**	**rs3764476**	**rs7235277**	**rs3794884**	**rs1667251**	**rs62093482**	**rs1791228**
V30M-1	rs28933979 (V30M)	0	0	0	0	0	0	0	0	0	0	0	0
V30M-2	rs28933979 (V30M)	0	1	1	1	0	0	1	1	1	0	0	1
F64L	rs121918091 (F64L)	0	1	1	1	0	0	1	1	1	0	0	0
E89Q	rs121918082 (E89Q)	0	0	0	0	0	0	0	0	0	0	0	0
V122I-1	rs76992529 (V122I)	0	0	1	1	1	1	0	0	0	0	0	1
V30M-3	rs28933979 (V30M)	0	0	0	0	0	0	0	0	0	0	1	0
V122I-2	rs76992529 (V122I)	0	1	1	1	0	0	1	1	1	1	0	1
I68L	rs121918085 (I68L)	1	1	1	1	0	0	1	1	1	0	0	1

Table 13. Detailed description of *TTR* intragenic haplotypes across different mutations. SNP=single nucleotide polymorphism; 0=absent; 1=present.

Among ATTRv patients carrying the V30M (p.Val50Met) mutation, the V30M-1 haplotype, entailing only V30M (p.Val50Met) variant, was the most frequent among Portuguese (70/142 alleles, 49%), Brazilian (15/142 alleles, 11%) and French (12/142 alleles, 8%). Contrarily, most of Swedish ATTRv V30M (p.Val50Met) patients carried a haplotype which entails, together with the V30M (p.Val50Met) variant, a single SNP, located in the 3'UTR, rs62093482 (V30M-3, 7/142 alleles, 5%), which was absent from other populations, except for one patient from the Italian cohort (**Fig**. **24**).

In our sample population, the V30M (p.Val50Met) and V122I (p.Val142Ile) were the pathogenic mutations associated to a greater number of haplotypes each. Haplotype frequency, divided by *TTR* pathogenic mutations (V30M and V122I) are reported in **Fig**. **25** and **26**, respectively. Indeed, V30M (p.Val50Met) haplotype was different between Portuguese/Brazilian and French ATTRv patients *vs* Swedish ATTRv kindreds (V30M-1 and 3, respectively). Another V30M (p.V30M) haplotype (V30M-2) was found across Italy (7/142 alleles, 5%), France (5/142 alleles, 3%), and Bulgaria (3/142 alleles, 2%). As concerns V122I (p.Val142Ile) haplotypes, the V122I-1 was present among Portuguese (9/19 alleles, 47%), and Brazilian (1/19 alleles, 5%) ATTRv kindreds. Contrarily, the V122I-2 haplotype was unique to the ATTRv Brazilian patients harboring V122I (p.Val142Ile) variant (6/19 alleles, 32%).

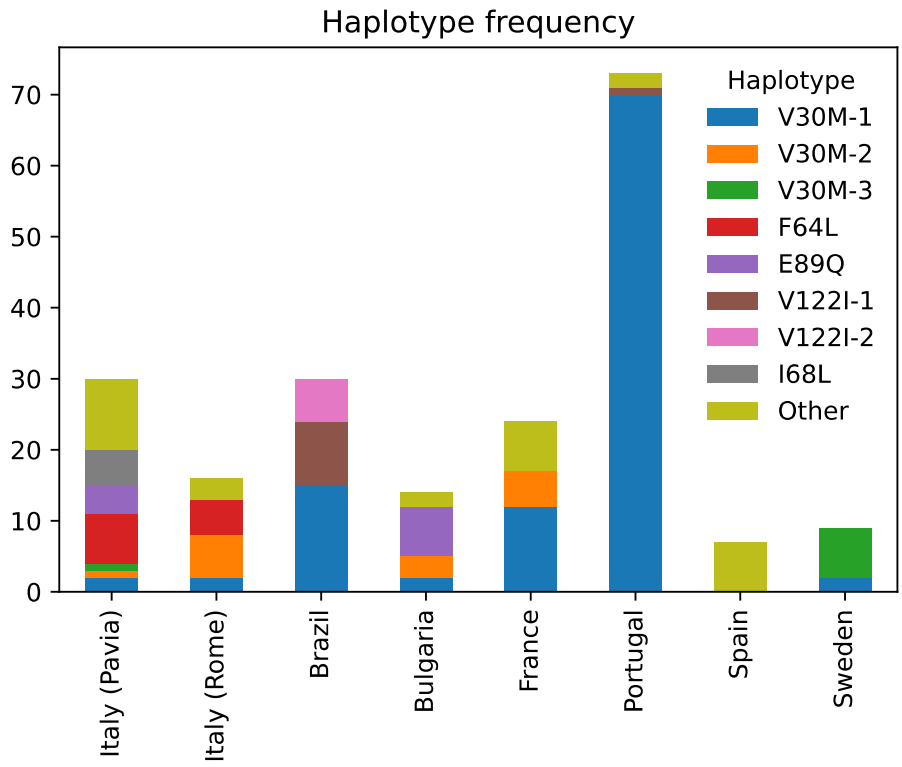

Fig. **24**. Haplotype frequency across our sample population, divided by Country.

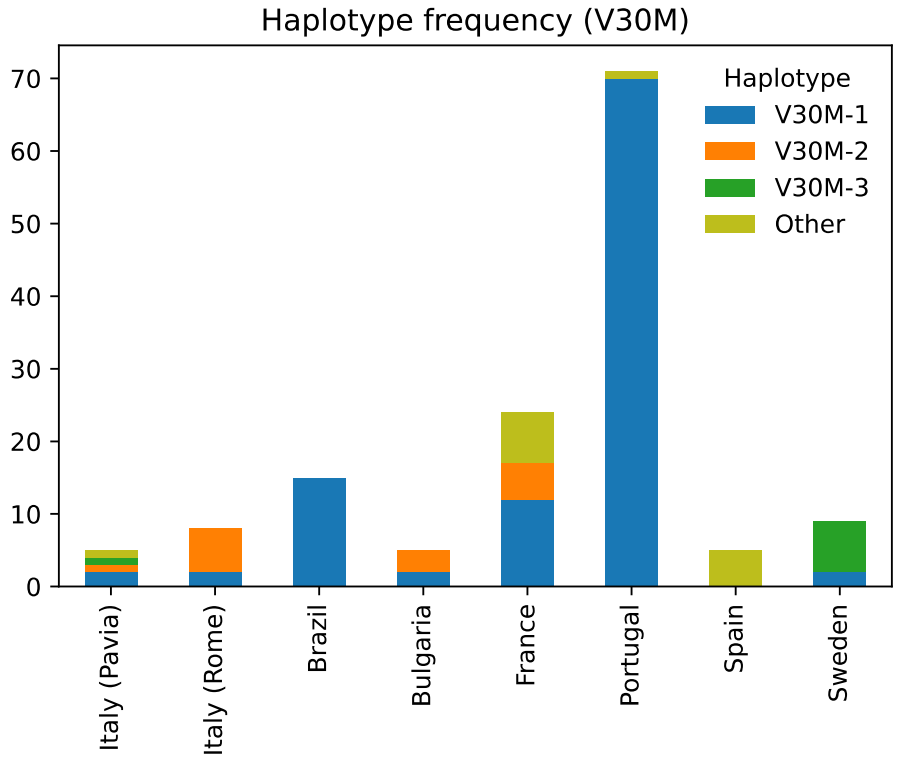

Fig. **25**. V30M haplotype frequency across our sample population, divided by Country.

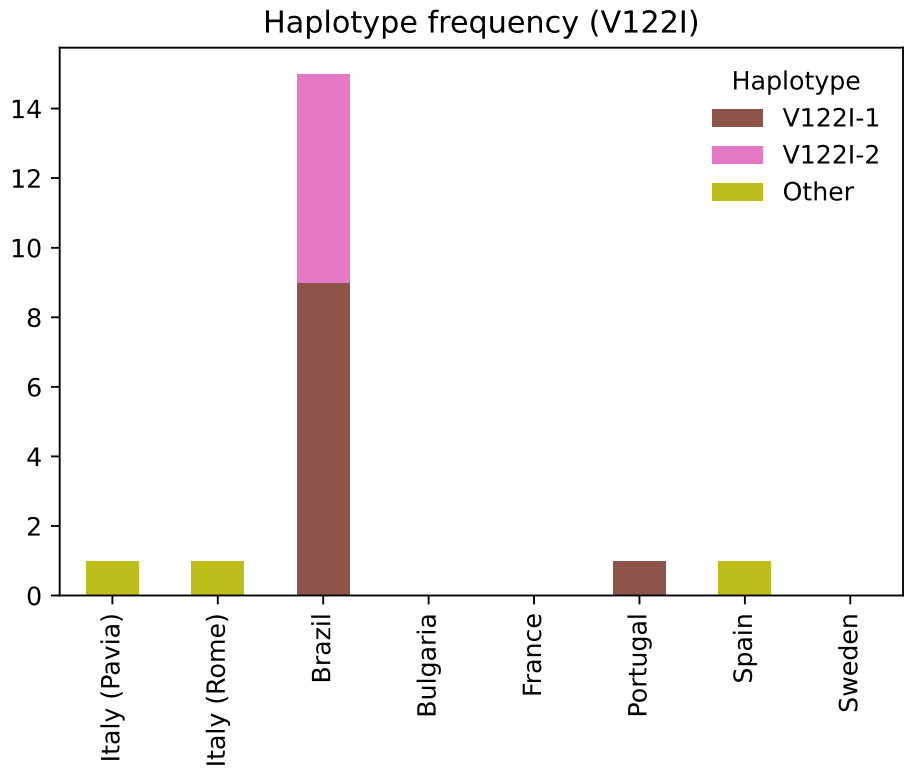

Fig. **26**. V122I haplotype frequency across our sample population, divided by Country.

3.5 Discussion

These are the preliminary results of a study stemming from a collaborative effort from many Centres worldwide aimed at better understanding the genetic variability underlying ATTR amyloidosis across different populations and ethnicities, either at *TTR* gene (in *cis*- or *trans*) or at genome-wide level, using genotype arrays and novel, third-generation, sequencing methods.

To date, n=52 Centres from n=19 Countries worldwide have been included. Overall, n=3596 DNA samples from ATTRv and ATTRwt patients, and controls, spanning across different populations and ethnicities, have been collected, and are ready for genotyping and long-read sequencing.

After a comprehensive literature review, a custom content entailing previously reported SNPs in *TTR* itself, distant meaningful genes, acting as possible modifiers of ATTRv or ATTRwt amyloidosis (e.g., *RBP4*, *AR*, *C1QA*, and *C1QC*), or other genes whose genetic variation has been previously linked to other significant diseases (e.g., light-chain amyloidosis), have been added to the backbone of standard GCRA.

Although preliminarily, we have started our work by trying to characterize the genetic variation surrounding the *TTR* gene in ATTRv amyloidosis symptomatic patients to define variant-disease associations which define different intragenic haplotypes.

An haplotype is a sequence of genetic variants which co-occur along a single chromosome since they are inherited together from one parent because of their genetic linkage[269]. Resolving haplotype structure is fundamental to track inheritance in human pedigrees and populations (linkage analysis and population genetics), to map regions of meiotic recombination, to identify variant-disease associations (association studies), to establish compound heterozygous states (clinical genetics), and to study allele-specific phenomena, as DNA methylation, or gene expression[221]. Phased haplotypes are also used to improve the power of GWA studies[270]. Accurate haplotype assignment can be easily achieved by novel third-generation sequencing technologies (LRS) provided by PacBio or Oxford Nanopore.

In our study n=323 *TTR* DNA samples from ATTRv symptomatic patients, mostly harboring V30M (p.Val50Met) variant (244/323, 75%), have been amplified by an optimized long-range PCR, and then sequenced on Sequel IIe System. Unfortunately, because of off-

target amplification or insufficient coverage, only n=201 *TTR* DNA samples have been effectively sequenced, and further analyzed.

LRS was able to confirm the *TTR* mutations reported by the referring clinicians in all the sequenced cases (n=201/201, 100%). The allele frequency of the well-known neutral G6S (p.Gly26Ser) polymorphism was equal to 5% (21 out of 402 alleles), which was in agreement with literature data[44]. In 5 out of 21 alleles (24%) this variant was *in cis*, while in the remaining n=16 alleles (76%) it was *in trans* with a pathogenic *TTR* variant, mostly V30M (p.Val50Met) mutation, according to the worldwide prevalence of *TTR* variants.

The G6S (p.Gly26Ser) was originally described in Scottish kindreds without amyloidosis. This variant, arising from a G→A transition (transition at a CG dinucleotide "hot spot") in codon 6 located in the N-terminal region, was previously found with an allele frequency of 5% in Caucasians, and of 1% in the African Americans, while it was not reported in any sample of Asian or African origin. These data were more easily explained by postulating a single Caucasian founder and by considering the admixture of "Caucasian" genes in the African American population. However, since this variant arose in a mutational hot spot, it could have arisen on multiple occasions, although, if this was the case, the absence of the SNP from Asian and African populations would be unexplained. The G6S (p.Gly26Ser) is thus taught to be a common non-amyloidogenic polymorphism among Caucasians[44].

LRS also helped identifying and phasing different intragenic haplotypes across our population, some of them defined only by the pathogenic *TTR* mutation, and others also by other *TTR* variants (SNPs) *in cis* with the pathogenic mutation itself. Overall, n=8 more frequent haplotypes have been identified. The most frequent haplotype was that defined only by the V30M (p.Val50Met) mutation itself (26%). Considering the haplotype distribution per Country, this haplotype was the most frequent across Portuguese (49%), Brazilian (11%), and French (8%) ATTRv V30M (p.Val50Met) patients. Indeed, as regards the Portuguese and Brazilian V30M (p.Val50Met) ATTRv patients, a common origin of the V30M (p.Val50Met) mutation has been previously hypothesized, which probably arose in Portugal and then spread from Portugal to Brazil with an age estimate of the most recent common ancestor (MRCA) of 750 and 650 years in Portuguese and Brazilian kindreds, respectively[67].

Contrarily, a different haplotype was found in the Swedish V30M (p.Val50Met) ATTRv patients with a corresponding age estimate for the MRCA of 375 years[67]. Notably, a single SNP, rs62093482, located in the 3' UTR, was previously found to be almost unique to the Swedish V30M (p.Val50Met) ATTRv patients. Indeed, this variant was found to be absent

from French and Japanese V30M (p.Val50Met) ATTRv patients, and uncommon among Portuguese V30M (p.Val50Met) ATTRv patients. Also, in our Swedish V30M (p.Val50Met) ATTRv patients the most common haplotype was that entailing the V30M (p.Val50Met) mutation and this SNP (5%), which was absent from the Portuguese and other populations, except for one single italian patient. However, although this SNP was initially taught to act as a microRNA binding site, possibly downregulating TTR levels and thus contributing to lower penetrance and later onset of ATTRv amyloidosis in the Swedish population[213], this was not further confirmed by functional studies[72,73].

Haplotypes associated to *TTR* pathogenic variants other than V30M (p.Val50Met) mutation have not been investigated so far. Apart from the V30M (p.Val50Met) variant, the V122I (p.Val142Ile) mutation was the other variant associated with more than one haplotype. Indeed, two different haplotypes have been found, both defined by the pathogenic mutation itself and five and eight different intronic variants, respectively, of which only three in common between the two (rs1080093, rs1080094, and rs1791228). Notably, while the first one was found both among Portuguese (47%) and Brazilian (5%) ATTRv kindreds, the second one was unique to the Brazilian ATTRv patients (32%), thus possibly pointing to a different founder effect, although this has to be further confirmed in a larger sample population.

Some SNPs, other than the rs62093482 mentioned above, were uniquely associated to certain pathogenic variants in certain populations, in detail: rs141035204, rs75517067 to the V122I (p.Val142Ile) variant among the Brazilian and Portuguese ATTRv patients, rs1667251 to the V122I (p.Val142Ile) variant in the Brazilian ATTRv kindreds, and rs116409170 to the I68L (p.Ile88Leu) variant in the Italian ATTRv patients. Contrarily, six SNPs (rs723744, rs1080093, rs1080094, rs3764476, rs7235277, and rs3794884) were common between four different haplotypes (V30M-2, F64L, V122I-2, and I68L).

Our study harbors some limitations. First, LRS was performed on a preliminary and rather small cohort of ATTRv symptomatic patients which has still not captured the genetic heterogeneity of the disease. Therefore, LRS has to be further extended to the whole cohort in the next months to possibly draw more meaningful considerations as regards variant-disease associations. Second, although targeted LRS allowed for rapid phasing of disease haplotypes (variants *in cis* with the pathogenic *TTR* mutation), the genomic region considered was rather small (approximately 9,000 bp) and did not allow for a proper distinction of haplotypes across different mutations and populations. A better definition of disease haplotypes might be

possible by a characterization of a larger genomic region surrounding, up- and downstream, *TTR* in a bigger cohort of ATTRv patients harboring different *TTR* pathogenic variants.

Third, variants transmitted by the non-carrying parent possibly harboring a trans-acting effect, were not considered. Finally, potential correlations with clinical variables, especially AOO, have not been investigated so far.

The collection of DNA *TTR* samples is still ongoing and we aim at reaching the target enrollment (> 6,000 samples, considering ATTRv and ATTRwt patients, and healthy controls) by the end of 2024. By December 2023 the genotyping of all already collected DNA *TTR* samples from ATTRv symptomatic patients will be carried out. Also, LRS will be extended to the same sample population in the next few months, looking both at *TTR* region itself and loci harboring genetic variations which will be identified by genotype arrays.

Correlations with different clinical variables, especially AOO, phenotype severity, and response to treatment will be considered since this will hopefully help clinicians to predict AOO in ATTRv patients, prompting earlier diagnosis, closer monitoring, and therapy initiation of this severe but treatable condition.

4. Bibliography

1. ANDRADE C. A PECULIAR FORM OF PERIPHERAL NEUROPATHY. *Brain*. 1952;75(3):408-427. doi:10.1093/brain/75.3.408
2. Sousa A, Andersson R, Drugge U, Holmgren G, Sandgren O. Familial Amyloidotic Polyneuropathy in Sweden: Geographical Distribution, Age of Onset, and Prevalence. *Hum Hered*. 1993;43(5):288-294. doi:10.1159/000154146
3. Kato-Motozaki Y, Ono K, Shima K, et al. Epidemiology of familial amyloid polyneuropathy in Japan: Identification of a novel endemic focus. *J Neurol Sci*. 2008;270(1-2):133-140. doi:10.1016/j.jns.2008.02.019
4. http://amyloidosismutations.com/mut-attr.php.
5. Benson MD, Buxbaum JN, Eisenberg DS, et al. Amyloid nomenclature 2020: update and recommendations by the International Society of Amyloidosis (ISA) nomenclature committee. *Amyloid*. 2020;27(4):217-222. doi:10.1080/13506129.2020.1835263
6. Planté-Bordeneuve V, Lalu T, Misrahi M, et al. Genotypic-phenotypic variations in a series of 65 patients with familial amyloid polyneuropathy. *Neurology*. 1998;51(3):708-714. doi:10.1212/WNL.51.3.708
7. Koike H, Tanaka F, Hashimoto R, et al. Natural history of transthyretin Val30Met familial amyloid polyneuropathy: Analysis of late-onset cases from non-endemic areas. *J Neurol Neurosurg Psychiatry*. 2012;83(2):152-158. doi:10.1136/jnnp-2011-301299
8. Coelho T, Ines M, Conceicaõ I, Soares M, De Carvalho M, Costa J. Natural history and survival in stage 1 Val30Met transthyretin familial amyloid polyneuropathy. *Neurology*. 2018;91(21):E1999-E2009. doi:10.1212/WNL.0000000000006543
9. Adams D, Gonzalez-Duarte A, O'Riordan WD, et al. Patisiran, an RNAi Therapeutic, for Hereditary Transthyretin Amyloidosis. *N Engl J Med*. 2018;379(1):11-21. doi:10.1056/nejmoa1716153
10. Adams D, Tournev IL, Taylor MS, et al. Efficacy and safety of vutrisiran for patients with hereditary transthyretin-mediated amyloidosis with polyneuropathy: a randomized clinical trial. *Amyloid*. 2023;30(1):18-26. doi:10.1080/13506129.2022.2091985
11. Benson MD, Waddington-Cruz M, Berk JL, et al. Inotersen Treatment for Patients with Hereditary Transthyretin Amyloidosis. *N Engl J Med*. 2018;379(1):22-31.

doi:10.1056/nejmoa1716793

12. Gillmore JD, Gane E, Taubel J, et al. CRISPR-Cas9 In Vivo Gene Editing for Transthyretin Amyloidosis. *N Engl J Med*. 2021;385(6):493-502. doi:10.1056/nejmoa2107454
13. Sousa A, Coelho T, Barros J, Sequeiros J. Genetic epidemiology of familial amyloidotic polyneuropathy (FAP)-type I in Póvoa do Varzim and Vila do Conde (north of Portugal). *Am J Med Genet*. 1995;60(6):512-521. doi:10.1002/ajmg.1320600606
14. Dardiotis E, Koutsou P, Papanicolaou EZ, et al. Epidemiological, clinical and genetic study of familial amyloidotic polyneuropathy in Cyprus. *Amyloid*. 2009;16(1):32-37. doi:10.1080/13506120802676948
15. Reinés J, Vera T, Martín M, et al. Epidemiology of transthyretin-associated familial amyloid polyneuropathy in the Majorcan area: Son Llàtzer Hospital descriptive study. *Orphanet J Rare Dis*. 2014;9(1):29. doi:10.1186/1750-1172-9-29
16. Cruz MW. Regional differences and similarities of familial amyloidotic polyneuropathy (FAP) presentation in Brazil. *Amyloid*. 2012;19(sup1):65-67. doi:10.3109/13506129.2012.673183
17. Reilly MM, Adams D, Booth DR, et al. Transthyretin gene analysis in European patients with suspected familial amyloid polyneuropathy. *Brain*. 1995;118(4):849-856. doi:10.1093/brain/118.4.849
18. Parman Y, Adams D, Obici L, et al. Sixty years of transthyretin familial amyloid polyneuropathy (TTR-FAP) in Europe. *Curr Opin Neurol*. 2016;29(Supplement 1):S3-S13. doi:10.1097/WCO.0000000000000288
19. Zhen DB, Swiecicki PL, Zeldenrust SR, Dispenzieri A, Mauermann ML, Gertz MA. Frequencies and geographic distributions of genetic mutations in transthyretin- and non-transthyretin-related familial amyloidosis. *Clin Genet*. 2015;88(4):396-400. doi:10.1111/cge.12500
20. Liu G, Ni W, Wang H, et al. Clinical features of familial amyloid polyneuropathy carrying transthyretin mutations in four Chinese kindreds. *J Peripher Nerv Syst*. 2017;22(1):19-26. doi:10.1111/jns.12196
21. Pan D, Bouligand J, Guiochon-Mantel A, Adams D. FAP in India: a first genetically proven case. *Orphanet J Rare Dis*. 2015;10(S1):P20. doi:10.1186/1750-1172-10-S1-P20
22. Schmidt HH, Waddington-Cruz M, Botteman MF, et al. Estimating the global

prevalence of transthyretin familial amyloid polyneuropathy. *Muscle Nerve*. 2018;57(5):829-837. doi:10.1002/mus.26034

23. Russo M, Obici L, Bartolomei I, et al. ATTRv amyloidosis Italian Registry: clinical and epidemiological data. *Amyloid*. 2020;27(4):259-265. doi:10.1080/13506129.2020.1794807
24. Adams D, Lozeron P, Theaudin M, et al. Regional difference and similarity of familial amyloidosis with polyneuropathy in France. *Amyloid*. 2012;19(sup1):61-64. doi:10.3109/13506129.2012.685665
25. Iorio A, De Angelis F, Di Girolamo M, et al. Most recent common ancestor of TTR Val30Met mutation in Italian population and its potential role in genotype-phenotype correlation. *Amyloid*. 2015;22(2):73-78. doi:10.3109/13506129.2014.994597
26. Sparkes RS, Sasaki H, Mohandas T, et al. Assignment of the prealbumin (PALB) gene (familial amyloidotic polyneuropathy) to human chromosome region 18q11.2?q12.1. *Hum Genet*. 1987;75(2):151-154. doi:10.1007/BF00591077
27. Tsuzuki T, Mita S, Maeda S, Araki S, Shimada K. Structure of the human prealbumin gene. *J Biol Chem*. 1985;260(22):12224-12227. doi:10.1016/S0021-9258(17)39013-0
28. Hiroyuki S, Naoko Y, Yasuyuki T, Yoshiyuki S. Structure of the chromosomal gene for human serum prealbumin. *Gene*. 1985;37(1-3):191-197. doi:10.1016/0378-1119(85)90272-0
29. Power DM, Elias NP, Richardson SJ, Mendes J, Soares CM, Santos CRA. Evolution of the Thyroid Hormone-Binding Protein, Transthyretin. *Gen Comp Endocrinol*. 2000;119(3):241-255. doi:10.1006/gcen.2000.7520
30. Ingenbleek Y, Young V. Transthyretin (Prealbumin) in Health and Disease: Nutritional Implications. *Annu Rev Nutr*. 1994;14(1):495-533. doi:10.1146/annurev.nu.14.070194.002431
31. Bellovino D, Morimoto T, Pisaniello A, Gaetani S. In Vitroandin VivoStudies on Transthyretin Oligomerization. *Exp Cell Res*. 1998;243(1):101-112. doi:10.1006/excr.1998.4137
32. Blake CCF, Geisow MJ, Oatley SJ, Rérat B, Rérat C. Structure of prealbumin: Secondary, tertiary and quaternary interactions determined by Fourier refinement at 1.8 Å. *J Mol Biol*. 1978;121(3):339-356. doi:10.1016/0022-2836(78)90368-6
33. Blake CCF, Geisow MJ, Swan IDA, Rerat C, Rerat B. Structure of human plasma prealbumin at 2.5 A resolution. *J Mol Biol*. 1974;88(1):1-12. doi:10.1016/0022-2836(74)90291-5

34. Minnella AM, Rissotto R, Antoniazzi E, et al. Ocular Involvement in Hereditary Amyloidosis. *Genes (Basel)*. 2021;12(7):955. doi:10.3390/genes12070955
35. Robbins J. Transthyretin from Discovery to Now. *Clin Chem Lab Med*. 2002;40(12). doi:10.1515/CCLM.2002.208
36. Enzyme Nomenclature. Recommendations 1978. Supplement 2: Corrections and Additions. *Eur J Biochem*. 1981;116(3):423-435. doi:10.1111/j.1432-1033.1981.tb05353.x
37. Noy N, Slosberg E, Scarlata S. Interactions of retinol with binding proteins: Studies with retinol-binding protein and with transthyretin. *Biochemistry*. 1992;31(45):11118-11124. doi:10.1021/bi00160a023
38. Blake CCF, Swan IDA, Rerat C, Berthou J, Laurent A, Rerat B. An X-ray study of the subunit structure of prealbumin. *J Mol Biol*. 1971;61(1):217-224. doi:10.1016/0022-2836(71)90218-X
39. Kanda Y, Goodman DS, Canfield RE, Morgan FJ. The Amino Acid Sequence of Human Plasma Prealbumin. *J Biol Chem*. 1974;249(21):6796-6805. doi:10.1016/S0021-9258(19)42128-5
40. Hamilton JA, Benson MD. Transthyretin: a review from a structural perspective. *Cell Mol Life Sci*. 2001;58(10):1491-1521. doi:10.1007/PL00000791
41. Fleming CE, Saraiva MJ, Sousa MM. Transthyretin enhances nerve regeneration. *J Neurochem*. 2007;103(2):831-839. doi:10.1111/j.1471-4159.2007.04828.x
42. Brouillette J, Quirion R. Transthyretin: A key gene involved in the maintenance of memory capacities during aging. *Neurobiol Aging*. 2008;29(11):1721-1732. doi:10.1016/j.neurobiolaging.2007.04.007
43. lves IL, Jacobson DR, Torres MF, Holmgren G, Buxbaum J SM. Transthyretin Ser6 as a neutral polymorphismin familial amyloidotic polyneuropathy. *Amyloid1996;3:242–4*.
44. Jacobson D, Alves I, Saraiva M, Thibodeau S, Buxbaum J. Transthyretin Ser 6 gene frequency in individuals without amyloidosis. *Hum Genet*. 1995;95(3). doi:10.1007/BF00225199
45. Hammarström P, Wiseman RL, Powers ET, Kelly JW. Prevention of Transthyretin Amyloid Disease by Changing Protein Misfolding Energetics. *Science (80-)*. 2003;299(5607):713-716. doi:10.1126/science.1079589
46. Uemichi T, Liepnieks JJ, Benson MD. A trinucleotide deletion in the transthyretin gene (AV122) in a kindred with familial amyloidotic polyneuropathy. *Neurology*.

1997;48(6):1667-1670. doi:10.1212/WNL.48.6.1667

47. Gorram F, Olsson M, Alarcon F, Nuel G, Anan I, Planté-Bordeneuve V. New data on the genetic profile and penetrance of hereditary Val30Met transthyretin amyloidosis in Sweden. *Amyloid*. 2021;28(2):84-90. doi:10.1080/13506129.2020.1841623

48. Jacobson DR, Alexander AA, Tagoe C, et al. The prevalence and distribution of the amyloidogenic transthyretin (TTR) V122I allele in Africa. *Mol Genet Genomic Med*. 2016;4(5):548-556. doi:10.1002/mgg3.231

49. Buxbaum JN, Ruberg FL. Transthyretin V122I (pV142I)* cardiac amyloidosis: an age-dependent autosomal dominant cardiomyopathy too common to be overlooked as a cause of significant heart disease in elderly African Americans. *Genet Med*. 2017;19(7):733-742. doi:10.1038/gim.2016.200

50. Gentile L, Di Bella G, Minutoli F, et al. Description of a large cohort of Caucasian patients with <scp>V122I ATTRv</scp> amyloidosis: Neurological and cardiological features. *J Peripher Nerv Syst*. 2020;25(3):273-278. doi:10.1111/jns.12385

51. Cappelli F, Frusconi S, Bergesio F, et al. The Val142Ile transthyretin cardiac amyloidosis. *J Cardiovasc Med*. 2016;17(2):122-125. doi:10.2459/JCM.0000000000000290

52. Mazzarotto F, Argirò A, Zampieri M, et al. Investigation on the high recurrence of the ATTRv-causing transthyretin variant Val142Ile in central Italy. *Eur J Hum Genet*. 2023;31(5):541-547. doi:10.1038/s41431-022-01235-2

53. Reilly MM, Staunton H, Harding AE. Familial amyloid polyneuropathy (TTR ala 60) in north west Ireland: a clinical, genetic, and epidemiological study. *J Neurol Neurosurg Psychiatry*. 1995;59(1):45-49. doi:10.1136/jnnp.59.1.45

54. González-Duarte A, Cárdenas-Soto K, Bañuelos CE, et al. Amyloidosis due to TTR mutations in Mexico with 4 distincts genotypes in the index cases. *Orphanet J Rare Dis*. 2018;13(1):107. doi:10.1186/s13023-018-0801-y

55. Wallace MR, Dwulet FE, Williams EC, Conneally PM, Benson MD. Identification of a new hereditary amyloidosis prealbumin variant, Tyr-77, and detection of the gene by DNA analysis. *J Clin Invest*. 1988;81(1):189-193. doi:10.1172/JCI113293

56. Hsieh ST. Amyloid neuropathy with transthyretin mutations: overview and unique Ala97Ser in Taiwan. *Acta Neurol Taiwan*. 2011;20(2):155-160. http://www.ncbi.nlm.nih.gov/pubmed/21739396

57. Almeida M do R, Ferlini A, Forabosco A, et al. Two transthyretin variants (TTR Ala-49 and TTR Gln-89) in two sicilian kindreds with hereditary amyloidosis. *Hum Mutat*.

1992;1(3):211-215. doi:10.1002/humu.1380010306

58. Durmuş-Tekçe H, Matur Z, Mert Atmaca M, et al. Genotypic and phenotypic presentation of transthyretin-related familial amyloid polyneuropathy (TTR-FAP) in Turkey. *Neuromuscul Disord*. 2016;26(7):441-446. doi:10.1016/j.nmd.2016.04.013
59. Saporta MAC, Zaros C, Cruz MW, et al. Penetrance estimation of TTR familial amyloid polyneuropathy (type I) in Brazilian families. *Eur J Neurol*. 2009;16(3):337-341. doi:10.1111/j.1468-1331.2008.02429.x
60. Plante-Bordeneuve V. Genetic study of transthyretin amyloid neuropathies: carrier risks among French and Portuguese families. *J Med Genet*. 2003;40(11):120e - 120. doi:10.1136/jmg.40.11.e120
61. Hellman U, Alarcon F, Lundgren HE, Suhr OB, Bonaiti-PelliÉ C, Planté-Bordeneuve V. Heterogeneity of penetrance in familial amyloid polyneuropathy, ATTR Val30Met, in the Swedish population. *Amyloid*. 2008;15(3):181-186. doi:10.1080/13506120802193720
62. Yamamoto K, Ikeda S, Hanyu N, Takeda S, Yanagisawa N. A pedigree analysis with minimised ascertainment bias shows anticipation in Met30-transthyretin related familial amyloid polyneuropathy. *J Med Genet*. 1998;35(1):23-30. doi:10.1136/jmg.35.1.23
63. Drugge U, Andersson R, Chizari F, et al. Familial amyloidotic polyneuropathy in Sweden: a pedigree analysis. *J Med Genet*. 1993;30(5):388-392. doi:10.1136/jmg.30.5.388
64. Lemos C, Coelho T, Alves-Ferreira M, et al. Overcoming artefact: anticipation in 284 Portuguese kindreds with familial amyloid polyneuropathy (FAP) ATTRV30M. *J Neurol Neurosurg Psychiatry*. 2014;85(3):326-330. doi:10.1136/jnnp-2013-305383
65. Bonaïti B, Alarcon F, Bonaïti-Pellié C, Planté-Bordeneuve V. Parent-of-origin effect in transthyretin related amyloid polyneuropathy. *Amyloid*. 2009;16(3):149-150. doi:10.1080/13506120903093944
66. Yoshioka K, Furuya H, Sasaki H, Saraiva MJM, Costa PP, Sakaki Y. Haplotype analysis of familial amyloidotic polyneuropathy. *Hum Genet*. 1989;82(1):9-13. doi:10.1007/BF00288262
67. Almeida M, Aoyama-Oishi N, Sakaki Y, et al. Haplotype analysis of common transthyretin mutations. *Hum Genet*. 1995;96(3). doi:10.1007/BF00210422
68. Zaros C, Genin E, Hellman U, et al. On the Origin of the Transthyretin Val30Met Familial Amyloid Polyneuropathy. *Ann Hum Genet*. 2008;72(4):478-484.

doi:10.1111/j.1469-1809.2008.00439.x

69. Ohmori H. Common origin of the Val30Met mutation responsible for the amyloidogenic transthyretin type of familial amyloidotic polyneuropathy. *J Med Genet*. 2004;41(4):e51-e51. doi:10.1136/jmg.2003.014803

70. Reilly MM, Adams D, Davis MB, Said G, Harding AE. Haplotype analysis of French, British and other European patients with familial amyloid polyneuropathy (met 30 and tyr 77). *J Neurol*. 1995;242(10):664-668. doi:10.1007/BF00866917

71. Soares ML, Coelho T, Sousa A, et al. Haplotypes and DNA sequence variation within and surrounding the transthyretin gene: genotype–phenotype correlations in familial amyloid polyneuropathy (V30M) in Portugal and Sweden. *Eur J Hum Genet*. 2004;12(3):225-237. doi:10.1038/sj.ejhg.5201095

72. Alves-Ferreira M, Coelho T, Santos D, et al. A Trans-acting Factor May Modify Age at Onset in Familial Amyloid Polyneuropathy ATTRV30M in Portugal. *Mol Neurobiol*. Published online May 19, 2017. doi:10.1007/s12035-017-0593-4

73. Norgren N, Hellman U, Ericzon BG, Olsson M, Suhr OB. Allele Specific Expression of the Transthyretin Gene in Swedish Patients with Hereditary Transthyretin Amyloidosis (ATTR V30M) Is Similar between the Two Alleles. Toft M, ed. *PLoS One*. 2012;7(11):e49981. doi:10.1371/journal.pone.0049981

74. Santos D, Coelho T, Alves-Ferreira M, et al. Variants in RBP4 and AR genes modulate age at onset in familial amyloid polyneuropathy (FAP ATTRV30M). *Eur J Hum Genet*. 2016;24(5):756-760. doi:10.1038/ejhg.2015.180

75. Soares ML, Coelho T, Sousa A, et al. Susceptibility and modifier genes in Portuguese transthyretin V30M amyloid polyneuropathy: complexity in a single-gene disease. *Hum Mol Genet*. 2005;14(4):543-553. doi:10.1093/hmg/ddi051

76. Dardiotis E, Koutsou P, Zamba-Papanicolaou E, et al. Complement C1Q polymorphisms modulate onset in familial amyloidotic polyneuropathy TTR Val30Met. *J Neurol Sci*. 2009;284(1-2):158-162. doi:10.1016/j.jns.2009.05.018

77. Dias A, Santos D, Coelho T, et al. C1 QA and C1 QC modify age-at-onset in familial amyloid polyneuropathy patients. *Ann Clin Transl Neurol*. 2019;6(4):748-754. doi:10.1002/acn3.748

78. Andreou S, Panayiotou E, Michailidou K, et al. Epidemiology of ATTRV30M neuropathy in Cyprus and the modifier effect of complement C1q on the age of disease onset. *Amyloid*. 2018;25(4):220-226. doi:10.1080/13506129.2018.1534731

79. Santos D, Coelho T, Alves-Ferreira M, et al. Familial amyloid polyneuropathy in

Portugal: New genes modulating age-at-onset. *Ann Clin Transl Neurol*. 2017;4(2):98-105. doi:10.1002/acn3.380

80. Lai Z, Colón W, Kelly JW. The Acid-Mediated Denaturation Pathway of Transthyretin Yields a Conformational Intermediate That Can Self-Assemble into Amyloid. *Biochemistry*. 1996;35(20):6470-6482. doi:10.1021/bi952501g
81. Colon W, Kelly JW. Partial denaturation of transthyretin is sufficient for amyloid fibril formation in vitro. *Biochemistry*. 1992;31(36):8654-8660. doi:10.1021/bi00151a036
82. Ihse E, Ybo A, Suhr O, Lindqvist P, Backman C, Westermark P. Amyloid fibril composition is related to the phenotype of hereditary transthyretin V30M amyloidosis. *J Pathol*. 2008;216(2):253-261. doi:10.1002/path.2411
83. Koike H, Nishi R, Ikeda S, et al. The morphology of amyloid fibrils and their impact on tissue damage in hereditary transthyretin amyloidosis: An ultrastructural study. *J Neurol Sci*. 2018;394:99-106. doi:10.1016/j.jns.2018.09.011
84. Koike H, Ando Y, Ueda M, et al. Distinct characteristics of amyloid deposits in early- and late-onset transthyretin Val30Met familial amyloid polyneuropathy. *J Neurol Sci*. 2009;287(1-2):178-184. doi:10.1016/j.jns.2009.07.028
85. Bergström J, Gustavsson Å, Hellman U, et al. Amyloid deposits in transthyretin-derived amyloidosis: cleaved transthyretin is associated with distinct amyloid morphology. *J Pathol*. 2005;206(2):224-232. doi:10.1002/path.1759
86. Ihse E, Suhr OB, Hellman U, Westermark P. Variation in amount of wild-type transthyretin in different fibril and tissue types in ATTR amyloidosis. *J Mol Med*. 2011;89(2):171-180. doi:10.1007/s00109-010-0695-1
87. COIMBRA A, ANDRADE C. FAMILIAL AMYLOID POLYNEUROPATHY: AN ELECTRON MICROSCOPE STUDY OF THE PERIPHERAL NERVE IN FIVE CASES. I. INTERSTITIAL CHANGES. *Brain*. 1971;94(2):199-206. doi:10.1093/brain/94.2.199
88. Ihse E, Rapezzi C, Merlini G, et al. Amyloid fibrils containing fragmented ATTR may be the standard fibril composition in ATTR amyloidosis. *Amyloid*. 2013;20(3):142-150. doi:10.3109/13506129.2013.797890
89. Okamoto S, Wixner J, Obayashi K, et al. Liver transplantation for familial amyloidotic polyneuropathy: Impact on Swedish patients' survival. *Liver Transplant*. 2009;15(10):1229-1235. doi:10.1002/lt.21817
90. Yazaki M, Mitsuhashi S, Tokuda T, et al. Progressive Wild-Type Transthyretin Deposition after Liver Transplantation Preferentially Occurs onto Myocardium in FAP

Patients. *Am J Transplant*. 2007;7(1):235-242. doi:10.1111/j.1600-6143.2006.01585.x

91. Yazaki M, Liepnieks JJ, Kincaid JC, Benson MD. Contribution of wild-type transthyretin to hereditary peripheral nerve amyloid. *Muscle Nerve*. 2003;28(4):438-442. doi:10.1002/mus.10452
92. Liepnieks JJ, Zhang LQ, Benson MD. Progression of transthyretin amyloid neuropathy after liver transplantation. *Neurology*. 2010;75(4):324-327. doi:10.1212/WNL.0b013e3181ea15d4
93. Merlini G, Bellotti V. Molecular Mechanisms of Amyloidosis. *N Engl J Med*. 2003;349(6):583-596. doi:10.1056/NEJMra023144
94. Westermark P, Sletten K, Johnson KH. Ageing and Amyloid Fibrillogenesis: Lessons from Apolipoprotein Al, Transthyretin and Islet Amyloid Polypeptide. In: ; 2007:205-227. doi:10.1002/9780470514924.ch13
95. Suhr OB, Lundgren E, Westermark P. One mutation, two distinct disease variants: unravelling the impact of transthyretin amyloid fibril composition. *J Intern Med*. 2017;281(4):337-347. doi:10.1111/joim.12585
96. Mangione PP, Verona G, Corazza A, et al. Plasminogen activation triggers transthyretin amyloidogenesis in vitro. *J Biol Chem*. 2018;293(37):14192-14199. doi:10.1074/jbc.RA118.003990
97. Thylén C, Wahlqvist J, Haettner E, Sandgren O, Holmgren G, Lundgren E. Modifications of transthyretin in amyloid fibrils: analysis of amyloid from homozygous and heterozygous individuals with the Met30 mutation. *EMBO J*. 1993;12(2):743-748. doi:10.1002/j.1460-2075.1993.tb05708.x
98. Mangione PP, Porcari R, Gillmore JD, et al. Proteolytic cleavage of Ser52Pro variant transthyretin triggers its amyloid fibrillogenesis. *Proc Natl Acad Sci*. 2014;111(4):1539-1544. doi:10.1073/pnas.1317488111
99. Marcoux J, Mangione PP, Porcari R, et al. A novel mechano-enzymatic cleavage mechanism underlies transthyretin amyloidogenesis. *EMBO Mol Med*. 2015;7(10):1337-1349. doi:10.15252/emmm.201505357
100. Koike H, Ikeda S, Takahashi M, et al. Schwann cell and endothelial cell damage in transthyretin familial amyloid polyneuropathy. *Neurology*. 2016;87(21):2220-2229. doi:10.1212/WNL.0000000000003362
101. Sousa MM, Du Yan S, Fernandes R, Guimarães A, Stern D, Saraiva MJ. Familial Amyloid Polyneuropathy: Receptor for Advanced Glycation End Products-Dependent Triggering of Neuronal Inflammatory and Apoptotic Pathways. *J Neurosci*.

2001;21(19):7576-7586. doi:10.1523/JNEUROSCI.21-19-07576.2001

102. Koike H, Misu K, Sugiura M, et al. Pathology of early- vs late-onset TTR Met30 familial amyloid polyneuropathy. *Neurology*. 2004;63(1):129-138. doi:10.1212/01.WNL.0000132966.36437.12

103. Adams D, Koike H, Slama M, Coelho T. Hereditary transthyretin amyloidosis: a model of medical progress for a fatal disease. *Nat Rev Neurol*. 2019;15(7):387-404. doi:10.1038/s41582-019-0210-4

104. Coutinho P, Martins da Silva A, Lopes Lima J RBA. Forty years of experience with type I amyloid neuropathy: review of 483 cases. *Amyloid and Amyloidosis*. 1980;Amsterdam:

105. Adams D, Coelho T, Obici L, et al. Rapid progression of familial amyloidotic polyneuropathy. *Neurology*. 2015;85(8):675-682. doi:10.1212/WNL.0000000000001870

106. Koike H. Type I (Transthyretin Met30) Familial Amyloid Polyneuropathy in Japan. *Arch Neurol*. 2002;59(11):1771. doi:10.1001/archneur.59.11.1771

107. Conceição I, De Carvalho M. Clinical variability in type I familial amyloid polyneuropathy (Val30Met): Comparison between late- and early-onset cases in Portugal. *Muscle Nerve*. 2007;35(1):116-118. doi:10.1002/mus.20644

108. Mariani L, Lozeron P, Théaudin M, et al. Genotype–phenotype correlation and course of transthyretin familial amyloid polyneuropathies in France. *Ann Neurol*. 2015;78(6):901-916. doi:10.1002/ana.24519

109. Cortese A, Vegezzi E, Lozza A, et al. Diagnostic challenges in hereditary transthyretin amyloidosis with polyneuropathy: avoiding misdiagnosis of a treatable hereditary neuropathy. *J Neurol Neurosurg Psychiatry*. 2017;88(5):457-458. doi:10.1136/jnnp-2016-315262

110. Lozeron P, Mariani LL, Dodet P, et al. Transthyretin amyloid polyneuropathies mimicking a demyelinating polyneuropathy. *Neurology*. 2018;91(2):e143-e152. doi:10.1212/WNL.0000000000005777

111. Théaudin M, Lozeron P, Algalarrondo V, et al. Upper limb onset of hereditary transthyretin amyloidosis is common in non-endemic areas. *Eur J Neurol*. 2019;26(3):497. doi:10.1111/ene.13845

112. Goyal NA, Mozaffar T. Tongue atrophy and fasciculations in transthyretin familial amyloid neuropathy. *Neurol Genet*. 2015;1(2):e18. doi:10.1212/NXG.0000000000000018

113. Cappellari M, Cavallaro T, Ferrarini M, et al. Variable presentations of TTR-related familial amyloid polyneuropathy in seventeen patients. *J Peripher Nerv Syst*. 2011;16(2):119-129. doi:10.1111/j.1529-8027.2011.00331.x
114. Kapoor M, Rossor AM, Laura M, Reilly MM. Clinical Presentation, Diagnosis and Treatment of TTR Amyloidosis. *J Neuromuscul Dis*. 2019;6(2):189-199. doi:10.3233/JND-180371
115. Finsterer J, Iglseder S, Wanschitz J, Topakian R, Löscher WN, Grisold W. Hereditary transthyretin-related amyloidosis. *Acta Neurol Scand*. 2019;139(2):92-105. doi:10.1111/ane.13035
116. Sekijima Y. Transthyretin (ATTR) amyloidosis: clinical spectrum, molecular pathogenesis and disease-modifying treatments. *J Neurol Neurosurg Psychiatry*. 2015;86(9):1036-1043. doi:10.1136/jnnp-2014-308724
117. Phelan D, Collier P, Thavendiranathan P, et al. Relative apical sparing of longitudinal strain using two-dimensional speckle-tracking echocardiography is both sensitive and specific for the diagnosis of cardiac amyloidosis. *Heart*. 2012;98(19):1442-1448. doi:10.1136/heartjnl-2012-302353
118. Martinez-Naharro A, Treibel TA, Abdel-Gadir A, et al. Magnetic Resonance in Transthyretin Cardiac Amyloidosis. *J Am Coll Cardiol*. 2017;70(4):466-477. doi:10.1016/j.jacc.2017.05.053
119. Gillmore JD, Maurer MS, Falk RH, et al. Nonbiopsy Diagnosis of Cardiac Transthyretin Amyloidosis. *Circulation*. 2016;133(24):2404-2412. doi:10.1161/CIRCULATIONAHA.116.021612
120. Glaudemans AWJM, van Rheenen RWJ, van den Berg MP, et al. Bone scintigraphy with 99m technetium-hydroxymethylene diphosphonate allows early diagnosis of cardiac involvement in patients with transthyretin-derived systemic amyloidosis. *Amyloid*. 2014;21(1):35-44. doi:10.3109/13506129.2013.871250
121. Rapezzi C, Quarta CC, Guidalotti PL, et al. Role of 99mTc-DPD Scintigraphy in Diagnosis and Prognosis of Hereditary Transthyretin-Related Cardiac Amyloidosis. *JACC Cardiovasc Imaging*. 2011;4(6):659-670. doi:10.1016/j.jcmg.2011.03.016
122. Perugini E, Guidalotti PL, Salvi F, et al. Noninvasive Etiologic Diagnosis of Cardiac Amyloidosis Using 99m Tc-3,3-Diphosphono-1,2-Propanodicarboxylic Acid Scintigraphy. *J Am Coll Cardiol*. 2005;46(6):1076-1084. doi:10.1016/j.jacc.2005.05.073
123. Sekijima Y, Ueda M, Koike H, Misawa S, Ishii T, Ando Y. Diagnosis and

management of transthyretin familial amyloid polyneuropathy in Japan: red-flag symptom clusters and treatment algorithm. *Orphanet J Rare Dis*. 2018;13(1):6. doi:10.1186/s13023-017-0726-x

124. Maia LF, Magalhaes R, Freitas J, et al. CNS involvement in V30M transthyretin amyloidosis: clinical, neuropathological and biochemical findings. *J Neurol Neurosurg Psychiatry*. 2015;86(2):159-167. doi:10.1136/jnnp-2014-308107
125. McColgan P, Viegas S, Gandhi S, et al. Oculoleptomeningeal Amyloidosis associated with transthyretin Leu12Pro in an African patient. *J Neurol*. 2015;262(1):228-234. doi:10.1007/s00415-014-7594-2
126. Lobato L, Rocha A. Transthyretin Amyloidosis and the Kidney. *Clin J Am Soc Nephrol*. 2012;7(8):1337-1346. doi:10.2215/CJN.08720811
127. Ferraro PM, D'Ambrosio V, Di Paolantonio A, et al. Renal Involvement in Hereditary Transthyretin Amyloidosis: An Italian Single-Centre Experience. *Brain Sci*. 2021;11(8):980. doi:10.3390/brainsci11080980
128. Reynolds MM, Veverka KK, Gertz MA, et al. Ocular Manifestations of Familial Transthyretin Amyloidosis. *Am J Ophthalmol*. 2017;183:156-162. doi:10.1016/j.ajo.2017.09.001
129. Maurer MS, Hanna M, Grogan M, et al. Genotype and Phenotype of Transthyretin Cardiac Amyloidosis. *J Am Coll Cardiol*. 2016;68(2):161-172. doi:10.1016/j.jacc.2016.03.596
130. Yang NCC, Lee MJ, Chao CC, et al. Clinical presentations and skin denervation in amyloid neuropathy due to transthyretin Ala97Ser. *Neurology*. 2010;75(6):532-538. doi:10.1212/WNL.0b013e3181ec7fda
131. González-Duarte A, Soto KC, Martínez-Baños D, et al. Familial amyloidosis with polyneuropathy associated with TTR Ser50Arg mutation. *Amyloid*. 2012;19(4):171-176. doi:10.3109/13506129.2012.712925
132. Carroll A, Dyck PJ, de Carvalho M, et al. Novel approaches to diagnosis and management of hereditary transthyretin amyloidosis. *J Neurol Neurosurg Psychiatry*. 2022;93(6):668-678. doi:10.1136/jnnp-2021-327909
133. Lane T, Fontana M, Martinez-Naharro A, et al. Natural History, Quality of Life, and Outcome in Cardiac Transthyretin Amyloidosis. *Circulation*. 2019;140(1):16-26. doi:10.1161/CIRCULATIONAHA.118.038169
134. Ruberg FL, Grogan M, Hanna M, Kelly JW, Maurer MS. Transthyretin Amyloid Cardiomyopathy. *J Am Coll Cardiol*. 2019;73(22):2872-2891.

doi:10.1016/j.jacc.2019.04.003

135. Adams D, Ando Y, Beirão JM, et al. Expert consensus recommendations to improve diagnosis of ATTR amyloidosis with polyneuropathy. *J Neurol*. 2021;268(6):2109-2122. doi:10.1007/s00415-019-09688-0

136. Dohrn MF, Röcken C, Bleecker JL, et al. Diagnostic hallmarks and pitfalls in late-onset progressive transthyretin-related amyloid-neuropathy. *J Neurol*. 2013;260(12):3093-3108. doi:10.1007/s00415-013-7124-7

137. Plante-Bordeneuve V, Ferreira A, Lalu T, et al. Diagnostic pitfalls in sporadic transthyretin familial amyloid polyneuropathy (TTR-FAP). *Neurology*. 2007;69(7):693-698. doi:10.1212/01.wnl.0000267338.45673.f4

138. Klein CJ, Vrana JA, Theis JD, et al. Mass Spectrometric–Based Proteomic Analysis of Amyloid Neuropathy Type in Nerve Tissue. *Arch Neurol*. 2011;68(2). doi:10.1001/archneurol.2010.261

139. Koike H, Kawagashira Y, Iijima M, et al. Electrophysiological features of late-onset transthyretin Met30 familial amyloid polyneuropathy unrelated to endemic foci. *J Neurol*. 2008;255(10):1526-1533. doi:10.1007/s00415-008-0962-z

140. Niklasson U, Olofsson BO, Bjerle P. Autonomic neuropathy in familial amyloidotic polyneuropathy. *Acta Neurol Scand*. 1989;79(3):182-187. doi:10.1111/j.1600-0404.1989.tb03736.x

141. Castro J, Miranda B, Castro I, de Carvalho M, Conceição I. The diagnostic accuracy of Sudoscan in transthyretin familial amyloid polyneuropathy. *Clin Neurophysiol*. 2016;127(5):2222-2227. doi:10.1016/j.clinph.2016.02.013

142. SUHR O, DANIELSSON Å, HOLMGREN G, STEEN L. Malnutrition and gastrointestinal dysfunction as prognostic factors for survival in familial amyloidotic polyneuropathy. *J Intern Med*. 1994;235(5):479-485. doi:10.1111/j.1365-2796.1994.tb01106.x

143. Dyck PJ, Davies JL, Litchy WJ, O'Brien PC. Longitudinal assessment of diabetic polyneuropathy using a composite score in the Rochester Diabetic Neuropathy Study cohort. *Neurology*. 1997;49(1):229-239. doi:10.1212/WNL.49.1.229

144. Denier C, Ducot B, Husson H, et al. A brief compound test for assessment of autonomic and sensory-motor dysfunction in familial amyloid polyneuropathy. *J Neurol*. 2007;254(12):1684-1688. doi:10.1007/s00415-007-0617-5

145. Raphael C, Briscoe C, Davies J, et al. Limitations of the New York Heart Association functional classification system and self-reported walking distances in chronic heart

failure. *Heart*. 2007;93(4):476-482. doi:10.1136/hrt.2006.089656

146. Damy T, Deux JF, Moutereau S, et al. Role of natriuretic peptide to predict cardiac abnormalities in patients with hereditary transthyretin amyloidosis. *Amyloid*. 2013;20(4):212-220. doi:10.3109/13506129.2013.825240
147. Gillmore JD, Damy T, Fontana M, et al. A new staging system for cardiac transthyretin amyloidosis. *Eur Heart J*. 2018;39(30):2799-2806. doi:10.1093/eurheartj/ehx589
148. Rocha A, Lobato L, Silva H, et al. Characterization of End-Stage Renal Disease After Liver Transplantation in Transthyretin Amyloidosis (ATTR V30M). *Transplant Proc*. 2011;43(1):189-193. doi:10.1016/j.transproceed.2010.11.014
149. Berk JL, Suhr OB, Obici L, et al. Repurposing Diflunisal for Familial Amyloid Polyneuropathy. *JAMA*. 2013;310(24):2658. doi:10.1001/jama.2013.283815
150. Merkies ISJ. Tafamidis for transthyretin familial amyloid polyneuropathy: A randomized, controlled trial. *Neurology*. 2013;80(15):1444.2-1445. doi:10.1212/01.wnl.0000429338.33391.87
151. Cortese A, Vita G, Luigetti M, et al. Monitoring effectiveness and safety of Tafamidis in transthyretin amyloidosis in Italy: a longitudinal multicenter study in a non-endemic area. *J Neurol*. 2016;263(5):916-924. doi:10.1007/s00415-016-8064-9
152. Adams D, Suhr OB, Dyck PJ, et al. Trial design and rationale for APOLLO, a Phase 3, placebo-controlled study of patisiran in patients with hereditary ATTR amyloidosis with polyneuropathy. *BMC Neurol*. 2017;17(1):1-12. doi:10.1186/s12883-017-0948-5
153. Dyck PJ, Kincaid JC, Dyck PJB, et al. Assessing mNIS+7Ionis and international neurologists' proficiency in a familial amyloidotic polyneuropathy trial. *Muscle and Nerve*. 2017;56(5):901-911. doi:10.1002/mus.25563
154. Suanprasert N, Berk JL, Benson MD, et al. Retrospective study of a TTR FAP cohort to modify NIS + 7 for therapeutic trials. *J Neurol Sci*. 2014;344(1-2):121-128. doi:10.1016/j.jns.2014.06.041
155. Dyck PJB, González-Duarte A, Obici L, et al. Development of measures of polyneuropathy impairment in hATTR amyloidosis: From NIS to mNIS + 7. *J Neurol Sci*. 2019;405(July):116424. doi:10.1016/j.jns.2019.116424
156. van Nes SI, Vanhoutte EK, van Doorn PA, et al. Rasch-built Overall Disability Scale (R-ODS) for immune-mediated peripheral neuropathies. *Neurology*. 2011;76(4):337-345. doi:10.1212/WNL.0b013e318208824b
157. Vinik EJ, Hayes RP, Oglesby A, et al. The Development and Validation of the Norfolk

QOL-DN, a New Measure of Patients' Perception of the Effects of Diabetes and Diabetic Neuropathy. *Diabetes Technol Ther*. 2005;7(3):497-508. doi:10.1089/dia.2005.7.497

158. Ticau S, Sridharan G V., Tsour S, et al. Neurofilament Light Chain as a Biomarker of Hereditary Transthyretin-Mediated Amyloidosis. *Neurology*. 2021;96(3):e412-e422. doi:10.1212/WNL.0000000000011090
159. Maia LF, Maceski A, Conceição I, et al. Plasma neurofilament light chain: an early biomarker for hereditary ATTR amyloid polyneuropathy. *Amyloid*. 2020;27(2):97-102. doi:10.1080/13506129.2019.1708716
160. Kapoor M, Foiani M, Heslegrave A, et al. Plasma neurofilament light chain concentration is increased and correlates with the severity of neuropathy in hereditary transthyretin amyloidosis. *J Peripher Nerv Syst*. 2019;24(4):314-319. doi:10.1111/jns.12350
161. Romano A, Primiano G, Antonini G, et al. Serum neurofilament light chain: a promising early diagnostic biomarker for hereditary transthyretin amyloidosis? *Eur J Neurol*. Published online September 19, 2023. doi:10.1111/ene.16070
162. Luigetti M, Guglielmino V, Romozzi M, et al. Nerve Conduction Studies of Dorsal Sural Nerve: Normative Data and Its Potential Application in ATTRv Pre-Symptomatic Subjects. *Brain Sci*. 2022;12(8):1037. doi:10.3390/brainsci12081037
163. Luigetti M, Di Paolantonio A, Guglielmino V, Romano A. Cutaneous silent period in ATTRv carriers: a possible early marker of nerve damage? *Neurol Sci*. 2022;43(12):6979-6982. doi:10.1007/s10072-022-06317-z
164. Kollmer J, Hund E, Hornung B, et al. In vivo detection of nerve injury in familial amyloid polyneuropathy by magnetic resonance neurography. *Brain*. 2015;138(3):549-562. doi:10.1093/brain/awu344
165. Kollmer J, Sahm F, Hegenbart U, et al. Sural nerve injury in familial amyloid polyneuropathy MR neurography vs clinicopathologic tools. *Neurology*. 2017;89(5):475-484. doi:10.1212/WNL.0000000000004178
166. Kollmer J, Hegenbart U, Kimmich C, et al. Magnetization transfer ratio quantifies polyneuropathy in hereditary transthyretin amyloidosis. *Ann Clin Transl Neurol*. 2020;7(5):799-807. doi:10.1002/acn3.51049
167. Holmgren G, Steen L, Suhr O, et al. Clinical improvement and amyloid regression after liver transplantation in hereditary transthyretin amyloidosis. *Lancet*. 1993;341(8853):1113-1116. doi:10.1016/0140-6736(93)93127-M

168. Tsuchiya A, Yazaki M, Kametani F, Takei Y ichi, Ikeda S ichi. Marked regression of abdominal fat amyloid in patients with familial amyloid polyneuropathy during long-term follow-up after liver transplantation. *Liver Transplant*. 2008;14(4):563-570. doi:10.1002/lt.21395

169. Yamamoto S, Wilczek HE, Nowak G, et al. Liver Transplantation for Familial Amyloidotic Polyneuropathy (FAP): A Single-Center Experience Over 16 Years. *Am J Transplant*. 2007;7(11):2597-2604. doi:10.1111/j.1600-6143.2007.01969.x

170. Wilczek HE, Larsson M, Ericzon BG. Long-term data from the Familial Amyloidotic Polyneuropathy World Transplant Registry (FAPWTR). *Amyloid*. 2011;18(sup1):193-195. doi:10.3109/13506129.2011.574354072

171. Conceição I, Evangelista T, Castro J, et al. Acquired amyloid neuropathy in a Portuguese patient after domino liver transplantation. *Muscle Nerve*. 2010;42(5):836-838. doi:10.1002/mus.21806

172. Ando Y, Terazaki H, Nakamura M, et al. A different amyloid formation mechanism: de novo oculoleptomeningeal amyloid deposits after liver transplantation. *Transplantation*. 2004;77(3):345-349. doi:10.1097/01.TP.0000111516.60013.E6

173. Sekijima Y, Dendle MA, Kelly JW. Orally administered diflunisal stabilizes transthyretin against dissociation required for amyloidogenesis. *Amyloid*. 2006;13(4):236-249. doi:10.1080/13506120600960882

174. Ibrahim M, Saint Croix GR, Lacy S, et al. The use of diflunisal for transthyretin cardiac amyloidosis: a review. *Heart Fail Rev*. 2022;27(2):517-524. doi:10.1007/s10741-021-10143-4

175. Merlini G, Planté-Bordeneuve V, Judge DP, et al. Effects of Tafamidis on Transthyretin Stabilization and Clinical Outcomes in Patients with Non-Val30Met Transthyretin Amyloidosis. *J Cardiovasc Transl Res*. 2013;6(6):1011-1020. doi:10.1007/s12265-013-9512-x

176. Coelho T, Maia LF, Martins da Silva A, et al. Tafamidis for transthyretin familial amyloid polyneuropathy: A randomized, controlled trial. *Neurology*. 2012;79(8):785-792. doi:10.1212/WNL.0b013e3182661eb1

177. Planté-Bordeneuve V, Gorram F, Salhi H, et al. Long-term treatment of transthyretin familial amyloid polyneuropathy with tafamidis: a clinical and neurophysiological study. *J Neurol*. 2017;264(2):268-276. doi:10.1007/s00415-016-8337-3

178. Lozeron P, Théaudin M, Mincheva Z, Ducot B, Lacroix C, Adams D. Effect on disability and safety of Tafamidis in late onset of Met30 transthyretin familial amyloid

polyneuropathy. *Eur J Neurol*. 2013;20(12):1539-1545. doi:10.1111/ene.12225
179. https://www.ema.europa.eu/en/medicines/human/orphan-designations/eu-3-06-401.
180. https://www.fda.gov/news-events/press-announcements/fda-approves-new-treatments-heart-disease-caused-serious-rare-disease-transthyretin-mediated.
181. Fox JC, Hellawell JL, Rao S, et al. First-in-Human Study of AG10, a Novel, Oral, Specific, Selective, and Potent Transthyretin Stabilizer for the Treatment of Transthyretin Amyloidosis: A Phase 1 Safety, Tolerability, Pharmacokinetic, and Pharmacodynamic Study in Healthy Adult Volunteers. *Clin Pharmacol Drug Dev*. 2020;9(1):115-129. doi:10.1002/cpdd.700
182. https://classic.clinicaltrials.gov/ct2/show/NCT03860935.
183. Obici L, Cortese A, Lozza A, et al. Doxycycline plus tauroursodeoxycholic acid for transthyretin amyloidosis: a phase II study. *Amyloid*. 2012;19 Suppl 1:34-36. doi:10.3109/13506129.2012.678508
184. Mallus MT, Rizzello V. Treatment of amyloidosis: present and future. *Eur Hear J Suppl*. 2023;25(Supplement_B):B99-B103. doi:10.1093/eurheartjsupp/suad082
185. Viney NJ, Guo S, Tai L, et al. Ligand conjugated antisense oligonucleotide for the treatment of transthyretin amyloidosis: preclinical and phase 1 data. *ESC Hear Fail*. 2021;8(1):652-661. doi:10.1002/ehf2.13154
186. Coelho T, Marques W, Dasgupta NR, et al. Eplontersen for Hereditary Transthyretin Amyloidosis With Polyneuropathy. *JAMA*. 2023;330(15):1448. doi:10.1001/jama.2023.18688
187. https://classic.clinicaltrials.gov/ct2/show/NCT04136171.
188. https://classic.clinicaltrials.gov/ct2/show/NCT03997383.
189. https://classic.clinicaltrials.gov/ct2/show/NCT04153149.
190. Adams D, Slama M. Hereditary transthyretin amyloidosis: current treatment. *Curr Opin Neurol*. 2020;33(5):553-561. doi:10.1097/WCO.0000000000000852
191. Dyck PJ, Overland CJ, Low PA, et al. Signs and symptoms versus nerve conduction studies to diagnose diabetic sensorimotor polyneuropathy: CI vs. NPhys trial. *Muscle and Nerve*. 2010;42(2):157-164. doi:10.1002/mus.21661
192. Dyck PJ, Overland CJ, Low PA, et al. "Unequivocally abnormal" vs "usual" signs and symptoms for proficient diagnosis of diabetic polyneuropathy: Cl vs N Phys trial. *Arch Neurol*. 2012;69(12):1609-1614. doi:10.1001/archneurol.2012.1481
193. Rooney WD, Berlow YA, Triplett WT, et al. Modeling disease trajectory in Duchenne muscular dystrophy. *Neurology*. 2020;94(15):E1622-E1633.

doi:10.1212/WNL.0000000000009244

194. Fischmann A, Hafner P, Fasler S, et al. Quantitative MRI can detect subclinical disease progression in muscular dystrophy. *J Neurol*. 2012;259(8):1648-1654. doi:10.1007/s00415-011-6393-2

195. Janssen B, Voet N, Geurts A, Van Engelen B, Heerschap A. Quantitative MRI reveals decelerated fatty infiltration in muscles of active FSHD patients. *Neurology*. 2016;86(18):1700-1707. doi:10.1212/WNL.0000000000002640

196. Paoletti M, Pichiecchio A, Piccinelli SC, et al. Advances in quantitative imaging of genetic and acquired myopathies: Clinical applications and perspectives. *Front Neurol*. 2019;10(FEB):1-21. doi:10.3389/fneur.2019.00078

197. Klickovic U, Zampedri L, Sinclair CDJ, et al. Skeletal muscle MRI differentiates SBMA and ALS and correlates with disease severity. *Neurology*. 2019;93(9):E895-E907. doi:10.1212/WNL.0000000000008009

198. Jenkins TM, Alix JJP, Fingret J, et al. Longitudinal multi - modal muscle - based biomarker assessment in motor neuron disease. *J Neurol*. 2020;267(1):244-256. doi:10.1007/s00415-019-09580-x

199. Morrow JM, Sinclair CDJ, Fischmann A, et al. MRI biomarker assessment of neuromuscular disease progression: A prospective observational cohort study. *Lancet Neurol*. 2016;15(1):65-77. doi:10.1016/S1474-4422(15)00242-2

200. Kugathasan U, Evans MRB, Morrow JM, et al. Development of MRC Centre MRI calf muscle fat fraction protocol as a sensitive outcome measure in Hereditary Sensory Neuropathy Type 1. *J Neurol Neurosurg Psychiatry*. Published online 2019:895-906. doi:10.1136/jnnp-2018-320198

201. Bas J, Ogier AC, Le Troter A, et al. Fat fraction distribution in lower limb muscles of patients with CMT1A A quantitative MRI study. *Neurology*. 2020;94(14). doi:10.1212/WNL.0000000000009013

202. Pridmore M, Castoro R, McCollum MS, Kang H, Li J, Dortch R. Length-dependent MRI of hereditary neuropathy with liability to pressure palsies. *Ann Clin Transl Neurol*. 2020;7(1):15-25. doi:10.1002/acn3.50953

203. Muzic SI, Paoletti M, Solazzo F, et al. Reproducibility of manual segmentation in muscle imaging. *Acta Myol myopathies cardiomyopathies Off J Mediterr Soc Myol*. 2021;40(3):116-123. doi:10.36185/2532-1900-052

204. Marty B, Baudin PY, Reyngoudt H, et al. Simultaneous muscle water T2 and fat fraction mapping using transverse relaxometry with stimulated echo compensation.

NMR Biomed. 2016;29(4):431-443. doi:10.1002/nbm.3459

205. Weigel M. Extended phase graphs: Dephasing, RF pulses, and echoes - Pure and simple. *J Magn Reson Imaging*. 2015;41(2):266-295. doi:10.1002/jmri.24619
206. Santini F, Deligianni X, Paoletti M, et al. Fast Open-Source Toolkit for Water T2 Mapping in the Presence of Fat From Multi-Echo Spin-Echo Acquisitions for Muscle MRI. *Front Neurol*. 2021;12(February):1-10. doi:10.3389/fneur.2021.630387
207. Smith DS, Berglund J, Kullberg J, Ahlström H, Avison MJ, Welch EB. Optimization of Fat-Water Separation Algorithm Selection and Options Using Image-Based Metrics with Validation by ISMRM Fat-Water Challenge Datasets. *Proc 21st Annu Meet ISMRM*. 2013;63(1):2413.
208. Berglund J, Kullberg J. Three-dimensional water/fat separation and T 2 * estimation based on whole-image optimization-Application in breathhold liver imaging at 1.5 T. *Magn Reson Med*. 2012;67(6):1684-1693. doi:10.1002/mrm.23185
209. Kelly JJ, Kyle RA, O'Brien PC, Dyck PJ. The natural history of peripheral neuropathy in primary systemic amyloidosis. *Ann Neurol*. 1979;6(1):1-7. doi:10.1002/ana.410060102
210. J. Schroeder, P. Tobler A-L Stalder et al. Intra-rater and inter-rater reliability of quantitative thigh muscle magnetic resonance imaging. *Imaging Med*. 2019;11 (2).
211. Agosti A, Shaqiri E, Paoletti M, et al. Deep learning for automatic segmentation of thigh and leg muscles. *Magn Reson Mater Physics, Biol Med*. 2022;35(3):467-483. doi:10.1007/s10334-021-00967-4
212. Rohm M, Markmann M, Forsting J, Rehmann R, Froeling M, Schlaffke L. 3D Automated Segmentation of Lower Leg Muscles Using Machine Learning on a Heterogeneous Dataset. *Diagnostics*. 2021;11(10):1747. doi:10.3390/diagnostics11101747
213. Koike H, Misu K, Sugiura M, et al. Pathology of early- vs late-onset TTR Met30 familial amyloid polyneuropathy. *Neurology*. 2004;63(1):129-138. doi:10.1212/01.WNL.0000132966.36437.12
214. Lichtenstein T, Sprenger A, Weiss K, et al. MRI biomarkers of proximal nerve injury in CIDP. *Ann Clin Transl Neurol*. 2018;5(1):19-28. doi:10.1002/acn3.502
215. Pinto M V., Milone M, Mauermann ML, et al. Transthyretin amyloidosis: Putting myopathy on the map. *Muscle Nerve*. 2020;61(1):95-100. doi:10.1002/mus.26723
216. Iorio A, De Lillo A, De Angelis F, et al. Non-coding variants contribute to the clinical heterogeneity of TTR amyloidosis. *Eur J Hum Genet*. 2017;25(9):1055-1060.

doi:10.1038/ejhg.2017.95

217. Snyder MW, Adey A, Kitzman JO, Shendure J. Haplotype-resolved genome sequencing: experimental methods and applications. *Nat Rev Genet*. 2015;16(6):344-358. doi:10.1038/nrg3903

218. Lieberman-Aiden E, van Berkum NL, Williams L, et al. Comprehensive Mapping of Long-Range Interactions Reveals Folding Principles of the Human Genome. *Science (80-)*. 2009;326(5950):289-293. doi:10.1126/science.1181369

219. Putnam NH, O'Connell BL, Stites JC, et al. Chromosome-scale shotgun assembly using an in vitro method for long-range linkage. *Genome Res*. 2016;26(3):342-350. doi:10.1101/gr.193474.115

220. Porubský D, Sanders AD, van Wietmarschen N, et al. Direct chromosome-length haplotyping by single-cell sequencing. *Genome Res*. 2016;26(11):1565-1574. doi:10.1101/gr.209841.116

221. Porubsky D, Garg S, Sanders AD, et al. Dense and accurate whole-chromosome haplotyping of individual genomes. *Nat Commun*. 2017;8(1):1293. doi:10.1038/s41467-017-01389-4

222. Moss DJH, Pardiñas AF, Langbehn D, et al. Identification of genetic variants associated with Huntington's disease progression: a genome-wide association study. *Lancet Neurol*. 2017;16(9):701-711. doi:10.1016/S1474-4422(17)30161-8

223. https://www.genomicsengland.co.uk.

224. Olsson M, Norgren N, Obayashi K, et al. A possible role for miRNA silencing in disease phenotype variation in Swedish transthyretin V30M carriers. *BMC Med Genet*. 2010;11(1):130. doi:10.1186/1471-2350-11-130

225. Boldbaatar B, Maenpaa E, Sikora Hanson J, Connors L. Analysis of the non-coding rs3764479 mutation in the proximal promoter of the transthyretin gene. *Amyloid*. 2019;26(sup1):83-84. doi:10.1080/13506129.2019.1583201

226. Alves-Ferreira M, Azevedo A, Coelho T, et al. Beyond Val30Met transthyretin (TTR): variants associated with age-at-onset in hereditary ATTRv amyloidosis. *Amyloid*. 2021;28(2):100-106. doi:10.1080/13506129.2020.1857236

227. Sikora JL, Logue MW, Chan GG, et al. Genetic variation of the transthyretin gene in wild-type transthyretin amyloidosis (ATTRwt). *Hum Genet*. 2015;134(1):111-121. doi:10.1007/s00439-014-1499-0

228. De Lillo A, De Angelis F, Di Girolamo M, et al. Phenome-wide association study of TTR and RBP4 genes in 361,194 individuals reveals novel insights in the genetics of

hereditary and wildtype transthyretin amyloidoses. *Hum Genet*. 2019;138(11-12):1331-1340. doi:10.1007/s00439-019-02078-6

229. https://www.alzforum.org/mutations/app.
230. Biffi A, Shulman JM, Jagiella JM, et al. Genetic variation at CR1 increases risk of cerebral amyloid angiopathy. *Neurology*. 2012;78(5):334-341. doi:10.1212/WNL.0b013e3182452b40
231. Yang HS, White CC, Chibnik LB, et al. UNC5C variants are associated with cerebral amyloid angiopathy. *Neurol Genet*. 2017;3(4):e176. doi:10.1212/NXG.0000000000000176
232. Chattopadhyay S, Thomsen H, Weinhold N, et al. Eight novel loci implicate shared genetic etiology in multiple myeloma, AL amyloidosis, and monoclonal gammopathy of unknown significance. *Leukemia*. 2020;34(4):1187-1191. doi:10.1038/s41375-019-0619-1
233. Meziane I, Huhn S, Filho MI da S, et al. Genome-wide association study of clinical parameters in immunoglobulin light chain amyloidosis in three patient cohorts. *Haematologica*. 2017;102(10):e411-e414. doi:10.3324/haematol.2017.171108
234. da Silva Filho MI, Försti A, Weinhold N, et al. Genome-wide association study of immunoglobulin light chain amyloidosis in three patient cohorts: comparison with myeloma. *Leukemia*. 2017;31(8):1735-1742. doi:10.1038/leu.2016.387
235. Saunders CN, Chattopadhyay S, Huhn S, et al. Search for AL amyloidosis risk factors using Mendelian randomization. *Blood Adv*. 2021;5(13):2725-2731. doi:10.1182/bloodadvances.2021004423
236. Dada S, Burger MC, Massij F, de Wet H, Collins M. Carpal tunnel syndrome: The role of collagen gene variants. *Gene*. 2016;587(1):53-58. doi:10.1016/j.gene.2016.04.030
237. Skuladottir AT, Bjornsdottir G, Ferkingstad E, et al. A genome-wide meta-analysis identifies 50 genetic loci associated with carpal tunnel syndrome. *Nat Commun*. 2022;13(1):1598. doi:10.1038/s41467-022-29133-7
238. Wiberg A, Ng M, Schmid AB, et al. A genome-wide association analysis identifies 16 novel susceptibility loci for carpal tunnel syndrome. *Nat Commun*. 2019;10(1):1030. doi:10.1038/s41467-019-08993-6
239. Yan W, Hao Z, Tang S, et al. A genome-wide association study identifies new genes associated with developmental dysplasia of the hip. *Clin Genet*. 2019;95(3):345-355. doi:10.1111/cge.13483
240. Patel B, Kleeman SO, Neavin D, et al. Shared genetic susceptibility between trigger

finger and carpal tunnel syndrome: a genome-wide association study. *Lancet Rheumatol*. 2022;4(8):e556-e565. doi:10.1016/S2665-9913(22)00180-1

241. Sood RF, Westenberg RF, Winograd JM, Eberlin KR, Chen NC. Genetic Risk of Trigger Finger: Results of a Genomewide Association Study. *Plast Reconstr Surg*. 2020;146(2):165e-176e. doi:10.1097/PRS.0000000000006982
242. Suri P, Stanaway IB, Zhang Y, et al. Genome-wide association studies of low back pain and lumbar spinal disorders using electronic health record data identify a locus associated with lumbar spinal stenosis. *Pain*. 2021;162(8):2263-2272. doi:10.1097/j.pain.0000000000002221
243. Yanik EL, Keener JD, Lin SJ, et al. Identification of a Novel Genetic Marker for Risk of Degenerative Rotator Cuff Disease Surgery in the UK Biobank. *J Bone Jt Surg*. 2021;103(14):1259-1267. doi:10.2106/JBJS.20.01474
244. Tashjian RZ, Kim SK, Roche MD, Jones KB, Teerlink CC. Genetic variants associated with rotator cuff tearing utilizing multiple population-based genetic resources. *J Shoulder Elb Surg*. 2021;30(3):520-531. doi:10.1016/j.jse.2020.06.036
245. Roos TR, Roos AK, Avins AL, et al. Genome-wide association study identifies a locus associated with rotator cuff injury. Raleigh S, ed. *PLoS One*. 2017;12(12):e0189317. doi:10.1371/journal.pone.0189317
246. Tashjian RZ, Granger EK, Farnham JM, Cannon-Albright LA, Teerlink CC. Genome-wide association study for rotator cuff tears identifies two significant single-nucleotide polymorphisms. *J Shoulder Elb Surg*. 2016;25(2):174-179. doi:10.1016/j.jse.2015.07.005
247. Teerlink CC, Cannon-Albright LA, Tashjian RZ. Significant association of full-thickness rotator cuff tears and estrogen-related receptor-β (ESRRB). *J Shoulder Elb Surg*. 2015;24(2):e31-e35. doi:10.1016/j.jse.2014.06.052
248. Kim SK, Nguyen C, Jones KB, Tashjian RZ. A genome-wide association study for shoulder impingement and rotator cuff disease. *J Shoulder Elb Surg*. 2021;30(9):2134-2145. doi:10.1016/j.jse.2020.11.025
249. Santos D, Coelho T, Alves-Ferreira M, et al. Large normal alleles of ATXN2 decrease age at onset in transthyretin familial amyloid polyneuropathy Val30Met patients. *Ann Neurol*. 2019;85(2):251-258. doi:10.1002/ana.25409
250. Ding D, Li K, Wang C, et al. ATXN2 polymorphism modulates age at onset in Machado-Joseph disease. *Brain*. Published online July 24, 2016:aww176. doi:10.1093/brain/aww176

251. Kullo IJ, Shameer K, Jouni H, et al. The ATXN2-SH2B3 locus is associated with peripheral arterial disease: an electronic medical record-based genome-wide association study. *Front Genet*. 2014;5. doi:10.3389/fgene.2014.00166
252. Yu F, Sabeti PC, Hardenbol P, et al. Positive Selection of a Pre-Expansion CAG Repeat of the Human SCA2 Gene. Abecasis G, ed. *PLoS Genet*. 2005;1(3):e41. doi:10.1371/journal.pgen.0010041
253. Medina-Suárez J, Rodríguez-Esparragón F, Sosa-Pérez C, et al. A Review of Genetic Polymorphisms and Susceptibilities to Complications after Aneurysmal Subarachnoid Hemorrhage. *Int J Mol Sci*. 2022;23(23):15427. doi:10.3390/ijms232315427
254. Deming Y, Filipello F, Cignarella F, et al. The MS4A gene cluster is a key modulator of soluble TREM2 and Alzheimer's disease risk. *Sci Transl Med*. 2019;11(505). doi:10.1126/scitranslmed.aau2291
255. Keikha M, Karbalaei M. Global distribution of ACE1 (rs4646994) and ACE2 (rs2285666) polymorphisms associated with COVID-19: A systematic review and meta-analysis. *Microb Pathog*. 2022;172:105781. doi:10.1016/j.micpath.2022.105781
256. Ma Y, Li Q, Chen J, et al. Angiotensin-Converting Enzyme 2 SNPs as Common Genetic Loci and Optimal Early Identification Genetic Markers for COVID-19. *Pathogens*. 2022;11(8):947. doi:10.3390/pathogens11080947
257. Khayat AS, de Assumpção PP, Meireles Khayat BC, et al. ACE2 polymorphisms as potential players in COVID-19 outcome. Pershouse MA, ed. *PLoS One*. 2020;15(12):e0243887. doi:10.1371/journal.pone.0243887
258. Jalaleddine N, Bouzid A, Hachim M, et al. ACE2 polymorphisms impact COVID-19 severity in obese patients. *Sci Rep*. 2022;12(1):21491. doi:10.1038/s41598-022-26072-7
259. Bakker MK, Cobyte S, Hennekam FAM, Rinkel GJE, Veldink JH, Ruigrok YM. Genome-wide linkage analysis combined with genome sequencing in large families with intracranial aneurysms. *Eur J Hum Genet*. 2022;30(7):833-840. doi:10.1038/s41431-022-01059-0
260. Živković M, Stanković A, Dinčić E, et al. The tag SNP for HLA-DRB1∗1501, rs3135388, is significantly associated with multiple sclerosis susceptibility: Cost-effective high-throughput detection by real-time PCR. *Clin Chim Acta*. 2009;406(1-2):27-30. doi:10.1016/j.cca.2009.05.004
261. Alghamdi J, Alaamery M, Barhoumi T, et al. Interferon-induced transmembrane protein-3 genetic variant rs12252 is associated with COVID-19 mortality. *Genomics*.

2021;113(4):1733-1741. doi:10.1016/j.ygeno.2021.04.002

262. Fedetz M, Matesanz F, Caro-Maldonado A, et al. OAS1 gene haplotype confers susceptibility to multiple sclerosis. *Tissue Antigens*. 2006;68(5):446-449. doi:10.1111/j.1399-0039.2006.00694.x

263. Zhou S, Butler-Laporte G, Nakanishi T, et al. A Neanderthal OAS1 isoform protects individuals of European ancestry against COVID-19 susceptibility and severity. *Nat Med*. 2021;27(4):659-667. doi:10.1038/s41591-021-01281-1

264. Gokul A, Arumugam T, Ramsuran V. Genetic Ethnic Differences in Human 2′-5′-Oligoadenylate Synthetase and Disease Associations: A Systematic Review. *Genes (Basel)*. 2023;14(2):527. doi:10.3390/genes14020527

265. Bakker MK, van der Spek RAA, van Rheenen W, et al. Genome-wide association study of intracranial aneurysms identifies 17 risk loci and genetic overlap with clinical risk factors. *Nat Genet*. 2020;52(12):1303-1313. doi:10.1038/s41588-020-00725-7

266. Zhou S, Ambalavanan A, Rochefort D, et al. RNF213 Is Associated with Intracranial Aneurysms in the French-Canadian Population. *Am J Hum Genet*. 2016;99(5):1072-1085. doi:10.1016/j.ajhg.2016.09.001

267. Gallagher MD, Posavi M, Huang P, et al. A Dementia-Associated Risk Variant near TMEM106B Alters Chromatin Architecture and Gene Expression. *Am J Hum Genet*. 2017;101(5):643-663. doi:10.1016/j.ajhg.2017.09.004

268. Mizrahi R, Rusjan PM, Kennedy J, et al. Translocator Protein (18 kDa) Polymorphism (rs6971) Explains in-vivo Brain Binding Affinity of the PET Radioligand [18 F]-FEPPA. *J Cereb Blood Flow Metab*. 2012;32(6):968-972. doi:10.1038/jcbfm.2012.46

269. https://www.nature.com/scitable/definition/haplotype-haplotypes-142/.

270. Nalls MA, Pankratz N, Lill CM, et al. Large-scale meta-analysis of genome-wide association data identifies six new risk loci for Parkinson's disease. *Nat Genet*. 2014;46(9):989-993. doi:10.1038/ng.3043